

University of Windsor

Scholarship at UWindor

Electronic Theses and Dissertations

Theses, Dissertations, and Major Papers

2019

Properties of Glass Aggregate Mortars

Kayle Karla Mei Mamitag Gorospe
University of Windsor

Follow this and additional works at: <https://scholar.uwindsor.ca/etd>

Recommended Citation

Gorospe, Kayle Karla Mei Mamitag, "Properties of Glass Aggregate Mortars" (2019). *Electronic Theses and Dissertations*. 7703.

<https://scholar.uwindsor.ca/etd/7703>

This online database contains the full-text of PhD dissertations and Masters' theses of University of Windsor students from 1954 forward. These documents are made available for personal study and research purposes only, in accordance with the Canadian Copyright Act and the Creative Commons license—CC BY-NC-ND (Attribution, Non-Commercial, No Derivative Works). Under this license, works must always be attributed to the copyright holder (original author), cannot be used for any commercial purposes, and may not be altered. Any other use would require the permission of the copyright holder. Students may inquire about withdrawing their dissertation and/or thesis from this database. For additional inquiries, please contact the repository administrator via email (scholarship@uwindsor.ca) or by telephone at 519-253-3000ext. 3208.

Properties of Glass Aggregate Mortars

By

Kayle Karla Mei Mamitag Gorospe

A Thesis
Submitted to the Faculty of Graduate Studies
through the Department of Civil and Environmental Engineering
in Partial Fulfillment of the Requirements for
the Degree of Master of Applied Science
at the University of Windsor

Windsor, Ontario, Canada

2019

© 2019 Karla Gorospe

Properties of Glass Aggregate Mortars

By

Kayle Karla Mei Mamitag Gorospe

APPROVED BY:

J. Sokolowski
Department of Mechanical, Automotive & Materials Engineering

T. Bolisetti
Department of Civil and Environmental Engineering

S. Das, Advisor
Department of Civil and Environmental Engineering

April 4, 2019

DECLARATION OF CO-AUTHORSHIP / PREVIOUS PUBLICATION

I. Co-Authorship

I hereby declare that this thesis incorporates material that is the result of joint research. Chapters 2, 3, and 4 of this thesis were co-authored with Mr. Emad Booya, and Dr. Hossein Ghaednia, under the supervision of Dr. Sreekanta Das. In all cases, the key ideas, primary contributions, experimental designs, data analysis, interpretation, and writing were performed by the author, and the contribution of co-authors was primarily through the provision of feedback on refinement of ideas, editing of the manuscript, and assistance with experimental testing.

I am aware of the University of Windsor Senate Policy on Authorship and I certify that I have properly acknowledged the contribution of other researchers to my thesis, and have obtained written permission from each of the co-author(s) to include the above material(s) in my thesis.

I certify that, with the above qualification, this thesis, and the research to which it refers, is the product of my own work.

II. Previous Publication

This thesis includes three (3) original papers that have been previously published/submitted for publication in peer reviewed journals, as follows:

Thesis Chapter	Publication title/full citation	Publication status
Chapter 2	Gorospe, K., Booya, E., Ghaednia, H., & Das, S. (2019). Effect of Various Glass Aggregates on the Shrinkage and Expansion of Cement Mortar. <i>Construction and Building Materials</i> , 210, 301 –311.	Published
Chapter 3	Gorospe, K., Booya, E., Ghaednia, H., & Das, S. Strength, Durability, and Thermal Properties of Glass Aggregate Mortars. <i>Materials in Civil Engineering</i> .	Accepted
Chapter 4	Gorospe, K., Booya, E., & Das, S. Durability of Glass Aggregate Mortars Containing Supplementary Cementitious Materials. <i>Building Engineering</i> .	Submitted

I certify that I have obtained a written permission from the copyright owner(s) to include the above published material(s) in my thesis. I certify that the above material describes work completed during my registration as a graduate student at the University of Windsor.

III. General

I declare that, to the best of my knowledge, my thesis does not infringe upon anyone's copyright nor violate any proprietary rights and that any ideas, techniques, quotations, or any other material from the work of other people included in my thesis, published or otherwise, are fully acknowledged in accordance with the standard referencing practices. Furthermore, to the extent that I have included copyrighted material that surpasses the bounds of fair dealing within the meaning of the Canada Copyright Act, I certify that I have obtained a written permission from the copyright owner(s) to include such material(s) in my thesis.

I declare that this is a true copy of my thesis, including any final revisions, as approved by my thesis committee and the Graduate Studies office, and that this thesis has not been submitted for a higher degree to any other University or Institution.

ABSTRACT

Glass as aggregates in cement mortars not only improves the sustainability of the material, but also promotes waste management. In addition, the inclusion of supplementary cementitious materials (SCMs) further enhances material properties and sustainability. The mechanical performance of glass aggregate mortars was evaluated by means of compressive strength, whereas durability was assessed through alkali silica reaction, water immersion absorption and sorptivity, chloride ion permeations, and plastic and drying shrinkage. Investigations into the thermal properties of glass aggregate mortars were also completed. Glass aggregates were found to reduce compressive strength; however, binary and ternary blends of SCMs can offset the reduction in strength associated with the glass addition. Furthermore, glass aggregates are effective in improving chloride ion permeability, absorption, sorptivity, and shrinkage due to their inherently low absorption capacity. SCMs further improve the durability properties by enhancing the microstructural properties of the cementitious matrix. Moreover, SCMs are required to reduce detrimental ASR expansions to acceptable levels. Glass aggregate mortars also show promising thermal insulation performance.

To Dad, Mom, and Dr. Das

ACKNOWLEDGEMENTS

First, I would like to thank my supervisor, Dr. Sreekanta Das, for encouraging me to pursue a master's degree and for his unwavering support and guidance throughout the entire journey. I am also very grateful for the many opportunities and challenges that he has presented me (though often not related to this thesis), which have facilitated the furtherance and expansion of my knowledge and practical experience in civil engineering. I would also like to acknowledge my committee members, Dr. Jerry Sokolowski and Dr. Tirupati Boliseti, for their time and effort in reviewing this thesis. Furthermore, I would like to acknowledge the Natural Sciences and Engineering Research Council of Canada (NSERC) and the University of Windsor for providing financial support.

My thanks and gratitude are also extended to Mr. Matt St. Louis and Mr. Jerome Finnerty for their time and assistance in the laboratory. Further, I would like to thank Ms. Sharon Lackie from the Great Lakes Institute for Environmental Research (GLIER) for her assistance with the SEM and EDS analyses.

My sincere appreciations also go out to Dr. Hossein (Hanif) Ghaednia for mentoring me throughout my graduate studies. Moreover, I would like to thank Mr. Emad Booya and Mr. Adeyemi Adesina for all their input and suggestions, and for sharing their knowledge and passion for concrete materials.

To my friends and colleagues: Amirreza Bastani, Babak Hajimohammadi, Behrouz Chegeni, Brodie Van Boxtel, Eric Hughes, Boluwatife Sobanke, Iyinoluwa Stephen, Jamshid Zohreh Heydariha, Jeeric Penales, John Bressan, Jothiarun Dhanapal, Navjot Singh, Rania Toufeili, Sachith Jayasuriya, and Soham Mitra – thank you for your assistance

in the lab and for your constant support and encouragement. You have made this experience much more enjoyable.

Lastly, I would like to express my deepest gratitude to my parents, Jerry and Raquel Gorospe, and my sisters, Karen and Kathleen, for their constant outpour of love and support. Thank you for believing in me and for always reminding me to persevere through the challenges and finish what I have started.

TABLE OF CONTENTS

DECLARATION OF CO-AUTHORSHIP / PREVIOUS PUBLICATION	iii
ABSTRACT.....	vi
DEDICATION.....	vii
ACKNOWLEDGEMENTS.....	viii
LIST OF TABLES.....	xiii
LIST OF FIGURES	xiiiiv

CHAPTER 1: GENERAL INTRODUCTION

1.1. Introduction.....	1
1.2. Literature Review.....	2
1.2.1. Glass Aggregates.....	2
1.2.2. Supplementary Cementitious Materials	6
1.3. Objectives.....	8
1.4. Experimental Methodology.....	9
1.5. Organization of the Thesis	9
1.6. References.....	10

CHAPTER 2: EFFECT OF VARIOUS GLASS AGGREGATES ON THE SHRINKAGE AND EXPANSION OF CEMENT MORTAR

2.1. Introduction.....	14
2.2. Experimental Procedure	18
2.2.1. Materials.....	19
2.2.2. Mixture Proportioning and Casting.....	21
2.2.3. Test Methodology.....	23
2.2.3.1. Restrained Plastic Shrinkage	23
2.2.3.2. Drying Shrinkage.....	24
2.2.3.3. Alkali Silica Reaction (ASR).....	25
2.3. Results and Discussion.....	26

2.3.1. Flow	26
2.3.2. Compressive Strength.....	27
2.3.3. Plastic Shrinkage	28
2.3.4. Drying Shrinkage.....	32
2.3.5. Alkali Silica Reaction.....	38
2.4. Conclusions.....	44
2.5. Acknowledgements	45
2.6. References	45

CHAPTER 3: STRENGTH, DURABILITY, AND THERMAL PROPERTIES OF GLASS AGGREGATE MORTARS

3.1. Introduction	49
3.2. Experimental Procedure	53
3.2.1. Materials	54
3.2.2. Mixture Proportioning and Casting	55
3.2.3. Test Methodology.....	57
3.2.3.1. Compressive Strength	57
3.2.3.2. Plastic Shrinkage.....	57
3.2.3.3. Absorption	59
3.2.3.4. Rapid Chloride Permeability	59
3.2.3.5. Thermal Conductivity	59
3.3. Results and Discussion.....	60
3.3.1. Compressive Strength.....	60
3.3.2. Plastic Shrinkage	64
3.3.3. Absorption	68
3.3.4. Rapid Chloride Permeability	69
3.3.5. Thermal Conductivity.....	71
3.4. Conclusions	73
3.5. Acknowledgements	75
3.6. References	75

CHAPTER 4: DURABILITY OF GLASS AGGREGATE MORTARS CONTAINING SUPPLEMENTARY CEMENTITIOUS MATERIALS

4.1. Introduction	80
4.2. Experimental Procedure	83
4.2.1. Materials	83
4.2.2. Mixture Proportioning	84
4.2.3. Test Methodology	87
4.2.3.1. Compressive Strength	87
4.2.3.2. Alkali Silica Reaction	87
4.2.3.3. Chloride Permeability	87
4.2.3.4. Sorptivity	88
4.3. Results and Discussion.....	89
4.3.1 Compressive Strength.....	89
4.3.2. Alkali Silica Reaction.....	93
4.3.3. Chloride Permeability.....	96
4.3.4. Sorptivity	100
4.3.5. Optimization.....	103
4.4. Conclusions.....	108
4.5. Acknowledgements	109
4.6. References	109
 CHAPTER 5: CONCLUSIONS AND RECOMMENDATIONS	
5.1. Mechanical Properties	113
5.2. Durability Properties	113
5.3. Thermal Properties	114
VITA AUCTORIS	115

LIST OF TABLES

CHAPTER 1

Table 1.1. Properties of sand and waste glass.....	3
--	---

CHAPTER 2

Table 2.1. Chemical composition of materials (%)	21
--	----

Table 2.2. Mass proportions of mortar mixtures.....	22
---	----

Table 2.3. Mortar flowability.....	27
------------------------------------	----

Table 2.4. EDS point analysis.....	43
------------------------------------	----

CHAPTER 3

Table 3.1. Chemical composition of materials (%)	55
--	----

Table 3.2. Mass proportions of mortar mixtures.....	56
---	----

CHAPTER 4

Table 4.1. Chemical composition of cementitious materials (%).....	84
--	----

Table 4.2. Mass proportions of mortar mixtures.....	86
---	----

Table 4.3. Statistical models of glass aggregate mortar properties.....	104
---	-----

Table 4.4. Optimization Criteria	105
--	-----

LIST OF FIGURES

CHAPTER 1

Figure 1.1. ASR mechanism	4
Figure 1.2. Classification of SCMs.....	7
Figure 1.3. Chemical composition of common SCMs.....	8

CHAPTER 2

Figure 2.1. Glass particles used in mortar.....	20
Figure 2.2. Schematic of the environmental test chamber	24
Figure 2.3. Plastic shrinkage specimen.....	25
Figure 2.4. 28-day compressive strength of glass aggregate mortars	30
Figure 2.5. Total crack area due to plastic shrinkage	31
Figure 2.6. Overlay cracks after 4 hours of testing.....	32
Figure 2.7. Development of drying shrinkage	34
Figure 2.8. Weight loss and shrinkage relation.....	36
Figure 2.9. ASR expansion of glass aggregate mortar.....	41
Figure 2.10. Deteriorated CG specimen immersed in NaOH solution for 14 days	43
Figure 2.11. EDS mapping of 14-day MG specimen exposed to NaOH solution	43

CHAPTER 3

Figure 3.1. Crushed glass aggregates.....	54
Figure 3.2. Glass bead aggregates.....	54
Figure 3.3. Plastic shrinkage restrain element with hemispherical protrusions.....	58
Figure 3.4. Setup of plastic shrinkage environmental test chamber	58
Figure 3.5. Testing procedure for thermal conductivity	60
Figure 3.6. Compressive strength of glass aggregate mortar at 20°C curing condition ...	61
Figure 3.7. Compressive strength of glass aggregate mortar at 50°C curing condition ...	63

Figure 3.8. Ettringite formation in MG specimen after 365 days of 50°C curing	64
Figure 3.9. Crack area and crack width analysis using ImageJ software	65
Figure 3.10. Development of plastic shrinkage cracks	66
Figure 3.11. Propagation of cracks in control specimen.....	67
Figure 3.12. Total plastic shrinkage crack area and maximum crack width.....	67
Figure 3.13. Plastic shrinkage crack patterns.....	68
Figure 3.14. 24-hour immersion absorption of glass aggregate mortars.....	69
Figure 3.15. RCPT of glass aggregate mortars	71
Figure 3.16. Thermal conductivity of glass aggregate mortars	73
CHAPTER 4	
Figure 4.1. Compressive strength	92
Figure 4.2. 14-day ASR expansion.....	95
Figure 4.3. Chloride permeability.....	99
Figure 4.4. Sorptivity	102
Figure 4.5. Desirability of mixtures containing FA	106
Figure 4.6. Desirability of mixtures containing SG.....	107

CHAPTER 1

GENERAL INTRODUCTION

1.1. Introduction

In recent years, there have been global initiatives towards the development of sustainable and environmentally-friendly building materials. This particularly applies to cementitious materials. First and foremost, the production of cement, which is the main binder used in concrete and mortar, produces significantly high carbon dioxide (CO₂) emissions. In fact, cement production is the third-largest source of anthropogenic CO₂ emissions after fossil fuels and land-use change [1]. Furthermore, the mining and transportation of natural aggregates also adds to the list of environmental impacts associated with the production of concrete and cement mortars. In order to enhance the sustainability of concrete and cement mortars, alternative binders and/or aggregates should be explored.

CO₂ emissions caused by cement production can be reduced by using supplementary cementitious materials (SCMs) as partial cement replacement. SCMs can either be obtained naturally or from waste by-products of various processes. Most SCMs do not possess any cementitious properties; however, some of these materials can react with Portland cement to form cementitious compounds [2]. Some of the commonly used SCMs are fly ash, slag, silica fume, and metakaolin.

Substituting natural aggregates with recycled aggregates can improve the sustainability of cementitious materials. In addition, the use of recycled aggregates also aids in waste management. Demolished concrete structures as well as recycled and

landfilled glass are examples of recycled aggregate sources. In this thesis, natural aggregate replacement with glass was established as the primary focus. However, SCMs were also incorporated to enhance mortar properties and to further improve sustainability.

1.2. Literature Review

1.2.1. Glass Aggregates

Glass is often considered a resource efficient material due to the abundance of the natural material it originates from. Glass is fully recyclable, which is one of its great benefits; however, millions of tonnes of glass, primarily in the form of bottles and jars, end up in landfills each year. It has been reported that in the United States alone, approximately 6.4 million tonnes of glass were landfilled in 2015 [3]. In Canada, complete data on the disposal of glass, specifically, is not available; however, Statistics Canada reports that of the 9.3 million tonnes of waste diverted in 2016, 4% is glass material [4]. On the other hand, the Essex-Windsor Solid Waste Authority reported that 3700 tonnes of glass, which comprises 70% of the glass disposed in the region, ended up in landfills in 2010 [5].

Although programs to improve glass recycling have been implemented globally, economic constraints, such as transportation costs, have hindered the progress of glass recycling and have resulted in the disposal of glass materials into landfills. Glass breaking during transit to recycling plants and concerns regarding contamination in the glass are other reasons for its disposal into landfills. The resulting low waste diversion rate of refuse glass therefore signifies the need for better waste management. Consequently, this concern has prompted much research into the repurposing of waste glass as a component of cementitious materials. The use of local glass as aggregates in concrete and cement mortar

can reduce production costs associated with the quarrying and transporting of natural aggregates. Moreover, the physical properties of glass itself can improve concrete properties. A comparison of the physical properties of sand and waste glass is presented in Table 1.1.

Table 1.1. Properties of sand and waste glass [6]

Properties	Sand	Waste glass
Specific gravity	2.57	2.19
Density (kg/m ³)	1688	1672
Absorption (%)	2.71	0.39
Pozzolanic index (%)	-	80

The use of glass as aggregates in concrete and mortar have been studied for the last 50 years. Nonetheless, earlier researches were focused on bituminous concrete for roads. Such studies were done by Foster [7], and Malisch et al. [8] in the 1970s. Studies on cement concrete and mortar containing glass aggregates were present in the 1970s and 1980s, but this research area did not expand until the 1990s and early 2000s. Most of the earlier studies in glass aggregate concrete and mortar focused on mechanical strength and expansion due to alkali silica reaction (ASR). These properties are still investigated in current studies; however, much attention has been given to the latter.

Many studies on the mechanical properties of glass aggregate concrete and mortar have been documented. Park et al. [9], Jin et al. [10], and Polley et al. [11] are some of the researchers who have completed comprehensive investigations on the fundamental mechanical properties of glass aggregate concrete and mortar. In general, compressive strength, tensile strength, and flexural strength is reduced when glass aggregates are used. The reduction in strength is linked to the weak bonding between the glass aggregates and

the cement matrix [10–12]. The high brittleness and low resistance to fracturing of glass aggregates have been reported as sources of strength reduction [13,14]. Microcracks within the glass aggregates have also been found to reduce strength [15,16]. The formation of these microcracks are often linked to the preparation of the aggregates (i.e. manual grinding).

The durability of glass aggregate concrete and mortar is often threatened by alkali silica reaction (ASR), which is a phenomenon that typically occurs when siliceous aggregates, such as glass, are used in cementitious materials (Figure 1.1). Alkalis (i.e. potassium (K^+) and sodium (Na^+)) in the pore solution form weak bonds with available hydroxide ions (OH^-). The dissolution of the alkali hydroxides produces free ions, which increase the pH of the cementitious material and causes a reaction with the silicon dioxide (SiO_2) in the glass aggregates. A hygroscopic silicate gel, composing of Na, K, Si, and Ca, is formed from the reaction. In the presence of moisture, the gels expand, and such expansion can cause cracking or the propagation of existing cracks in the material.

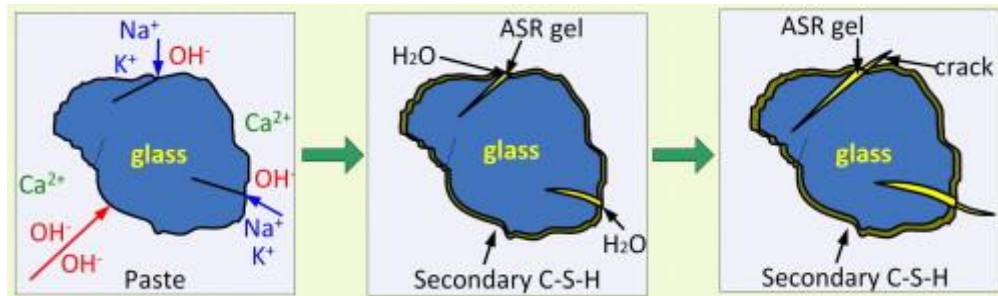


Figure 1.1. ASR mechanism [17]

Contrasting reports can be found in literature regarding ASR expansion of glass aggregate concrete and mortar. Some studies claim that glass aggregates cause deleterious ASR expansions, whereas others report acceptable levels of expansion [12,18,19,16]. In

summarizing the various results on ASR, it is concluded that the level of expansion is dependent on the size of the glass particles used. Specifically, glass aggregates of finer particle size results in lower expansions. In fact, some researchers have found that fine glass aggregates exhibit pozzolanic properties [20,21]. Studies also suggest that finer particles of glass aggregates minimize induced swelling pressures, reduces the stress intensity factor that causes expansion, and increases the volume of the interfacial transition zone (ITZ), providing porous space for expansion to freely occur without detrimental effects [22–24]. Nonetheless, more recent studies propose that ASR occurs only within intraparticle cracks in the glass [16,25].

Other durability properties such as water immersion absorption and sorptivity, chloride ion permeations, carbon resistance, and sulphate attack have all been investigated in literature. General findings agree that glass aggregates are effective in improving these properties [13,15,26]. Moreover, drying shrinkage of glass aggregate mortars, which is a qualitative assessment of durability, have also been studied and results show that glass aggregates reduce shrinkage strains [13].

Although research on glass aggregate concrete and mortar has spanned many decades, there are still some gaps in the literature. In particular, further research is needed to assess the durability of mature concrete and mortar. There is also no known literature on the plastic shrinkage of concrete and mortar consisting of glass aggregates. This property should be examined as the formation of early-age cracks can adversely affect durability and serviceability. Further, the thermal properties of glass aggregate concrete and mortar have rarely been investigated. Glass itself has excellent thermal properties, so there is great potential for the improvement of insulation properties of concrete and mortar.

1.2.2. Supplementary Cementitious Materials

In 2016, it was estimated that the global production of cement generated 2.2 Gt of CO₂ and it is expected that the level of cement production will resume growth in the coming years [27]. Hence, there is a need for viable alternatives to cement. One such alternative is supplementary cementitious materials (SCMs). Most concrete structures today consist of SCMs as partial cement replacement due to its advantageous properties and environmental benefit. SCMs envelope many types of materials that vary in origin, chemical and mineralogical composition, and particle characteristics [28]. Some common synthetic SCMs include fly ash, slag, and silica fume. These SCMs are derived from waste by-products of coal, steel, and silicon metal and ferrosilicon alloy plants, respectively. SCMs can also be obtained naturally. Examples of natural SCMs include, volcanic ash, calcined shale or clay, and metakaolin. Figure 1.2. outlines a general classification scheme of SCMs, while Figure 1.3. presents the chemical composition of common SCMs.

In general, SCMs improve the consistency and workability of concrete and mortar by increasing the volume of fines in the mixture. However, greater volumes of fine particles reduce bleeding rates, which can cause plastic shrinkage cracks [2]. SCMs enhance the microstructure of the cementitious matrix through pore-size refinement, matrix densification, and interfacial transition zone refinement [29–31]. These enhancements in the microstructure typically improves strength and permeability properties. Nonetheless, studies have also shown that the reactivity of SCMs can affect concrete properties. For example, the slow reaction rate of fly ash results in lower early-age compressive strength, whereas the high hydration activity of slag results in higher early-age compressive strength [32,33]. In addition, the chemical composition of SCMs greatly influences the performance

and behaviour of concrete and mortar. Specifically, SCMs with higher compositions of SiO_2 are very effective in mitigating expansions associated with ASR [34].

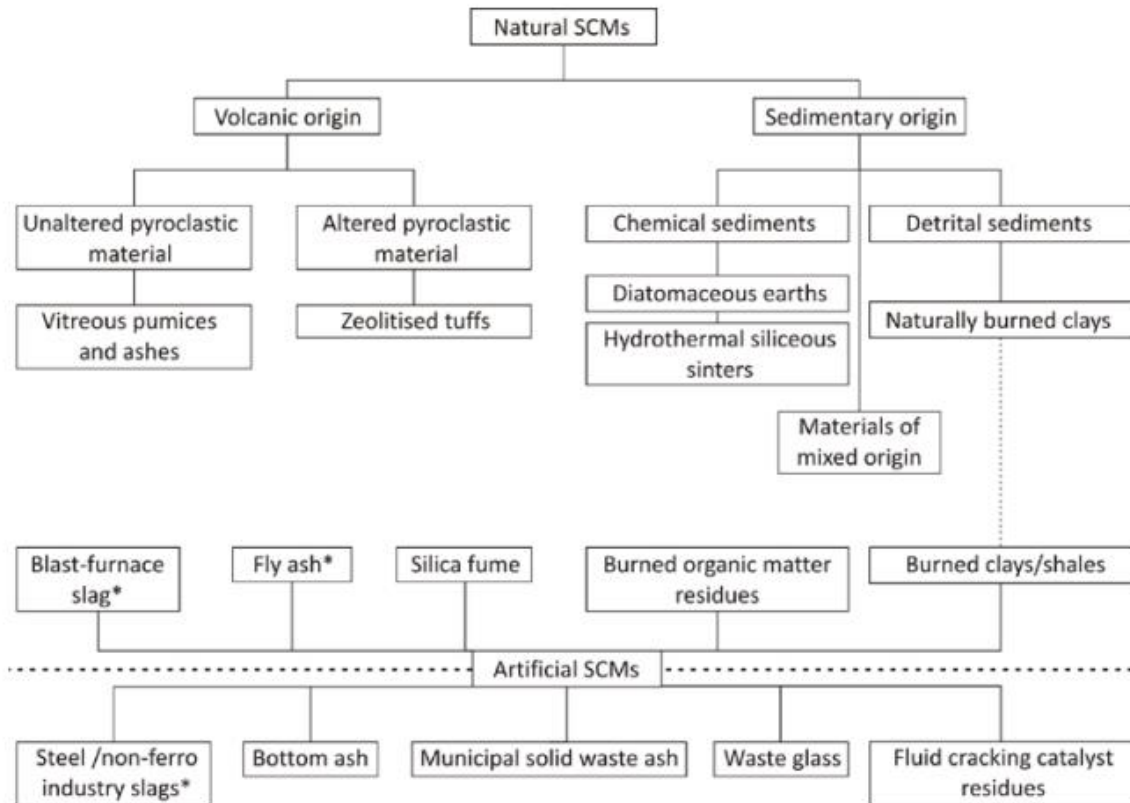


Figure 1.2. Classification of SCMs [28]

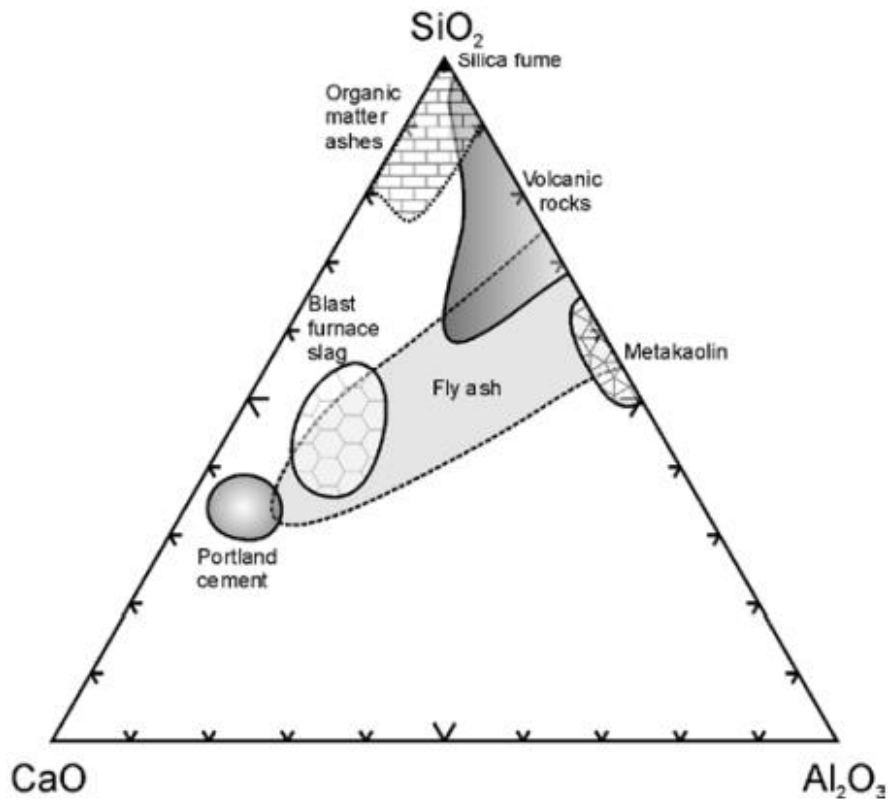


Figure 1.3. Chemical composition of common SCMs [28]

1.3. Objectives

The purpose of this thesis is to study the applicability of glass aggregates as a sustainable and environmentally-friendly alternative to natural aggregates in cement mortars. The influence of binary and ternary cementitious blends was also examined. The suitability of glass aggregate mortars was evaluated in terms of mechanical, durability, and thermal performance. This thesis also aimed to fill gaps in literature, specifically regarding plastic shrinkage.

1.4. Experimental Methodology

The objectives of this thesis were achieved through experimental investigations. Three types of glass aggregates – crushed glass, glass beads, and expanded glass – were used in the production of the mortar mixtures. Supplementary cementitious materials (SCMs) were also incorporated in binary and ternary systems as partial cement replacement. The SCMs used include fly ash, slag, silica fume, and metakaolin. The mechanical properties of glass aggregate mortars were evaluated by means of compressive strength testing, whereas durability was assessed through alkali silica reaction (ASR), chloride permeability, water immersion absorption, sorptivity, plastic shrinkage, and drying shrinkage. Thermal conductivity was also examined. Specific experimental procedures, namely the mixture design and test methodologies, are presented in detail within Chapters 2, 3, and 4.

1.5. Organization of the Thesis

This thesis is written in manuscript format and is divided into five chapters as follows:

1. Chapter 1, which is entitled “General Introduction,” presents an overview of the thesis topic and the literature review. The objectives of the study and the test methodologies undertaken are also discussed in this chapter.
2. Chapter 2 is entitled “Effect of Various Glass Aggregates on the Shrinkage and Expansion of Cement Mortar.” This chapter studies the influence of crushed glass, glass beads, and expanded glass on volumetric changes of cement mortars. Specifically,

- plastic and drying shrinkage, and alkali silica reaction (ASR) expansion were examined.
3. Chapter 3 is entitled “Strength, Durability, and Thermal Properties of Glass Aggregate Mortars.” The study presented in this chapter shows the applicability of mixed glass aggregates for building and construction materials through the testing of compressive strength, plastic shrinkage, water immersion absorption, and rapid chloride permeability.
 4. Chapter 4 is entitled “Durability of Glass Aggregate Mortars Containing Supplementary Cementitious Materials.” This chapter focuses on the effects of using supplementary cementitious materials as partial replacement of cement in glass aggregate mortars. Compressive strength, ASR, chloride permeability, and sorptivity was investigated.
 5. Chapter 5, which is entitled “Conclusions and Recommendations,” draws conclusions from the studies undertaken and provides recommendations for future work.

1.6. References

- [1] R.M. Andrew, Global CO₂ emissions from cement production, 1928-2017, *Earth System Science Data*. 10 (2018) 2213–2239.
- [2] National Ready Mixed Concrete Association (NRMCA), CIP 30 - Supplementary Cementitious Materials. <https://www.nrmca.org/aboutconcrete/cips/30p.pdf>, 2000.
- [3] United States Environmental Protection Agency (USEPA), Facts and Figures about Materials, Waste and Recycling - Glass: Material-Specific Data. <https://www.epa.gov/facts-and-figures-about-materials-waste-and-recycling/glass-material-specific-data>, 2018 (accessed 20 February 2019).
- [4] Statistics Canada, Materials diverted, by type, <https://www150.statcan.gc.ca/t1/tb11/en/tv.action?pid=3810003401>, n.d. (accessed 3 March 2019).

- [5] exp. Services Inc., Essex Windsor Solid Waste Authority: Waste Recycling Strategy. (2011).
- [6] Z.Z. Ismail, E.A. AL-Hashmi, Recycling of waste glass as a partial replacement for fine aggregate in concrete, *Waste Management*. 29 (2009) 655–659.
- [7] C.W. Foster, Use of waste glass as asphaltic concrete aggregate, *Masters Theses*. 7187 (1970).
- [8] W.R. Malisch, D.E. Day, B.G. Wixson, Use of domestic waste glass as aggregate in bituminous concrete, *Highway Research Board*. (1970) 1–10.
- [9] S.B. Park, B.C. Lee, J.H. Kim, Studies on mechanical properties of concrete containing waste glass aggregate, *Cement and Concrete Research*. 34 (2004) 2181–2189.
- [10] W. Jin, C. Meyer, S. Baxter, “Glascrete” - concrete with glass aggregate, *ACI Structural Journal*. 97 (2000) 208–213.
- [11] C. Polley, S.M. Cramer, R.V. de la Cruz, Potential for using waste glass in portland cement concrete, *Journal of Materials in Civil Engineering*. 10 (2002) 210–219.
- [12] T.C. Ling, C.S. Poon, A comparative study on the feasible use of recycled beverage and CRT funnel glass as fine aggregate in cement mortar, *Journal of Cleaner Production*. 29–30 (2012) 46–52.
- [13] J.R. Wright, C. Cartwright, D. Fura, F. Rajabipour, Fresh and hardened properties of concrete incorporating recycled glass as 100% sand replacement, *Journal of Materials in Civil Engineering*. 26 (2014) 4014073.
- [14] N. Almesfer, J. Ingham, Effect of waste glass on the properties of concrete, *Journal of Materials in Civil Engineering*. 26 (2014) 6014022.
- [15] K.H. Tan, H. Du, Use of waste glass as sand in mortar: Part I - Fresh, mechanical and durability properties, *Cement and Concrete Composites*. 35 (2013) 118–126.
- [16] F. Rajabipour, H. Maraghechi, G. Fischer, Investigating the alkali-silica reaction of recycled glass aggregates in concrete materials, *Journal of Materials in Civil Engineering*. 22 (2010) 1201–1208.
- [17] H. Du, K.H. Tan, Effect of particle size on alkali-silica reaction in recycled glass mortars, *Construction and Building Materials*. 66 (2014) 275–285.
- [18] İ.B. Topçu, M. Canbaz, Properties of concrete containing waste glass, *Cement and Concrete Research*. 34 (2004) 267–274.

- [19] R. Idir, M. Cyr, A. Tagnit-Hamou, Use of fine glass as ASR inhibitor in glass aggregate mortars, *Construction and Building Materials*. 24 (2010) 1309–1312.
- [20] M. Kamali, A. Ghahremaninezhad, Effect of glass powders on the mechanical and durability properties of cementitious materials, *Construction and Building Materials*. 98 (2015) 407–416.
- [21] K. Afshinnia, P.R. Rangaraju, Mitigating alkali-silica reaction in concrete: Effectiveness of ground glass powder from recycled glass, *Transportation Research Record Journal of the Transportation Research Board*. 2508 (2015) 65–72.
- [22] Z.P. Bazant, A. Steffens, Mathematical model for kinetics of alkali-silica reaction in concrete, *Cement and Concrete Research*. 30 (2000) 419–428.
- [23] Z.P. Bazant, Z. Goanfseup, M. Christian, Fracture mechanics of ASR in concretes with waste glass particles of different sizes, *Journal of Engineering Mechanics*. 126 (2000) 226–232.
- [24] A. Suwito, W. Jin, Y. Xi, C. Meyer, A mathematical model for the pessimum size effect of ASR in concrete, *Concrete Science and Engineering*. 4 (2002) 23–34.
- [25] H. Du, K.H. Tan, Use of waste glass as sand in mortar: Part II - Alkali-silica reaction and mitigation methods, *Cement and Concrete Composites*. 35 (2013) 109–117.
- [26] S. De Castro, J. De Brito, Evaluation of the durability of concrete made with crushed glass aggregates, *Journal of Cleaner Production*. 41 (2013) 7–14.
- [27] International Energy Agency (IEA), *Cement: Tracking Clean Energy Progress*. <https://www.iea.org/tcep/industry/cement/>, 2019 (accessed 3 March 2019).
- [28] R. Snellings, G. Mertens, J. Elsen, Supplementary cementitious materials, *Reviews in Mineralogy and Geochemistry*. 74 (2012) 211–278.
- [29] R. Siddique, Utilization of silica fume in concrete: Review of hardened properties, *Resources, Conservation and Recycling*. 55 (2011) 923–932.
- [30] M. Sharfuddin Ahmed, O. Kayali, W. Anderson, Chloride penetration in binary and ternary blended cement concretes as measured by two different rapid methods, *Cement and Concrete Composites*. 30 (2008) 576–582.
- [31] P. Dinakar, K.G. Babu, M. Santhanam, Durability properties of high volume fly ash self compacting concretes, *Cement and Concrete Composites*. 30 (2008) 880–886.
- [32] R.O. Lane, J.F. Best, Properties and use of fly ash in portland cement concrete, *Concrete International*. 4 (1982) 81–92.

- [33] M.F. Bazhuni, M. Kamali, A. Ghahremaninezhad, An investigation into the properties of ternary and binary cement pastes containing glass powder, *Frontiers of Structural and Civil Engineering*. (2018) 1–10.
- [34] M. Thomas, The effect of supplementary cementing materials on alkali-silica reaction: A review, *Cement and Concrete Research*. 41 (2011) 1224–1231.

CHAPTER 2

EFFECT OF VARIOUS GLASS AGGREGATES ON THE SHRINKAGE AND EXPANSION OF CEMENT MORTAR

2.1. Introduction

Glass is a versatile material and it is utilized in many building applications including claddings in facades, curtain and partition walls, and most notably building fenestrations. Though glass as a construction material is fairly dated, the development of durable concrete composed of recycled glass particles is currently being explored with the endeavours of alleviating the growing waste problem encountered by many landfills today. Over the years, glass as a substitute to fine aggregates, coarse aggregates, or even cement in concrete has been much researched as efforts in waste management have expanded [1–5]. Consumer products such as beverage containers, television screens, and computer monitors are a few of the sources for glass aggregates that have previously been used in the investigation of such concrete composites.

Preparation of post-consumer glass for use as aggregate or cementitious material in concrete is as simple as crushing it to the desired size. This method of preparation is commonly employed by many researchers who obtain glass materials directly from local recycling plants. Post-consumer glass can also be further processed to create new products such as expanded glass, a material that can be used in lightweight concrete. Typically, these products are commercially available for purchase.

The use of recycled glass in concrete is not only a sustainable solution, but has also been proven to be feasible [6,7]. Nonetheless, there are properties of glass aggregate

concrete, such as alkali silica reaction (ASR) expansion, that require further investigation as some discrepancies in results have been reported. The main reasons for the inconsistencies in the findings can be attributed to the presence of impurities in the recycled glass, the colour of the glass, and the preparation of the glass aggregates used in these studies. Assorted coloured glass varies in chemical composition as different metal oxides are added during the glass production stage. The colour of glass has been reported to have an observable effect on the durability of concrete. On the other hand, preparation of glass aggregates by manual crushing has led to micro-cracks for certain types and/or colours of glass, thus affecting durability and mechanical properties as well [8,9].

Early research in glass aggregate concrete was mainly focused on mechanical properties such as compressive strength, modulus of elasticity, and splitting tensile strength. In general, regardless of the type, incorporating glass particles in concrete results in a reduction in mechanical strength as replacement amount increases. The primary cause of the reduction in mechanical properties was determined to be weak bonding at the interfacial region between the glass particles and the cement matrix [10–12]. However, Taha and Nounu [3] found insignificant differences in strength between control specimen containing 0% waste glass and specimens containing 50% and 100% waste glass. Nevertheless, a study conducted by Mardani-Aghabaglou et al. [11] suggests that the mechanical properties are acceptable up to 60% replacement of fine glass aggregates with particle sizes ranging from 0 to 4 mm.

In recent years, studies on the durability of glass aggregate concrete have expanded [6,11]. Several studies on durability have indicated some concerns of potentially deleterious expansion triggered by ASR between the alkaline cement and the silica-rich

glass particles; however, there has been contrasting reports. Specifically, Topçu and Canbaz [7] found that specimens containing coarse waste glass aggregates ranging from 4 to 16 mm in size results in lower expansions compared to control specimens containing 0% waste glass. Specimens containing 100% waste glass were observed to have the lowest expansion. On the other hand, Ling and Poon [5] reported that glass particles less than 5 mm in size result in greater expansion compared to specimens containing no glass aggregates. The study also showed higher ASR expansion with increasing glass content. Furthermore, Tan and Du [8,13] studied the effects of different coloured glass aggregates from recycled soda-lime bottles prepared by manual crushing. In the study, it was observed that increasing the amount of brown, green, and mixed coloured glass reduces expansion. This trend was found to be opposite for specimens containing clear glass. The study then concluded that the primary cause of the conflicting results was not the colour of the glass, rather the manufacturing process of the glass bottles used, which influences the degree of micro-cracking sustained after crushing. This inference corroborates the findings of Rajabipour et al. [9] and Shayan and Xu [1] as intraparticle cracks in the glass particles were identified as a major instigator of unwarranted ASR expansions.

The addition of fibres, lithium compounds, and pozzolans such as fly ash and silica fumes, have been employed to control excessive ASR expansions [3,14]. Binary and ternary mixtures of supplementary cementitious materials containing finely ground glass has also been found to mitigate expansion due to ASR [15]. According to Schwarz et al. [16] fine glass powder is effective in reducing detrimental ASR expansion though fly ash is much more effective. Furthermore, glass particles finer than 50 μm have been reported to exhibit pozzolanic properties, which can reduce ASR expansion [17,18]. Hence,

expansion is reduced as glass aggregate particle size becomes finer. Nonetheless, many studies have reported particle size ranges in which detrimental expansion does not occur. In particular, Jin et al. [19] found that ASR can be avoided by grinding glass to pass sieve No. 50 (300 μm). However, Idir et al. [20] found that glass aggregates smaller than 1000 μm does not cause any detrimental expansion due to ASR, thereby concluding that it is not necessary to use glass in the form of fines. Moreover, studies using expanded glass aggregates have established negligible ASR expansion because of the porosity of the particles [21,22].

Apart from deleterious expansions, cement-based materials are subject to volumetric contraction or shrinkage. Shrinkage in hardened concrete is referred to as drying shrinkage. Studies have shown that glass aggregates are effective in reducing long-term drying shrinkage of concrete due to its low absorption capacity [8]. Further, Wright et al. [10] suggests that the higher elastic modulus of glass aggregate concrete compared to normal concrete may be a reason for the reduction in drying shrinkage. Specifically, for 45% replacement of sand with glass aggregate, Kou and Poon [23] found an 18% decrease in drying shrinkage when compared to 0% glass aggregate. On the other hand, for porous aggregates like expanded glass, pre-wetting of the aggregates, prior to incorporating into the concrete mix, is typically done to compensate for the high water absorption of lightweight glass particles. Thus, the resulting effect of such preparation is an improved resistance to drying shrinkage [24,25]. Nonetheless, studies on the shrinkage behaviour of glass aggregate concrete is incomplete as early-age plastic shrinkage has not been reported. Plastic shrinkage is the volumetric contraction of freshly placed concrete. Cracking due to plastic shrinkage predominantly transpires because of rapid evaporation of free surface

water, though factors such as the fines content, water-cement ratio, and admixtures are known to influence such detrimental behaviour, which is a concern in the concrete industry [26].

The gap in literature concerning the effects of glass aggregates on early-age plastic shrinkage has prompted the current study as no known reports on plastic shrinkage of cement-based materials containing glass aggregates have been investigated. In addition, since the type and preparation of glass aggregates can influence ASR expansion, as evident in the contradicting reports on ASR, deleterious expansion was studied for the glass aggregates used. Furthermore, with many studies focussing on only one type of glass aggregate in concrete and cement mortar specimens, this study was aimed at broadening the field of study by evaluating the effectiveness of combining various types of glass aggregates, which has rarely been done. Thus, to provide a comprehensive study on the durability of glass aggregates, in terms of volumetric changes, the dimensional stability with respect to restrained plastic shrinkage, drying shrinkage, and ASR expansion were investigated to quantify the cracking resistance of glass aggregate mortar at an early-age and in the long-term. Flowability and compressive strength of glass aggregate mortar were also examined.

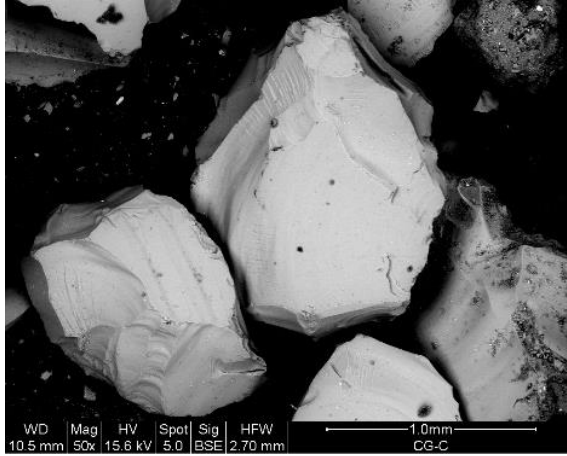
2.2. Experimental Procedure

This research was undertaken using an experimental method. Cement mortar containing different types of glass aggregates, namely, crushed glass, glass beads, and expanded glass, were used as a replacement of sand. Flowability, compressive strength,

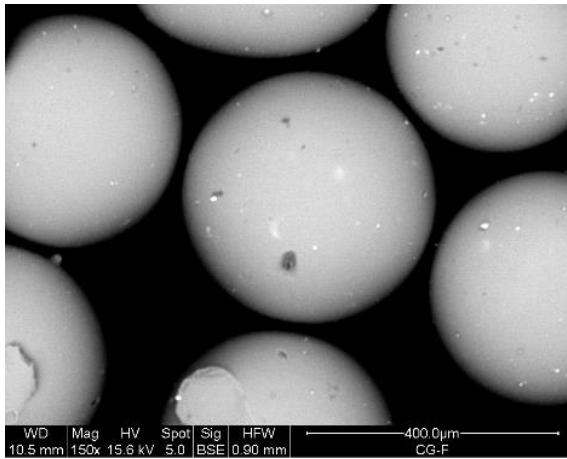
restrained plastic shrinkage, drying shrinkage, and ASR expansion of glass aggregate mortars were investigated.

2.2.1. Materials

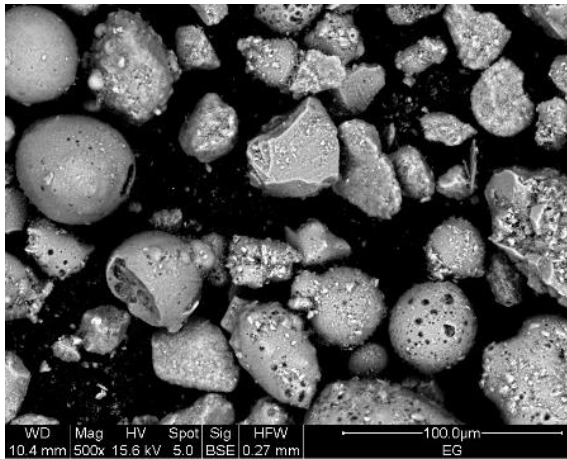
All mortar specimen were prepared using Type 10 general use Portland cement conforming to CSA A3001 [27] and natural sand aggregates with a fineness modulus of 2.63. Commercially purchased crushed glass, glass beads, and expanded glass with sizes ranging from 600 to 850 μm , 250 to 425 μm , and 40 to 125 μm , respectively were also used as fine aggregates (Figure 2.1). The densities of the crushed glass, glass beads, and expanded glass are 2499 kg/m^3 , 1249 kg/m^3 , and 530 kg/m^3 , respectively. As shown in Figure 2.1, the three types of glass aggregates differ in shape. These images were taken using scanning electron microscopy (SEM) at a magnification of 50x to 500x. The crushed glass [Figure 2.1(a)] consists of particles with irregular geometry, whereas the glass beads [Figure 2.1(b)] have consistent spherical shapes. On the other hand, the expanded glass [Figure 2.1(c)] has more variable features; the shapes of some particles are characteristically spherical, while other particles exhibit irregular geometry. Additionally, expanded glass particles contain multiple voids in its glass structure, which is expected from the manufacturing process. The chemical compositions of the materials are presented in Table 2.1.



(a)



(b)



(c)

Figure 2.1. Glass particles used in mortar: (a) crushed glass at 50x magnification (b) glass beads at 150x magnification (c) expanded glass at 500x magnification

Table 2.1. Chemical composition of materials (%)

Analyte Symbol	Cement	Sand	Crushed glass	Glass bead	Expanded glass
CaO	62.3	19.17	10.46	9.17	8.74
SiO ₂	18.2	46.65	70.88	71.55	68.59
Al ₂ O ₃	4.5	6.6	2.25	0.72	6.28
Fe ₂ O ₃ (T)	2.76	3.07	1.29	0.66	0.47
MnO	-	0.063	0.024	0.01	0.015
MgO	3.1	2.68	1.3	3.72	1.42
Na ₂ O	0.22	1.13	12.85	13.82	12.94
K ₂ O	0.45	1.24	0.64	0.13	0.43
SO ₃	3.47	-	-	-	-
TiO ₂	0.21	0.27	0.09	0.03	0.23
P ₂ O ₅	-	0.07	0.02	0.01	0.03
Co ₃ O ₄	-	< 0.005	< 0.005	< 0.005	< 0.005
CuO	-	0.006	0.023	< 0.005	0.016
NiO	-	< 0.003	< 0.003	< 0.003	0.003
Cr ₂ O ₃	-	< 0.01	0.08	0.01	0.05
V ₂ O ₅	-	0.007	< 0.003	< 0.003	0.004
LOI	4.8	16.43	-	-	-

2.2.2. Mixture Proportioning and Casting

The test matrix is shown in Table 2.2. The specimen names were chosen to indicate the main attributes of the test specimens. The first letter of the name corresponds to the type of glass aggregate substituted. Hence, CG refers to crushed glass, GB refers to glass bead, MG refers to mixed glass (mixture of crushed glass and glass bead), and EG refers to expanded glass. The following number indicates the percentage of sand replacement. For example, the specimen designation MG-30 indicates replacement of sand with mixed glass at 30%. Mortar mixtures were cast with a water/cement ratio of 0.5 and cement to fine aggregates ratio of 1:2 by mass. The composition of fine aggregates varied by type and amount of glass replacement. The first set of specimens, denoted as MG for mixed

glass, consists of crushed glass and glass beads at a ratio of 2:1, to keep the proportion of fine aggregates well-graded. MG specimens were studied at 30% and 50% replacement of natural sand. Specimens containing only crushed glass (CG), and only glass beads (GB), were also studied at 30% and 50% replacement to study how each glass type contributes to the behaviour of MG specimens. Expanded glass (EG) specimens were only examined at 5% and 10% replacement as increasing the amount of EG beyond 10% produced mixtures that were not workable. Superplasticizer was only added to EG specimens at a dosage of 2.5 mL/kg of cement to improve workability. In subsequent discussions, MG, CG, and GB specimens will be considered as Group 1 specimens, whereas EG specimens will be considered as Group 2 specimens.

Table 2.2. Mass proportions of mortar mixtures

Specimen Designation	Cement	Water	Fine aggregates			
			Sand	Crushed glass	Glass bead	Expanded glass
Control	1	0.5	2	-	-	-
MG-30	1	0.5	1.4	0.4	0.2	-
MG-50	1	0.5	1	0.67	0.33	-
CG-30	1	0.5	1.4	0.6	-	-
CG-50	1	0.5	1	1	-	-
GB-30	1	0.5	1.4	-	0.6	-
GB-50	1	0.5	1	-	1	-
EG-05	1	0.5	1.9	-	-	0.1
EG-10	1	0.5	1.8	-	-	0.2

Mortar mixtures were prepared using a set sequence and procedure to ensure the consistency of the produced specimens. Cement, sand, and glass aggregates were combined and mixed until the materials were well distributed. Water was slowly added to the dry materials and was mixed using a laboratory pan mixer for three minutes. For expanded

glass mixtures, superplasticizer was added to the water prior to combining with the dry materials. Mortar flow was then measured according to ASTM C1437 [28].

2.2.3. Test Methodology

2.2.3.1. Restrained Plastic Shrinkage

The setup and procedure for restrained plastic shrinkage were conducted in accordance with ASTM C1579 [29] using a modified method of the tests established by Banthia and Gupta [30], and Branston et al. [31]. The restrained plastic shrinkage test was performed in an environmental chamber (Figure 2.2) operating at a temperature of 40°C (\pm 2°C) and a relative humidity of 15% (\pm 3%) to accelerate the development of shrinkage cracks. A heater fan connected to a temperature and humidity controller was used to produce uniform airflow over the test specimens and to maintain the set environmental conditions. Furthermore, a plexiglass cover was also used to sustain the heat and uniform airflow, and to allow for observation of cracks during testing. The operating conditions resulted in an evaporation rate of 1 kg/m²/h.

As illustrated in Figure 2.3, concrete elements, 40 x 80 x 500 mm in dimension, with hemispherical protrusions were used to provide internal restraint to 30 mm of mortar overlay. Figure 2.3(a) shows the plan view and cross-section view of a typical concrete restraint element, while Figure 2.3(b) shows the cross-section of the restraint element with mortar overlay. Forms were carefully removed after 1.5 hours in the environmental chamber to increase overlay exposure to airflow. Testing resumed for an additional 2.5 hours, for a total test period of 4 hours. The average width of each crack was measured

using a 240x magnification digital microscope, and the total crack area was recorded. The mean value of two specimens which were tested simultaneously is reported in this paper.

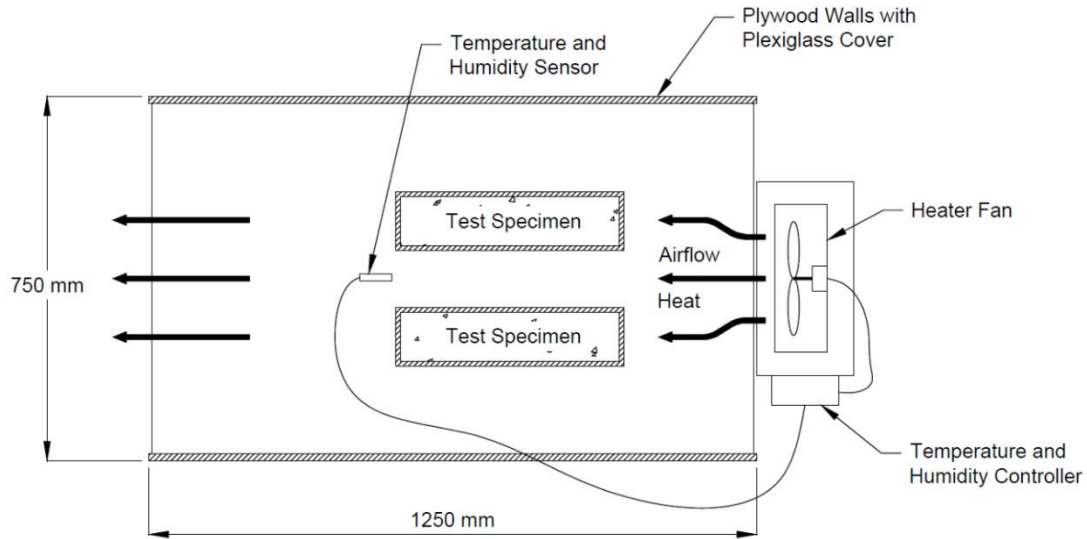


Figure 2.2. Schematic of the environmental test chamber

2.2.3.2. Drying Shrinkage

Drying shrinkage test of 25 x 25 x 250 mm mortar bars was performed in accordance with ASTM C596 [32]. Specimens were cured in moulds for 24 hours prior to curing in ambient temperature water for 48 hours. After 72 hours, the specimens were wiped dry and an initial reading was obtained using a length comparator. Mortar bars were placed in air storage, at a controlled temperature of 22°C ($\pm 1^\circ\text{C}$) and relative humidity of 40% ($\pm 2\%$), and length readings were taken after 4, 11, 18, 25, and 32 days. The weight of the mortar bars was recorded concurrently, with the 4-day air storage reading taken as the reference for weight loss calculations. In this paper, the mean values reported for each mixture designation are based on four identical test specimens.

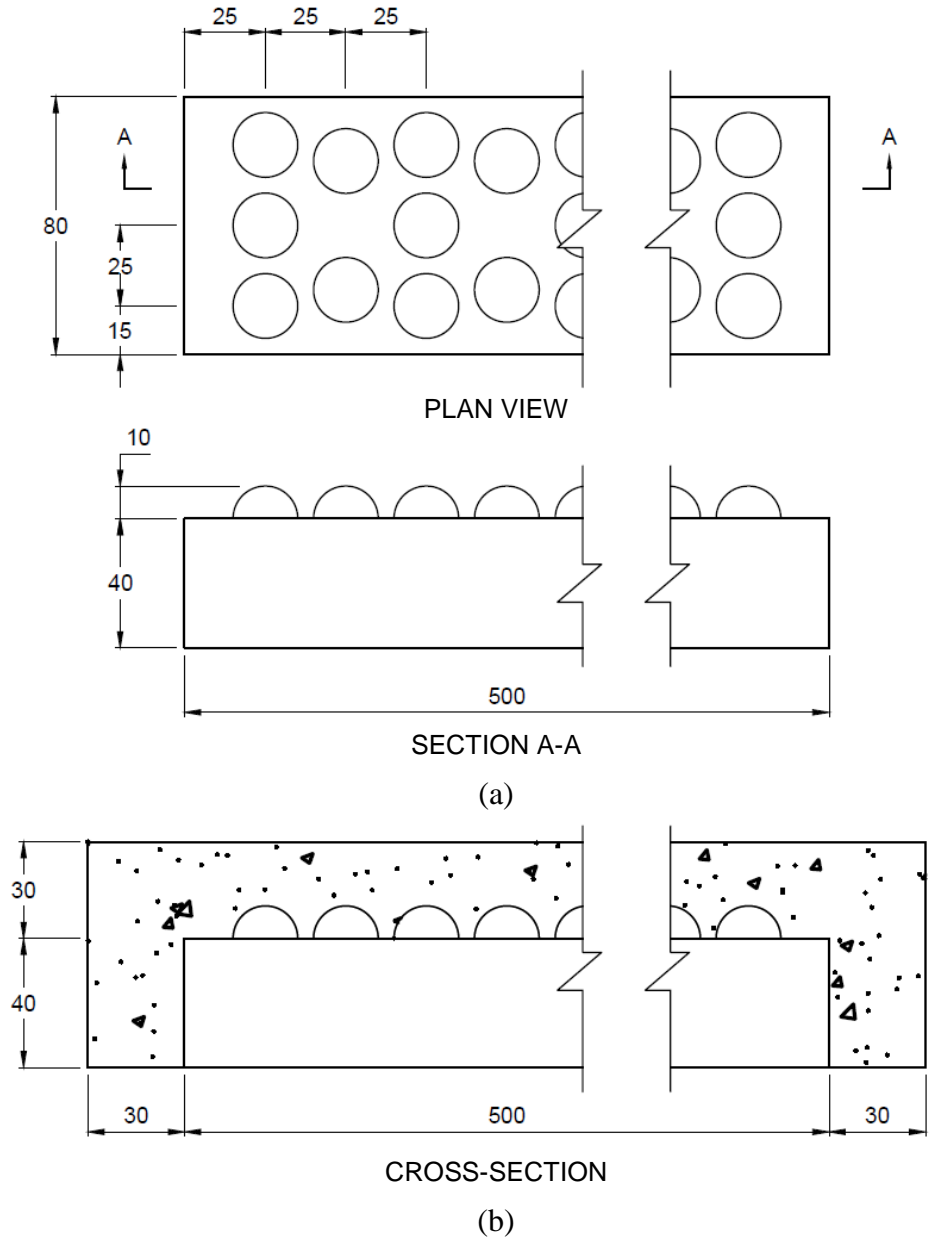


Figure 2.3. Plastic shrinkage specimen: (a) concrete restraint element (b) element with overlay

2.2.3.3. Alkali Silica Reaction (ASR)

As per ASTM C1260 [33], expansion of mortar specimens due to deleterious aggregates can be evaluated by means of the alkali silica reaction (ASR). Test specimens were cured in moulds for 24 hours prior to curing in water at 80°C (± 2°C) for an additional

24 hours. Initial length readings were then measured within 30 seconds of removing the specimens from the water. Mortar bars were cured in 1 mol NaOH solution at 80°C ($\pm 2^\circ\text{C}$) for a minimum of 14 days to accelerate the ASR process. After 14 days in NaOH (16 days after casting), specimens with expansions less than 0.10% were considered innocuous, while expansions greater than 0.20% were considered potentially deleterious. Expansion between the innocuous and deleterious zone indicated the presence of aggregates with both innocuous and deleterious properties. Thus, the testing was extended to 28 days (30 days after casting) for specimens falling in this intermediate zone. MG specimens, after 14 days of exposure to NaOH, were also examined by means of scanning electron microscopy (SEM) and energy dispersive x-ray spectroscopy (EDS) to further examine the development of ASR. It is important to note that the alkali content of the cement has little significance in any expansion that occurs as the alkalinity of the NaOH solution dominates.

2.3. Results and Discussion

2.3.1. Flow

The flowability of MG, CG, and GB mixtures is reduced as replacement amount increases. However, results of the test indicate that the flowability of glass aggregate specimens at 30% replacement was either similar or slightly better than the control specimen. These findings are attributed to the low absorption capacity of crushed glass and glass beads, which retain free water in the mortar mixture. GB mixtures were observed to be more workable than CG mixtures due to the geometry of the GB aggregates. The angularity of crushed glass results in greater shear stress, impeding the flow of the mixtures. In general, adding expanded glass in cement mortar mixtures result in

undesirably low flowability because of the fineness and porosity of the glass particles, which tend to absorb free water. Nonetheless, the flow for EG-05 and EG-10 reported in Table 2.3 were noticeably high since superplasticizer was used for these mixtures. No other mixes used superplasticizer. Table 2.3 shows the resulting flow for all mixtures.

Table 2.3. Mortar flowability

Specimen Designation	Initial (mm)	Final (mm)	Flow (%)
Control	100	225	125
MG-30	100	240	140
MG-50	100	220	120
CG-30	100	220	124
CG-50	100	210	110
GB-30	100	235	135
GB-50	100	210	120
EG-05	100	255	155
EG-10	100	230	130

2.3.2. Compressive Strength

Figure 2.4 shows the average 28-day compressive strength of glass aggregate mortar, prepared and tested as per ASTM C109 [34]. In comparison to the control mixture, an increase in crushed glass and glass bead content resulted in a decrease in compressive strength by as much as 20% and 32% at a replacement of rate of 30% and 50%, respectively. The weak bond between the glass aggregates and the cement matrix is attributed to the unfavourable effect on the strength. Though angular aggregates like CG provide better bonding than spherical aggregates like GB, it was observed that GB specimens exhibited higher compressive strength compared to the CG specimens. The higher compressive strength of GB specimens is primarily due to the finer size and

spherical shape of the glass aggregates. Smaller glass particle sizes result in higher compressive strength as reported by Shao et al. [35]. Further, the spherical shape of GB reduces void content, thereby improving strength. The strength of MG specimens, at a replacement rate of 30%, appropriately falls between the GB and CG results. However, it should be noted that at 50% replacement, the MG and GB specimens have comparable strength.

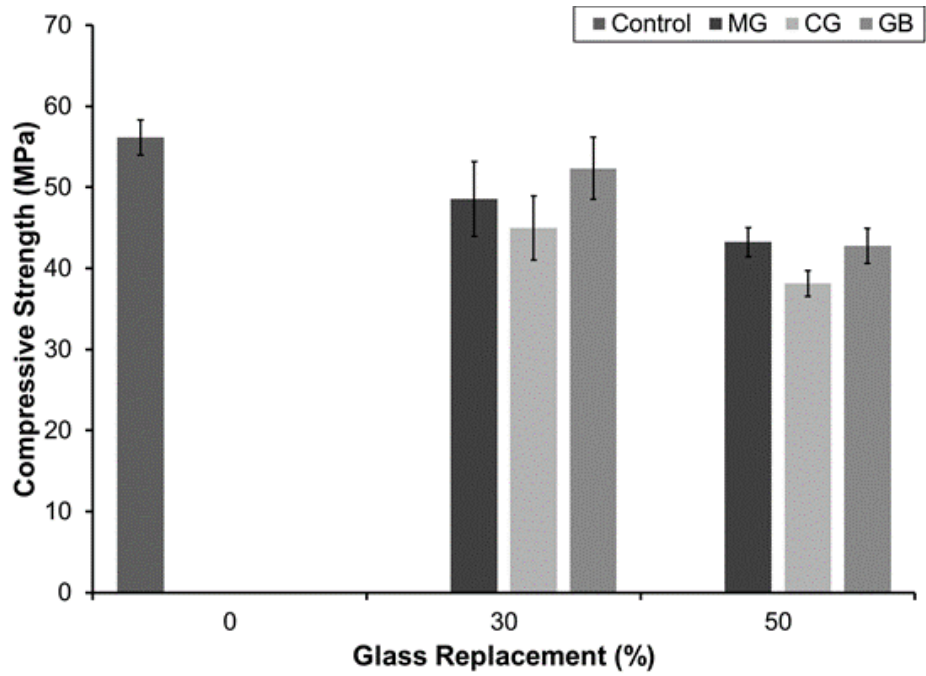
The compressive strength of EG specimens, though still lower than the control specimen, is relatively higher than the MG, CG, and GB specimens, even though the amounts of replacement of sand by expanded glass aggregates were only 5% and 10%. Similar to GB specimens, the strength of EG specimens is attributed to the fineness of the glass particles and its inherent pozzolanic characteristics [36]. Hence, increasing the proportion of EG aggregates resulted in an increase in strength. The 28-day compressive strength of EG-10 specimen was 55 MPa, which is only 3% less than the compressive strength of the control specimen.

2.3.3. Plastic Shrinkage

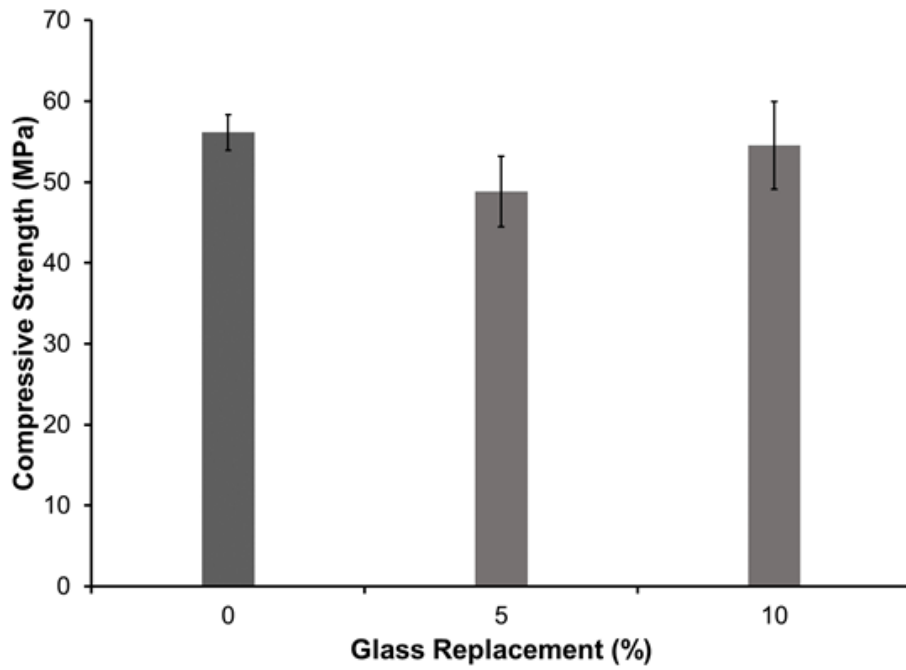
Cracking due to plastic shrinkage of cement mortar and concrete primarily transpires when the evaporation rate exceeds the bleeding rate. Rapid evaporation of moisture at early stages of placement causes contraction stresses in the capillary pores of concrete and cement mortar. Cracks then develop due to the low tensile strength of plastic concrete and its inability to resist the capillary pressure [26]. Figure 2.5 presents the results obtained from the restrained plastic shrinkage tests. Figure 2.5(a) indicates that incorporating CG and GB aggregates in mortar is effective in reducing the total crack area

induced by plastic shrinkage. The positive influence of CG and GB is attributed to the low water absorption capacity of these glass aggregates compared to natural sand aggregate, which implies increased bleeding of the mortar in CG and GB mixes. Hence, higher amounts of CG and GB as a replacement of sand resulted in greater resistance to plastic shrinkage cracks and an overall reduction in total crack area. At equivalent replacement amounts, CG performed better than GB. Specifically, the total crack areas of CG specimens were significantly lower than GB specimens by 76% and 85% at 30% and 50% replacements, respectively. In addition, the total crack area of MG specimens fell between CG and GB specimens. The better plastic shrinkage performance of CG specimen as compared to GB specimen is likely due to the angular geometry and larger size of the CG aggregates, which provide better resistance to tensile stresses induced by the increase in capillary pressure during rapid evaporation.

Little to no bleeding was visually observed for EG specimens due to the high absorption capacity of the aggregates. Consequently, as shown in Figure 2.5(b), EG specimens were more susceptible to plastic shrinkage cracks compared to the control specimen. The use of superplasticizer in the EG mixtures may have also contributed to the increase in total crack area [26]. Figure 2.6 shows the resulting cracks for select specimens.

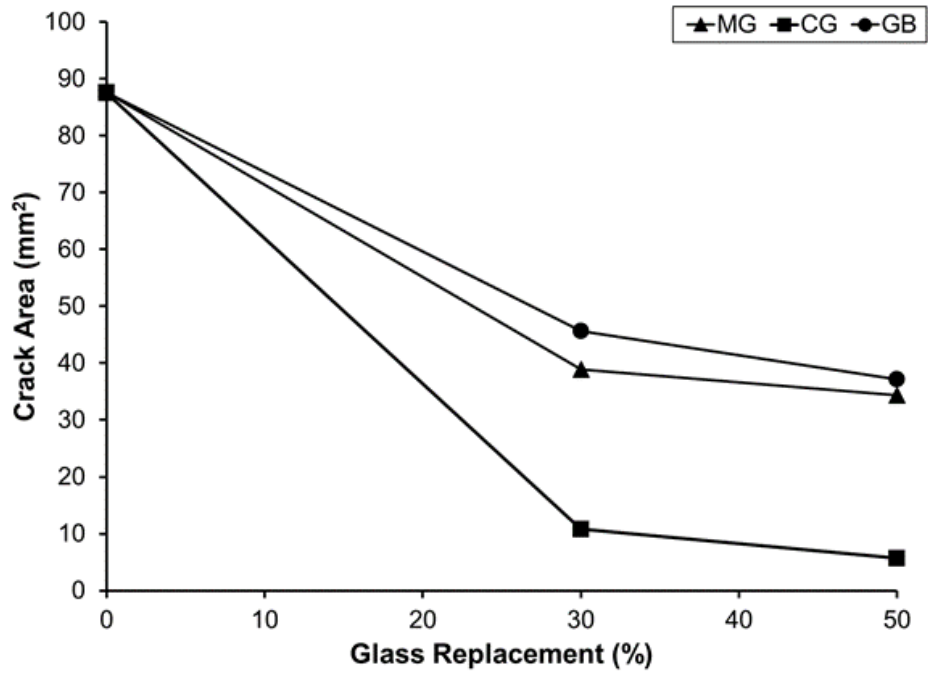


(a)

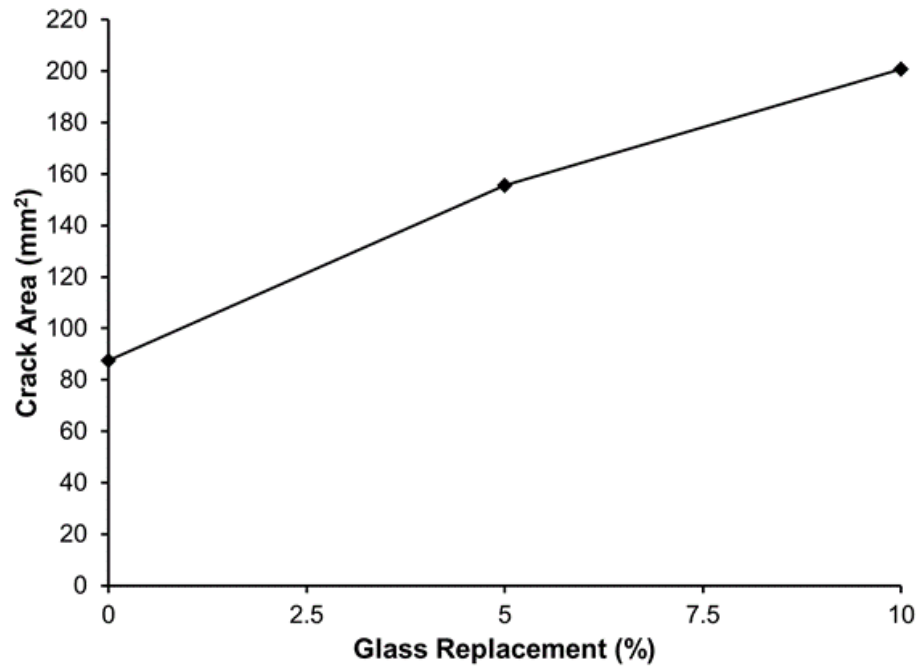


(b)

Figure 2.4. 28-day compressive strength of glass aggregate mortars (a) Group 1 specimens – MG, CG, and GB mortar (b) Group 2 specimens – EG



(a)



(b)

Figure 2.5. Total crack area due to plastic shrinkage (a) Group 1 specimens – MG, CG, and GB mortar (b) Group 2 specimens – EG

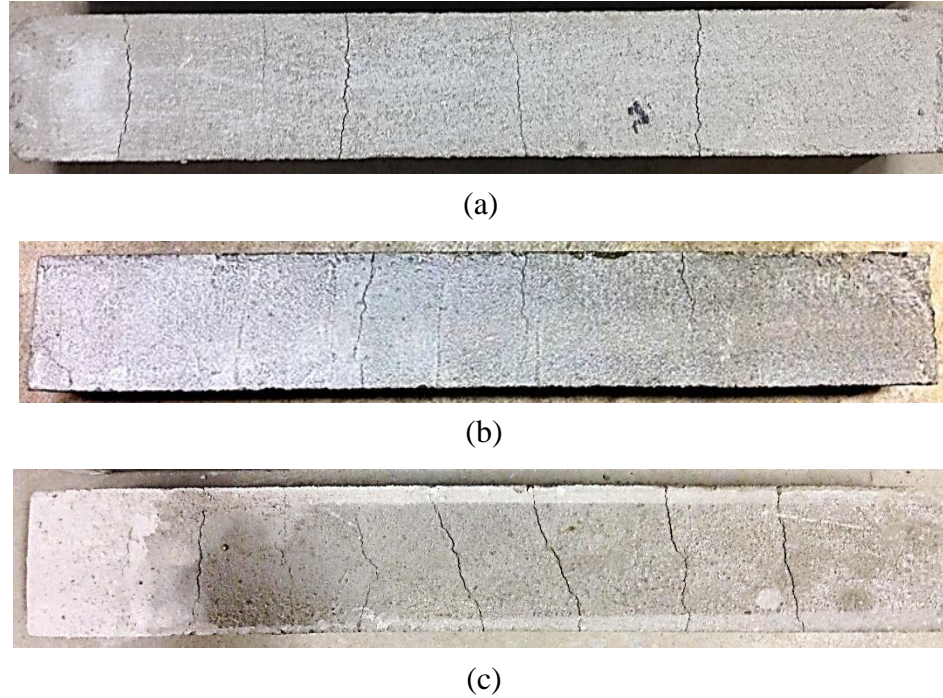


Figure 2.6. Overlay cracks after 4 hours of testing (a) Control (88 mm² crack area) (b) MG-30 (47 mm² crack area) (c) EG-10 (218 mm² crack area)

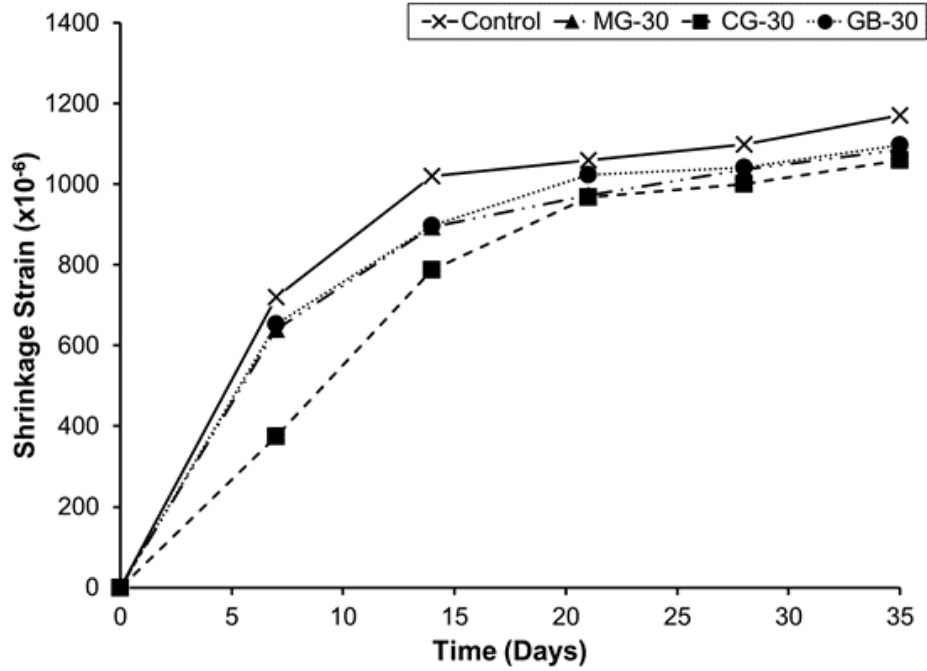
2.3.4. Drying Shrinkage

Drying shrinkage is a phenomenon caused by moisture loss in the pores of cement-based materials. Typically, the cement paste in concrete and cement mortar exhibit the largest shrinkage; however, aggregates provide a restraining effect that reduces the magnitude of the shrinkage [37]. When restrained, drying shrinkage in concrete and cement mortar can result in cracking. Cracks can negatively affect durability as cracks provide passages to deleterious substances. Additionally, shrinkage cracks can result in strength reductions as cracks can penetrate deeper into the concrete over time [37]. Thus, the evaluation of drying shrinkage is significant in the overall study of durability.

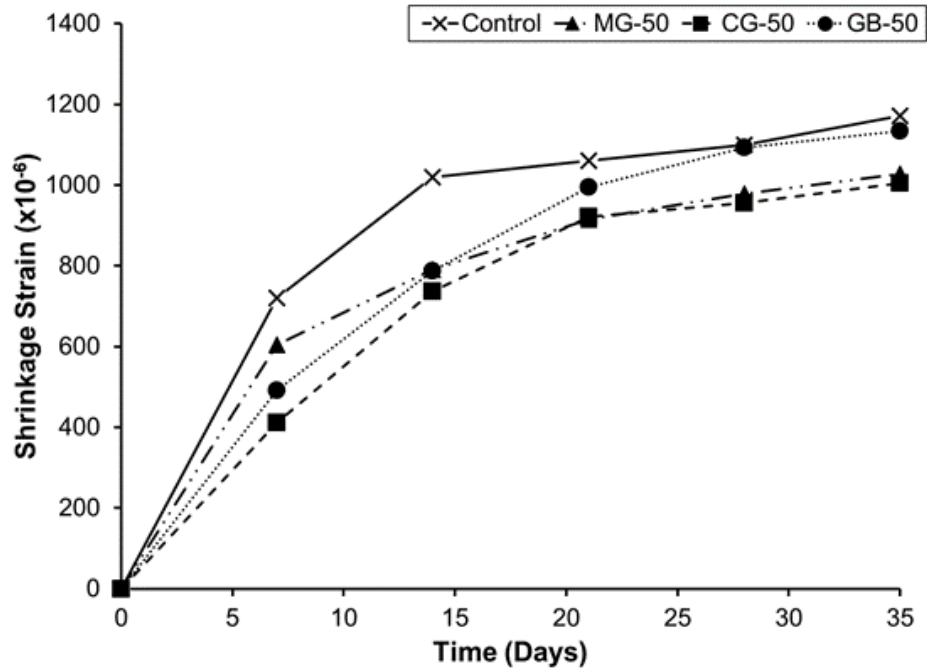
Figure 2.7 shows the development of drying shrinkage over time. As can be observed in this figure, MG, CG, and GB specimens were effective in reducing drying

shrinkage. However, EG specimens exhibited an opposite trend. The CG specimens showed the least shrinkage. This is due to the angularity of the glass, which provided better restraint compared to the GB particles. EG specimens experienced shrinkage greater than the control specimen, which can be associated to the high porosity and tendency of the particles to absorb the free water in the mix, thereby increasing volumetric contraction. It should be noted that the effect of EG on drying shrinkage of cement mortar found in the current study contradicts some earlier findings where a reduction in shrinkage was observed [25]. Unlike these earlier reports, the aggregates used in this study were not pre-wetted prior to casting. It is also important to note that the shrinkage strains of EG-05 and EG-10 were quite comparable and the difference between these two specimens is negligible. It is probable that the amounts of glass replacements (5% and 10%) in these mortar mixtures are too close to witness any distinct difference.

Since drying shrinkage is associated with loss of moisture, the strong relation between the shrinkage strain and the weight loss of glass aggregate mortar, as shown in Figure 2.8, was expected. Analysis of the trends indicate that mortar specimens containing GB aggregates are far more durable than mortar specimens containing MG and CG aggregates as GB specimens resulted in less weight loss for a particular value of the shrinkage strain. For example, weight loss of MG-30, CG-30, and GB-30 can be interpolated as 1.3%, 1.5%, and 1.1%, respectively, for the shrinkage strain of 1000×10^{-6} . Therefore, although GB specimens result in higher shrinkage strain over time (Figure 2.7), it is far more durable than MG and CG specimens in terms of weight loss. Again, the results of EG-5 and EG-10 are very similar.

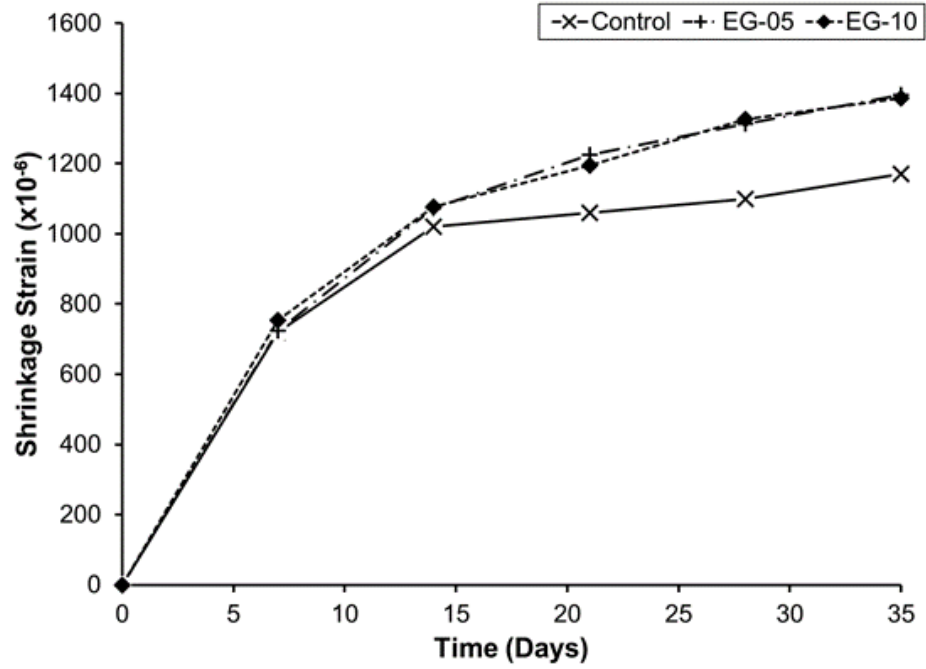


(a)



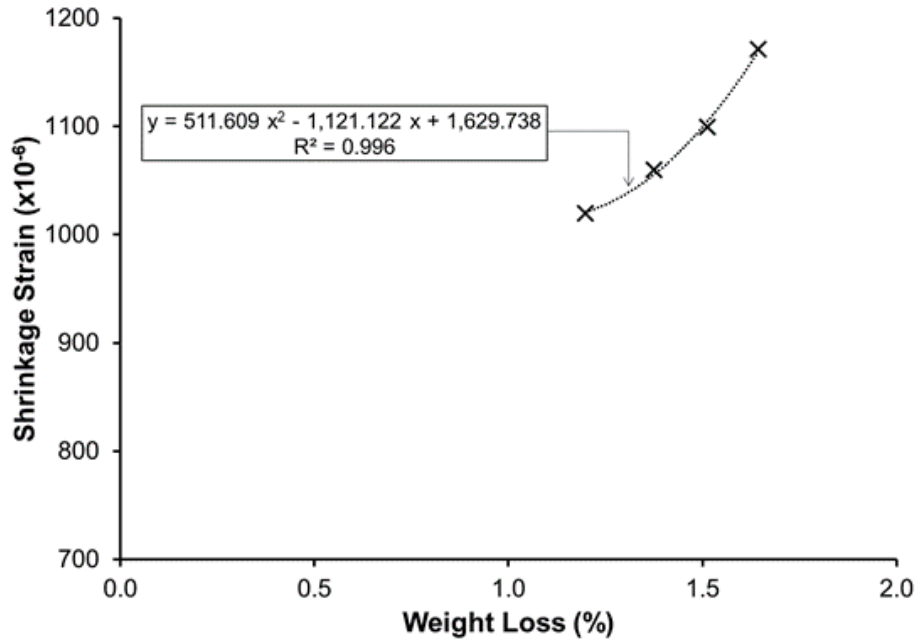
(b)

Figure 2.7. Development of drying shrinkage (a) Group 1 specimens at 30% replacement (b) Group 1 specimens at 50% replacement

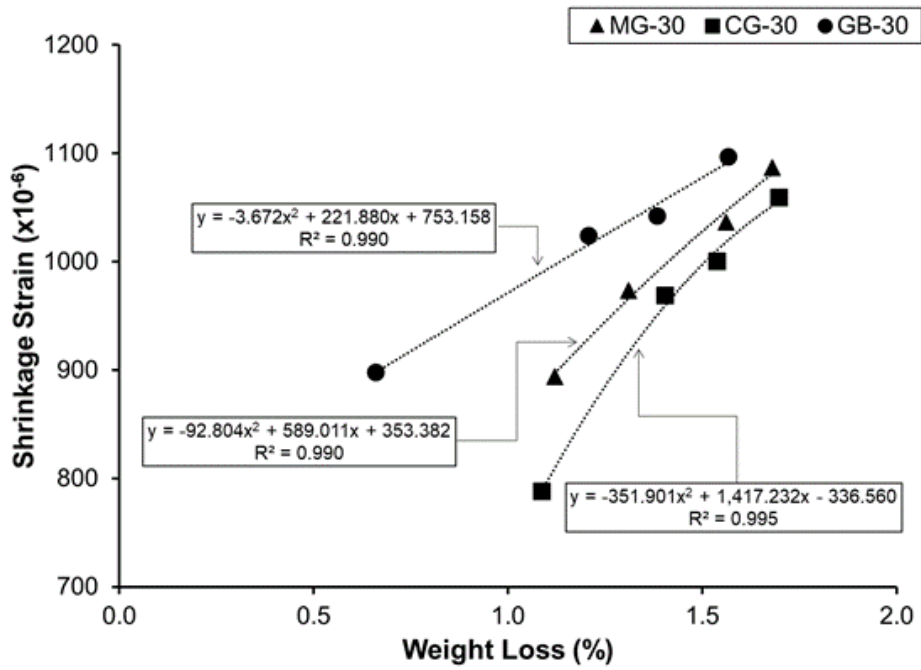


(c)

Figure 2.7. (cont.) Development of drying shrinkage (c) Group 2 specimens

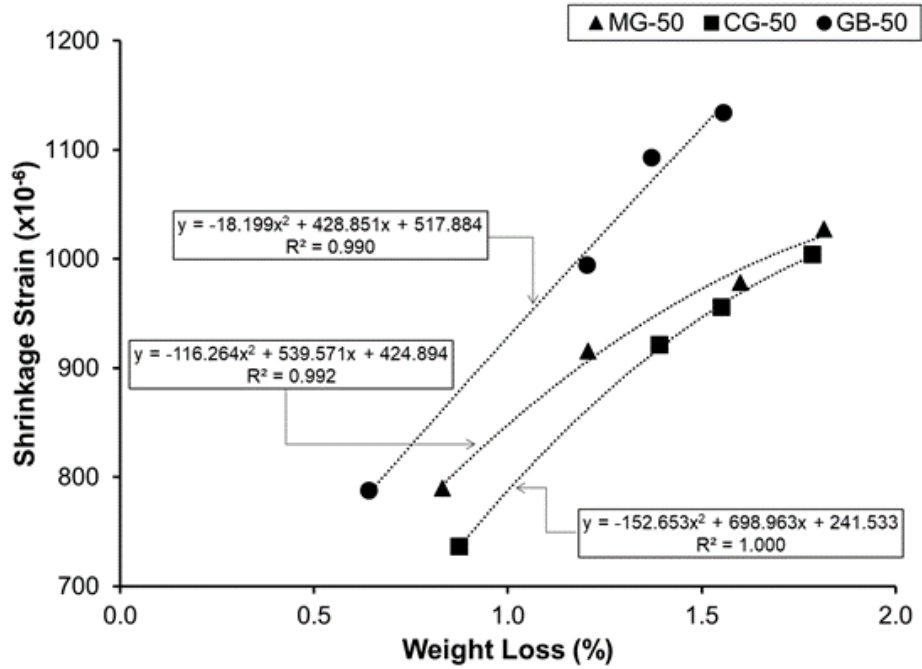


(a)

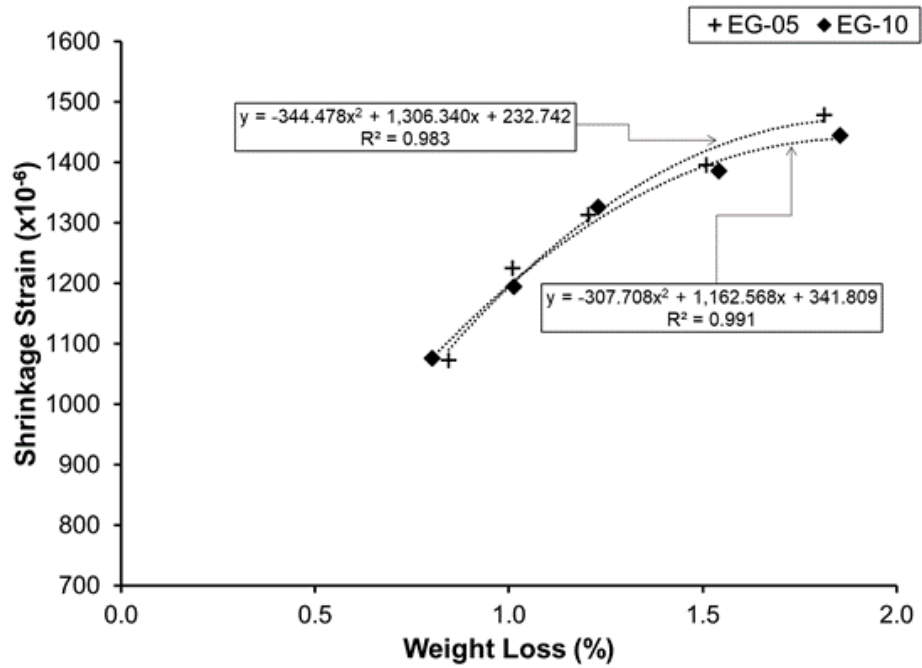


(b)

Figure 2.8. Weight loss and shrinkage relation (a) Control (b) Group 1 specimens at 30% replacement



(c)



(d)

Figure 2.8. (cont.) Weight loss and shrinkage relation (c) Group 1 specimens at 50% replacement (d) Group 2 specimens

2.3.5. Alkali Silica Reaction

It is generally presumed that incorporating glass aggregates in cement mortar increases the risk of potentially deleterious internal expansion caused by ASR. Nonetheless, many recent findings have disproved this assumption [9,13]. The current study found that not all glass aggregates exhibit deleterious behaviour (Figure 2.9). As can be found in Figure 2.9(a), CG specimens showed excessive expansion after 14 days in NaOH solution, exceeding the deleterious zone boundary of 0.20% [33]. Figure 2.10 shows an example of how surface cracking occurred in a CG specimen after immersing in NaOH solution for 14 days. This figure also shows that the specimen was separated into two pieces. Conversely, it was found that even after 28 days in NaOH solution, GB specimens [Figure 2.9(b)] did not surpass the deleterious zone, but exceeded the ASTM C1260 threshold of 0.10% [33]. The GB specimen also performed better than the control specimen. Figure 2.9(c) shows that the combined effect of CG and GB aggregates in MG specimens resulted in significant expansion reduction of 47% and 52%, as compared to CG specimens, for the replacement amounts of 30% and 50%, respectively. Since the chemical compositions of the CG and GB are nearly similar, as presented in Table 2.2, it can be concluded that the underlying explanation for the differing performance of CG and GB is predominantly due to the size of the glass particles. Shayan and Xu [1] and Rajabipour et al. [9] concluded that glass particle size above 0.60 mm can result in considerably higher expansion, while particle size below 0.30 mm causes little to no deleterious expansion. Since GB aggregates have higher proportion of fines compared to CG, GB specimens were less susceptible to deleterious expansion. It should be noted that the control specimen just meets the deleterious zone after 14 days in NaOH solution. This indicates that the curing

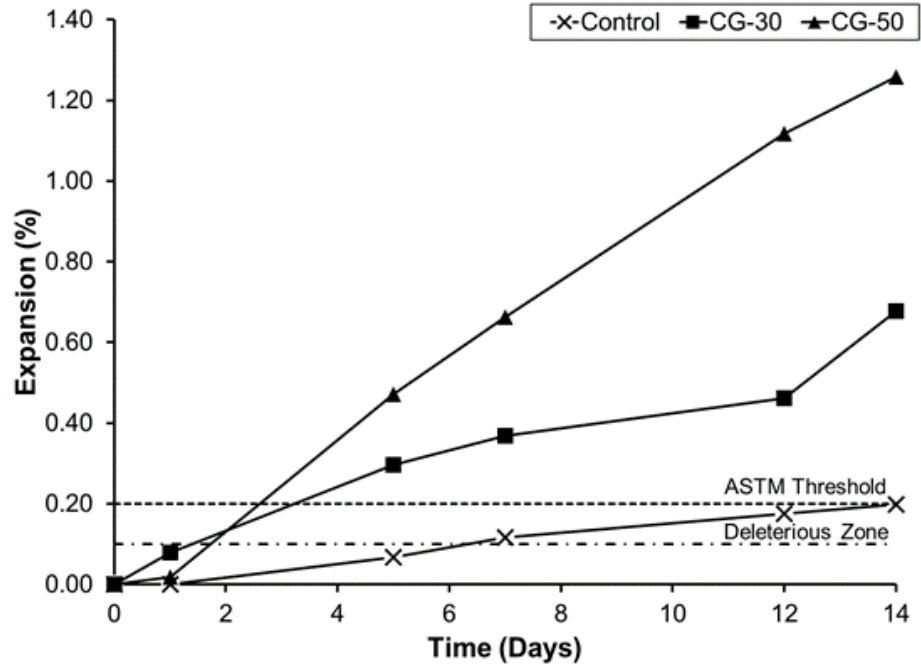
condition used in this study was effective in accelerating ASR induced expansion. A similar observation was found by Topçu, and Canbaz [7]. Nevertheless, the results obtained from this study concludes that different glass aggregates cause varying degrees of ASR expansion. Specifically, in relation to the control specimen, a detrimental effect was realized for specimens containing CG aggregates, while a beneficial effect was observed for specimens containing GB aggregates.

There is quite the contrast between the behaviour of EG specimens and the specimens made of the other glass aggregates. As can be found from Figure 2.9(d), performance of both EG-05 and EG-10 specimen were comparable, and both exhibited a negligible expansion of approximately 0.04%. Additionally, no surface cracking developed on the specimens throughout the entire duration of the test. It is likely that the impact of any internal expansions caused by ASR was absorbed by the multiple voids of these lightweight aggregates. Carsana and Bertolini [21] also undertook a study to determine the effect of ASR on specimens made with expanded glass. SEM images presented by Carsana and Bertolini indicated that internal fractures occur within the expanded glass aggregates; however, ASR did not have any effect at the interfacial zone between the aggregate and the cement matrix.

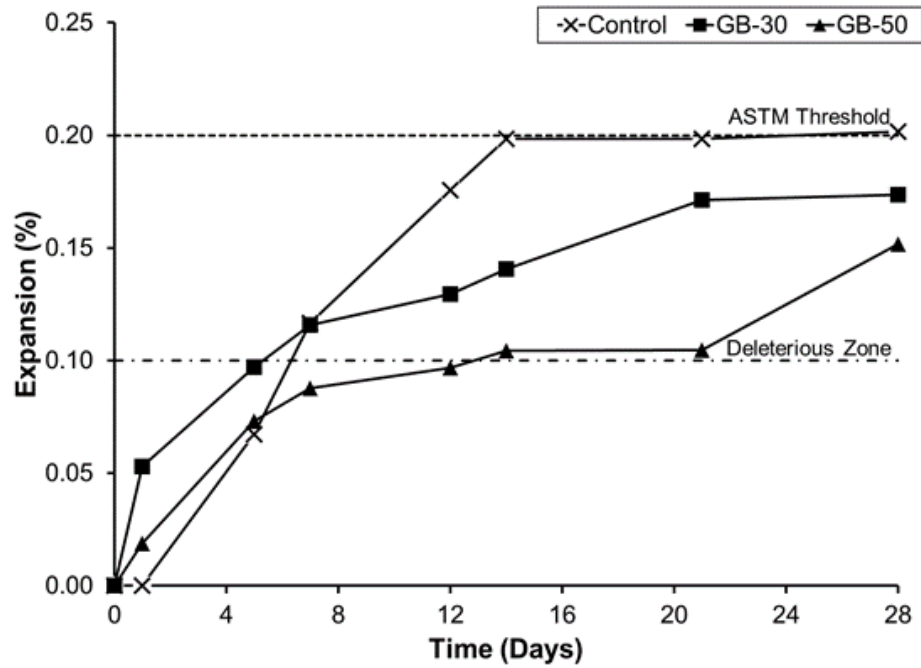
It is important to note that several studies contradict the use of the accelerated mortar bar method (ASTM C1260) for determining ASR since the severe testing environment has the potential of falsely identifying nonreactive aggregates as reactive [38,39]. According to Munir et al. [40], ASTM C1260 best determines the reactivity of marginally to moderately reactive aggregates. Although ASTM C1260 results can be over-conservative, the speed of testing has been determined to be a significant practical

advantage, which is why this test was used. Nonetheless, comparison of test results with a longer-term test method should be considered in future studies.

EDS mapping of an MG specimen that has been immersed in NaOH solution for 14 days is depicted in Figure 2.11. This figure indicates a glass particle in red, which is composed of primarily SiO_2 , surrounded by a layer of reacted silica and calcium in yellow. The area in blue represents the cement which is predominantly CaO. The grey area at the top of the image indicates a valley in the topology and hence, sufficient information from this zone could not be obtained by EDS mapping analysis. It may be due to the fact that a glass particle was de-bonded in this area. The chemical compositions of the specimen were determined at the different spots as shown in Figure 2.11 and summarized in Table 2.4. As expected, the unreacted glass, designated as Spot 1, has high SiO_2 content with a high ratio of SiO_2 to CaO (SiO_2/CaO), while the cement matrix, designated as spot 4, has high CaO content with a very low SiO_2/CaO . Spots 2 and 3, located in the yellow zone of the EDS map, were found to have a SiO_2/CaO of 2.11 and 0.9, respectively. According to Rajabipour et al. [9], SiO_2/CaO values between 0.2 and 1 suggests pozzolanic reaction resulting in the formation of calcium silicate hydrate (CSH). On the other hand, SiO_2/CaO values between 1 and 5 suggests the formation of expansive ASR gel. SiO_2/CaO at spot 3 is clearly CSH. However, there is a possibility of ASR gel formation at spot 2 though there is also a likelihood that EDS detected a higher content of SiO_2 since the spot is at the interface of the glass and cement matrix.

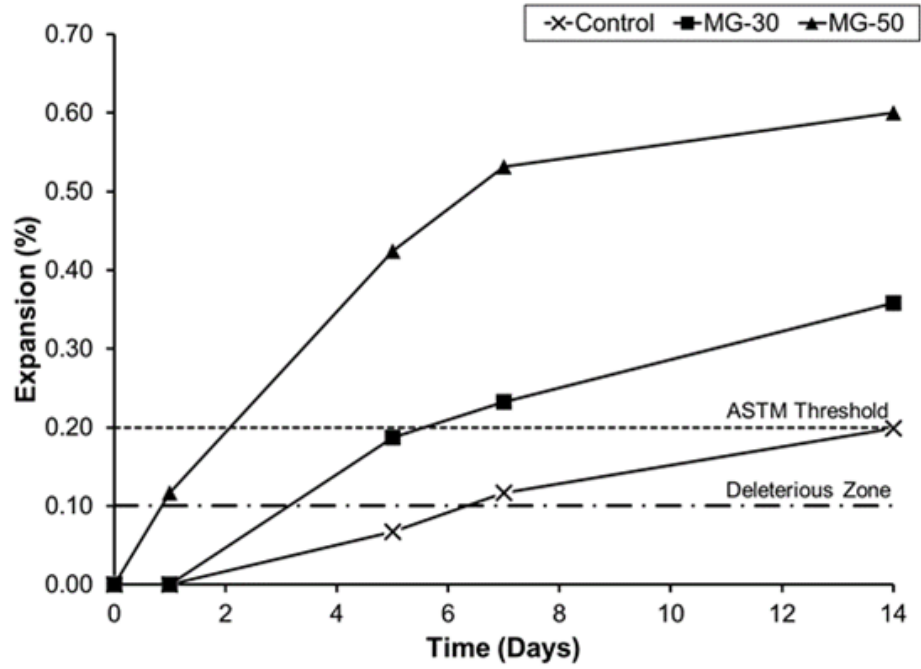


(a)

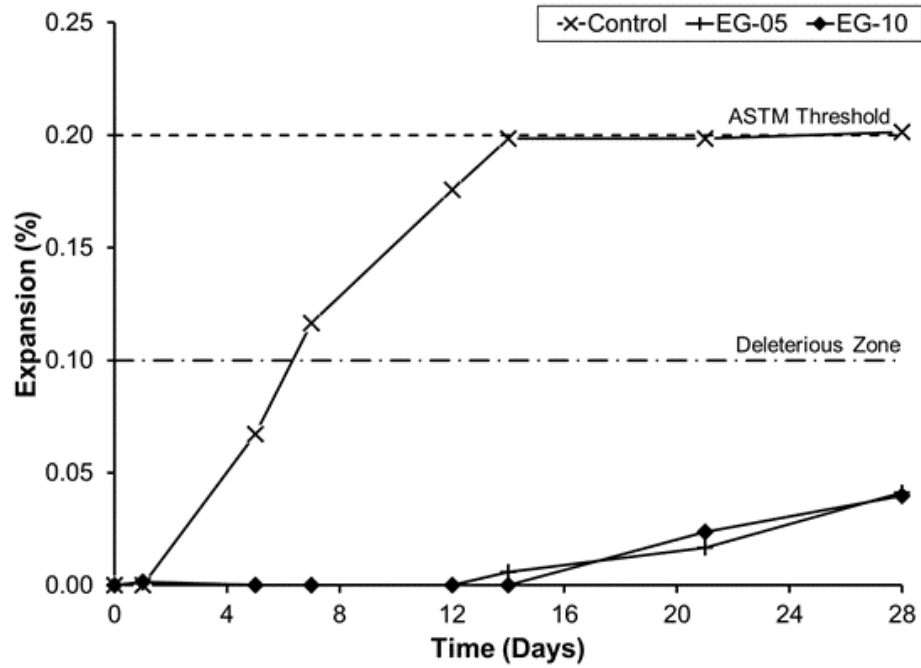


(b)

Figure 2.9. ASR expansion of glass aggregate mortar (a) Crushed glass (b) Glass beads



(c)



(d)

Figure 2.9. (cont.) ASR expansion of glass aggregate mortar (c) Mixed glass
(d) Expanded glass



Figure 2.10. Deteriorated CG specimen immersed in NaOH solution for 14 days

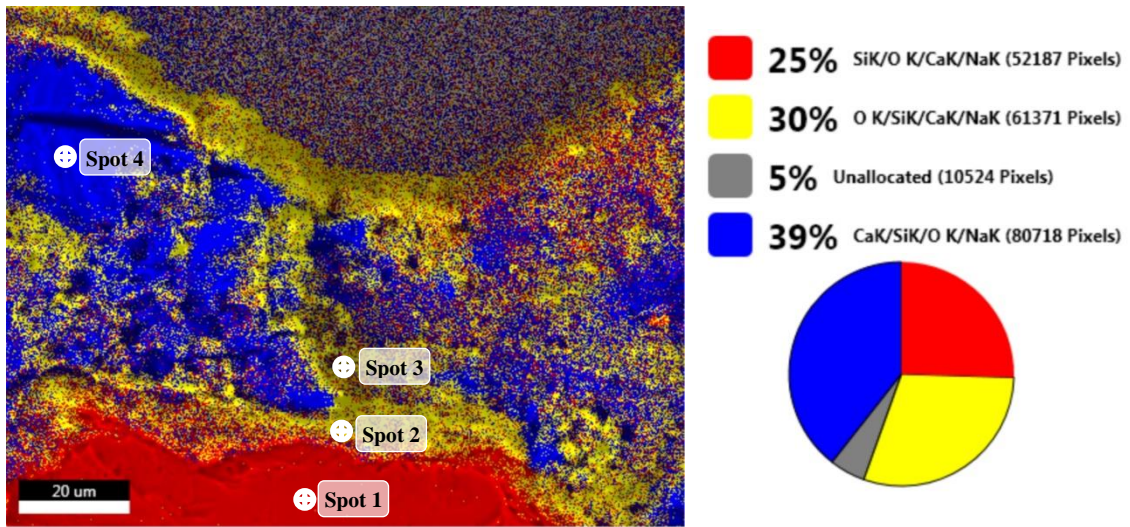


Figure 2.11. EDS mapping of 14-day MG specimen exposed to NaOH solution

Table 2.4. EDS point analysis

Spot ID	Chemical composition (wt %)			SiO ₂ /CaO	Description
	SiO ₂	CaO	Na ₂ O		
1	42.84	8.04	1.14	5.34	Unreacted glass
2	42.46	20.15	2.78	2.11	Pozzolanic CSH or ASR gel
3	31.40	34.78	6.96	0.90	Pozzolanic CSH
4	12.99	68.42	2.25	0.19	Cement

2.4. Conclusions

This study examined the effect of incorporating a variety of glass aggregate in cement mortar. Crushed glass, glass beads, and a mixture of the two were used to determine the effect of these aggregates on the performance of cement mortar. Mortar with expanded glass aggregates was also studied for possible integration with other glass aggregates in a future research. This study found that the use of glass aggregates in cement mortar can be of great benefit if a suitable type and amount of glass aggregate is chosen. The conclusions of this study are summarised as follows. It should be noted that the conclusions may be limited to the specimens used and the scope of the work.

1. It is generally presumed that the addition of glass aggregates increases the risk of ASR, though outcomes of several recent studies do not agree with this. Nonetheless, the current study concludes that not all glass aggregates result in deleterious expansions. In fact, ASR in specimens with expanded glass aggregates was beneficial and it resulted in a negligible expansion of 0.04%; in comparison, the expansion of the control specimen was 0.2%. This study found that ASR depends on the size of the glass aggregate. Finer glass aggregates help in reducing the deleterious expansions due to pozzolanic properties. Further, the porosity of glass aggregates also affects the ASR induced expansion. Higher porosity helps in reducing the expansion. Hence, negligible ASR induced expansion (0.04%) was observed for expanded glass aggregate mortar specimens.
2. The low absorption ability of crushed glass and glass bead aggregates causes increased bleeding of the mortar mixtures and this results in a greater resistance to plastic and drying shrinkage. On the contrary, expanded glass aggregate has high porosity and

fineness. Thus, incorporation of this aggregate results in high absorption of free water which causes a reduction in the workability and an increase in volumetric contraction. However, the relationship between shrinkage strain and weight loss suggests that at a particular strain, the mortar mix made of expanded glass aggregate exhibited the least weight loss. Thus, this mix was found to be more durable than the mixes made of other glass aggregates.

3. In general, incorporation of glass aggregate in the cement mortar causes reduction in its compressive strength ranging from 3% to 32%. This reduction is associated to weak bonding between glass aggregates and the cement matrix at the interfacial transition zone. However, incorporation of glass bead and expanded glass aggregates results in reverting some of the loss in strength caused by weak bonding. This happens because finer glass particles have inherent pozzolanic properties. The study found that there was only a 3% reduction in the 28-day compressive strength for EG-10 specimen.

2.5. Acknowledgements

The authors acknowledge the Natural Sciences and Engineering Research Council of Canada for the financial support provided to Karla Gorospe in the form of the Canada Graduate Scholarship.

2.6. References

- [1] A. Shayan, A. Xu, Value-added utilisation of waste glass in concrete, *Cement and Concrete Research*. 34 (2004) 81–89.
- [2] V. Corinaldesi, G. Gnappi, G. Moriconi, A. Montenero, Reuse of ground waste glass as aggregate for mortars, *Waste Management*. 25 (2005) 197–201.

- [3] B. Taha, G. Nounu, Utilizing waste recycled glass as sand/cement replacement in concrete, *Journal of Materials in Civil Engineering*. 21 (2009) 709–721.
- [4] T.C. Ling, C.S. Poon, Properties of architectural mortar prepared with recycled glass with different particle sizes, *Materials & Design*. 32 (2011) 2675–2684.
- [5] T.C. Ling, C.S. Poon, A comparative study on the feasible use of recycled beverage and CRT funnel glass as fine aggregate in cement mortar, *Journal of Cleaner Production*. 29–30 (2012) 46–52.
- [6] S. De Castro, J. De Brito, Evaluation of the durability of concrete made with crushed glass aggregates, *Journal of Cleaner Production*. 41 (2013) 7–14.
- [7] İ.B. Topçu, M. Canbaz, Properties of concrete containing waste glass, *Cement and Concrete Research*. 34 (2004) 267–274.
- [8] K.H. Tan, H. Du, Use of waste glass as sand in mortar: Part I - Fresh, mechanical and durability properties, *Cement and Concrete Composites*. 35 (2013) 118–126.
- [9] F. Rajabipour, H. Maraghechi, G. Fischer, Investigating the alkali-silica reaction of recycled glass aggregates in concrete materials, *Journal of Materials in Civil Engineering*. 22 (2010) 1201–1208.
- [10] J.R. Wright, C. Cartwright, D. Fura, F. Rajabipour, Fresh and hardened properties of concrete incorporating recycled glass as 100% sand replacement, *Journal of Materials in Civil Engineering*. 26 (2014) 4014073.
- [11] A. Mardani-Aghabaglou, M. Tuyan, K. Ramyar, Mechanical and durability performance of concrete incorporating fine recycled concrete and glass aggregates, *Materials Structures*. 48 (2015) 2629–2640.
- [12] S.H. Chen, H.Y. Wang, J.W. Zhou, Investigating the properties of lightweight concrete containing high contents of recycled green building materials, *Construction and Building Materials*. 48 (2013) 98–103.
- [13] H. Du, K.H. Tan, Use of waste glass as sand in mortar: Part II - Alkali-silica reaction and mitigation methods, *Cement and Concrete Composites*. 35 (2013) 109–117.
- [14] S. Guo, Q. Dai, X. Sun, X. Xiao, R. Si, J. Wang, Reduced alkali-silica reaction damage in recycled glass mortar samples with supplementary cementitious materials, *Journal of Cleaner Production*. 172 (2018) 3621–3633.
- [15] K. Afshinnia, P.R. Rangaraju, Efficiency of ternary blends containing fine glass powder in mitigating alkali – silica reaction, *Construction and Building Materials*. 100 (2015) 234–245.

- [16] N. Schwarz, H. Cam, N. Neithalath, Influence of a fine glass powder on the durability characteristics of concrete and its comparison to fly ash, *Cement and Concrete Composites*. 30 (2008) 486–496.
- [17] M. Kamali, A. Ghahremaninezhad, Effect of glass powders on the mechanical and durability properties of cementitious materials, *Construction and Building Materials*. 98 (2015) 407–416.
- [18] K. Afshinnia, P.R. Rangaraju, Impact of combined use of ground glass powder and crushed glass aggregate on selected properties of Portland cement concrete, *Construction and Building Materials*. 117 (2016) 263–272.
- [19] W. Jin, C. Meyer, S. Baxter, “Glascrete” - concrete with glass aggregate, *ACI Structural Journal*. 97 (2000) 208–213.
- [20] R. Idir, M. Cyr, A. Tagnit-Hamou, Use of fine glass as ASR inhibitor in glass aggregate mortars, *Construction and Building Materials*. 24 (2010) 1309–1312.
- [21] M. Carsana, L. Bertolini, Durability of lightweight concrete with expanded glass and silica fume, *ACI Materials Journal*. 114 (2017) 207–213.
- [22] V. Ducman, A. Mladenovič, J.S. Šuput, Lightweight aggregate based on waste glass and its alkali-silica reactivity, *Cement and Concrete Research*. 32 (2002) 223–226.
- [23] S.C. Kou, C.S. Poon, Properties of self-compacting concrete prepared with recycled glass aggregate, *Cement and Concrete Composites*. 31 (2009) 107–113.
- [24] T. Fujiwara, Effect of aggregate on drying shrinkage of concrete, *Journal of Advanced Concrete Technology*. 6 (2008) 31–44.
- [25] J. Ye, S. Hu, F. Wang, Y. Zhou, Z. Liu, Effect of pre-wetted light-weight aggregate on internal relative humidity and autogenous shrinkage of concrete, *Journal of Wuhan University of Technology-Mater. Sci. Ed.* 21 (2006) 134–137.
- [26] P.J. Uno, Plastic shrinkage cracking and evaporation formulas, *ACI Materials Journal*. 95 (1998) 365–375.
- [27] CSA A3001, Cementitious materials used in concrete, Canadian Standards Association., Mississauga, Ontario, 2013.
- [28] ASTM C1437, Standard test method for flow of hydraulic cement mortar, ASTM International, West Conshohocken, PA, 2015.
- [29] ASTM C1579, Standard test method for evaluating plastic shrinkage cracking of restrained fiber reinforced concrete (using a steel form insert), ASTM International, West Conshohocken, PA, 2013.

- [30] N. Banthia, R. Gupta, Test method for evaluation of plastic shrinkage cracking in fiber-reinforced cementitious materials, *Experimental Techniques*. 31 (2007) 44–48.
- [31] J. Branston, S. Das, S.Y. Kenno, C. Taylor, Influence of basalt fibres on free and restrained plastic shrinkage, *Cement and Concrete Composites*. 74 (2016) 182–190.
- [32] ASTM C596, Standard test method for drying shrinkage of mortar containing hydraulic cement, ASTM International, West Conshohocken, PA, 2017.
- [33] ASTM C1260, Standard test method for potential alkali reactivity of aggregates (mortar-bar method), ASTM International, West Conshohocken, PA, 2014.
- [34] ASTM C109, Standard test method for compressive strength of hydraulic cement mortars (using 2-in. or [50mm] cube specimens), ASTM International, West Conshohocken, PA, 2016.
- [35] Y. Shao, T. Lefort, S. Moras, D. Rodriguez, Studies on concrete containing ground waste glass, *Cement and Concrete Research*. 30 (2000) 91–100.
- [36] H. Du, K.H. Tan, Concrete with recycled glass as fine aggregates, *ACI Materials Journal*. 111 (2014) 47–57.
- [37] ACI Committee 224, ACI 224.1R-07: Causes, evaluation and repair of cracks in concrete structures, *Technical Documents*. (2007) 26.
- [38] D. Lu, B. Fournier, P.E. Grattan-Bellew, Evaluation of accelerated test methods for determining alkali-silica reactivity of concrete aggregates, *Cement and Concrete Composites*. 28 (2006) 546–554.
- [39] F. Golmakani, R.D. Hooton, Comparison of laboratory performance tests used to assess alkali-silica reactivity, in: *Proceedings, Annual Conference - Canadian Society for Civil Engineering*, 2016.
- [40] M.J. Munir, S. Abbas, A.U. Qazi, M.L. Nehdi, S.M.S. Kazmi, Role of test method in detection of alkali – silica reactivity of concrete aggregates, *Proceedings of the Institution of Civil Engineers - Construction Materials*. 171 (2017) 203–221.

CHAPTER 3

STRENGTH, DURABILITY, AND THERMAL PROPERTIES OF GLASS AGGREGATE MORTARS

3.1. Introduction

In 2014, 2,990,000 tons of glass, primarily in the form of containers, such as bottles and jars, were recycled in the United States [1]. Nonetheless, economic constraints, such as transportation costs, have led to the disposal of recyclable glass materials into landfills. Research on concrete containing glass aggregates initiated around the 1970s as a method of controlling the disposal of refuse glass. Most earlier studies explored the use of glass aggregates in bituminous concrete for roads [2,3]. Since then, studies on glass aggregate concrete have expanded due to the growing concerns in waste management.

There is much potential for the construction applications of recycled glass aggregates as additives to concrete and even masonry systems. In fact, concrete containing glass aggregates have been shown to be environmentally friendly and feasible as the use of glass aggregates can minimize waste and lower the cost of concrete production [4,5]. However, concerns regarding the susceptibility of glass aggregates to alkali silica reaction (ASR) when combined with cement has deterred its widespread use in the concrete industry. Nonetheless, recent studies have suggested general methods, such as the use of lithium compounds and pozzolans, for controlling and mitigating detrimental expansions due to ASR [6,7].

In recent years, there has been extensive research on the influence of glass as aggregate replacement in concrete and cement mortar. The mechanical properties of glass

concrete and glass mortar have been heavily studied as strength is critical for any building material. The compressive strength of concrete containing glass aggregates has been generally found to be lower than the strength of normal plain cement concrete, with the reduction in strength increasing as the glass content increases [8,9]. However, studies by Taha and Nounu [7] reported minor effect of recycled glass sand on the compressive strength of concrete at 50% and 100% replacement levels after 28 days and 364 days, respectively. Mardani-Aghabalou et al. [10] also found insignificant differences between the strength of glass concrete and sand concrete after 28 days. Conversely, Ismail and Al-Hashmi [11] observed a minor increase in compressive strength of 20% waste glass concrete after 28 days. According to Idir et al. [12], an increase in strength is characteristic of finer glass particles, which exhibit pozzolanic properties. Particularly, Idir et al. [12] found a strength increase of 30 – 35 MPa in glass aggregate mortars with glass particles finer than 80 μm . Afshinnia and Rangaraju [13] and Kamali and Ghahremaninezhad [14] also found that an increase in compressive strength was attributed to glass particles finer than 50 μm .

Some studies have concluded that the weak bonding between the cement paste and glass aggregates is the underlying cause of strength reduction [15,16]. Almesfer and Ingham [17] also suggested that the high brittleness of glass leads to cracking upon loading, which results in incomplete adhesion with the cement paste. Moreover, Wright et al. [15] stated that soda-lime glass aggregates have lower resistance to fracturing compared to sand aggregates. Hence, flexural and tensile properties have been found to exhibit similar results as that of compressive strength [9,18].

Plastic shrinkage in concrete and cement mortar occurs at early stages of casting when the evaporation rate of surface water surpasses the bleed rate of the concrete. Plastic shrinkage cracks rarely impair strength, specifically in concrete floors and pavements; however, the growth of the cracks can affect serviceability and long-term durability as the cracks provide a passage for chlorides and other deleterious agents [19]. In reinforced concrete structures, cracks can result in corrosion of reinforcement bars, which can ultimately cause strength reduction. Modifications in the mixture design as well as proper placing and curing practices are a few methods of reducing the occurrence of plastic shrinkage cracks. In addition, fibres can be used to control plastic shrinkage cracks. This has been well studied in many aspects of concrete construction materials [20–22]. Nonetheless, there is no known literature on the plastic shrinkage of concrete or cement mortar containing glass aggregates, though several studies on drying shrinkage do exist. These studies conclude that glass aggregates reduce drying shrinkage and microcracking [16,23]. Although the magnitudes of plastic and drying shrinkage cannot be correlated [24], the mechanisms of both types of shrinkage suggest that the impermeability of glass aggregates can control plastic shrinkage as well. Studies are required to validate this assumption and fill the gap in the literature.

Even without cracks, penetration of aggressive agents like soluble salts are common concerns in porous materials like concrete. Penetration of substances can occur through different transport mechanisms (diffusion, absorption, or permeation) and can deteriorate steel reinforcements, initiate chemical degradation of concrete, and contribute to the development of frost damage [25]. Fortunately, it is in good agreement that concrete and cement mortar containing glass aggregates have low absorption capacity due to the

impermeable nature of glass [7,16]. However, De Castro and De Brito [4] found that the absorption performance of glass aggregate concrete was similar to that of regular concrete. This study stated that the size of the replaced aggregates may have influenced the absorption results.

The impermeable nature of glass aggregates has also shown positive effects in terms of rapid chloride permeability of concrete and cement mortars. Wright et al. [15] and Tan and Du [9] have concluded that glass aggregate concrete provides greater resistance to chloride ion permeability since glass is understood to have little to no internal porosity. Furthermore, the greater resistance of mortar to chloride permeability is attributed to the packing efficiency of the glass, which is enhanced with finer gradations. Conversely, De Castro and De Brito [4], have claimed that adding glass does not significantly change the chloride ion permeability behaviour of concrete because the quality of the cement governs the chloride penetration. Nonetheless, previous studies on the penetration of substances into glass aggregate concrete were for specimens at the age of 28 days. Hence, further studies on the transport of substances into mature concrete is necessary.

According to Delgado et al. [26], penetration of moisture in porous building materials not only causes degradation, in terms of strength and durability, but can also change thermal conductivity. Thermal conductivity is the rate at which heat passes through a material. Lower thermal conductivity indicates better insulating properties, which can increase energy savings. The thermal properties of aggregates highly influence the thermal conductivity of concrete materials [27]. Thus, since glass has a lower thermal conductivity than sand, concrete with glass aggregates generally has a lower thermal conductivity. Yun et al. [28] found a 42% decrease in thermal conductivity when glass bubbles are

incorporated into concrete. In addition, Alani et al. [29] studied the thermal performance of screeds (a cementitious material that is typically laid over concrete subfloors) containing 100% glass aggregates. The study found a decrease in the thermal conductivity of glass screeds by almost 50% when compared to sand screeds. Nonetheless, there are gaps in the literature regarding the thermal conductivity of glass aggregate concrete or mortar. Specifically, the effect of specimen age on thermal conductivity has yet to be addressed by researchers. Further, the effect of various glass aggregate type has not been studied.

The objective of this study is to evaluate the suitability of glass aggregates for future building construction applications. Compressive strength of cement mortars was evaluated, and durability was assessed qualitatively through plastic shrinkage, and quantitatively through water immersion absorption and rapid chloride permeability tests. There is no known research on the propagation of plastic shrinkage cracks in glass aggregate mortars, and there is limited research on the penetration of substances in mature concrete. Thus, this study serves to fill gaps in the literature. Furthermore, with few studies on the thermal conductivity of glass aggregate mortar, this property was assessed in this study to validate and add to the current literature.

3.2. Experimental Procedure

Cement mortars containing varying proportions of crushed glass and glass bead aggregates as replacements of natural sand were assessed for compressive strength, plastic shrinkage, immersion absorption, rapid chloride permeability, and thermal conductivity. Testing was conducted at specimen ages of 28, 90, and 365 days. The experimental method followed in this study is described in the subsequent sections.

3.2.1. Materials

Type GUL Portland limestone cement, conforming to CAN/CSA-A3001 [30], was used in the preparation of all cement mortar specimens. Fine aggregates comprised of natural sand with a fineness modulus of 2.63 and commercially purchased glass particles made from 100% recycled glass. Two types of glass aggregates were used – crushed glass (CG) (Figure 3.1) and glass beads (GB) (Figure 3.2). Crushed glass aggregates had particle sizes ranging from 850 to 600 μm and a density of 2499 kg/m^3 . Glass bead aggregates had particle sizes ranging from 125 to 40 μm and a density of 1249 kg/m^3 . The chemical properties of the materials, obtained through X-ray fluorescence (XRF) analysis, are presented in Table 3.1.



Figure 3.1. Crushed glass aggregates

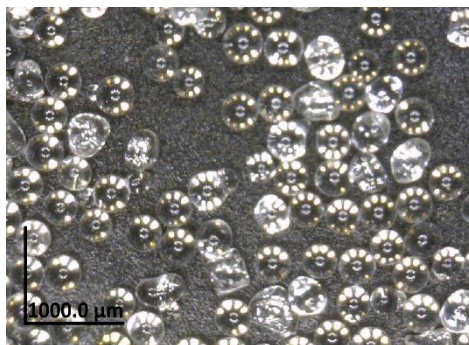


Figure 3.2. Glass bead aggregates

Table 3.1. Chemical composition of materials (%)

Analyte symbol	Cement	Sand	Crushed glass	Glass bead
CaO	62.3	19.17	10.46	9.17
SiO ₂	18.2	46.65	70.88	71.55
Al ₂ O ₃	4.5	6.6	2.25	0.72
Fe ₂ O ₃ (T)	2.76	3.07	1.29	0.66
MnO	-	0.063	0.024	0.01
MgO	3.1	2.68	1.3	3.72
Na ₂ O	0.22	1.13	12.85	13.82
K ₂ O	0.45	1.24	0.64	0.13
SO ₃	3.47	-	-	-
TiO ₂	0.21	0.27	0.09	0.03
P ₂ O ₅	-	0.07	0.02	0.01
Co ₃ O ₄	-	< 0.005	< 0.005	< 0.005
CuO	-	0.006	0.023	< 0.005
NiO	-	< 0.003	< 0.003	< 0.003
Cr ₂ O ₃	-	< 0.01	0.08	0.01
V ₂ O ₅	-	0.007	< 0.003	< 0.003
LOI	4.8	16.43	-	-

3.2.2. Mixture Proportioning and Casting

The cement to fine aggregate (sand and glass) ratio and water to cement ratio were maintained at 1:2 by mass. Natural sand was replaced with glass particles at varying amounts of 30%, 50%, 70%, and 100% by mass of the aggregates (sand). The composition of the total glass replacement was 67% crushed glass and 33% glass beads to keep the fine aggregates well-graded. The control mortar specimen contained no glass aggregates. Table 3.2 summarizes the mixture proportions for all cement mortar specimens used in this study. The mixture designation indicates that the specimens consist of a combination of two types of glass aggregates (CG and GB) as the notation “MG” refers to mixed glass. This specification is followed by the percentage of sand replaced with glass. Thus, MG-30

denotes a specimen with fine aggregates comprised of 30% glass (crushed glass and glass beads).

Table 3.2. Mass proportions of mortar mixtures

Mixture designation	Cement	Water	Fine aggregates		
			Sand	Crushed glass	Glass bead
Control	1.0	0.5	2.0	-	-
MG-30	1.0	0.5	1.4	0.40	0.20
MG-50	1.0	0.5	1.0	0.67	0.33
MG-70	1.0	0.5	0.6	0.93	0.47
MG-100	1.0	0.5	-	1.33	0.67

A set sequence and procedure were followed in the preparation of each cement mortar mixture to ensure the consistency of the specimens produced. Firstly, the cement, sand, and glass were combined and mixed until all materials were uniformly distributed. Water was slowly added to the dry materials in batches as it was mixed in a laboratory pan mixer. The total duration of mixing was three minutes. Superplasticizer was not required in any of the mixes as the low absorption of the glass particles retained free water at the surface, improving workability.

3.2.3. Test Methodology

3.2.3.1. Compressive Strength

The compressive strength of 50 mm mortar cubes was tested for each mixture at 28, 90, and 365 days after casting. Test specimens were cured in a lime-water bath, as per ASTM C192 [31] and ASTM C511 [32], at standard conditions of 20°C and at accelerated conditions of 50°C. A universal testing machine was used to apply uniaxial compressive load for which the ultimate load was recorded and used in calculating the compressive strength. In accordance with ASTM C109 [33], six specimens for each mixture and each curing condition were tested.

3.2.3.2. Plastic Shrinkage

Plastic shrinkage test procedures were based on ASTM C1579 [34]. Internal restraint was provided using a modified method established by Branston et al. [20] and Banthia and Gupta [35]. As illustrated in Figure 3.3, 500 x 320 x 50 mm concrete restraint elements with 10 mm hemispherical protrusions were used for a 30 mm mortar overlay. Plastic shrinkage tests were performed in an environmental chamber (Figure 3.4) operating at a temperature of 40°C ($\pm 2^\circ\text{C}$) and a relative humidity of 15% ($\pm 3\%$). Two heater fans and a humidifier were used to maintain the set environmental conditions, which resulted in an evaporation rate of 1 kg/m²/h. The total duration of the test was six hours.

Plastic shrinkage test specimens were analyzed by means of image processing. A digital camera was propped above the environmental chamber to capture an image of the test specimen at 1-minute intervals, for the entire duration of the test. *ImageJ* software was

then used to quantify the total crack area and maximum crack width. Further explanation on the *ImageJ* analysis is provided in the discussion section.

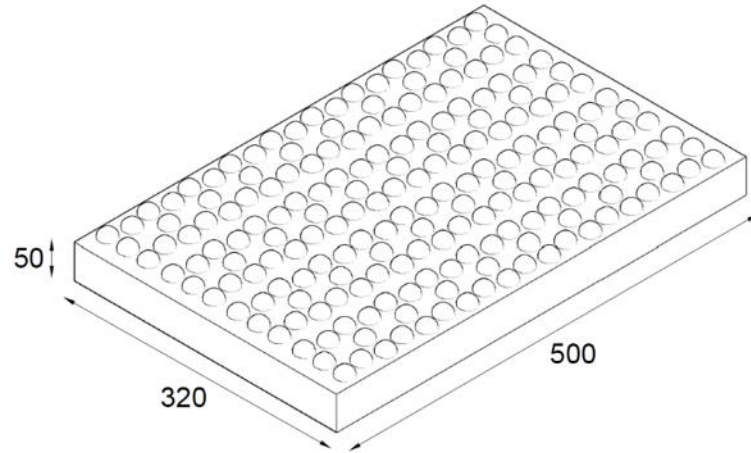


Figure 3.3. Plastic shrinkage restrain element with hemispherical protrusions

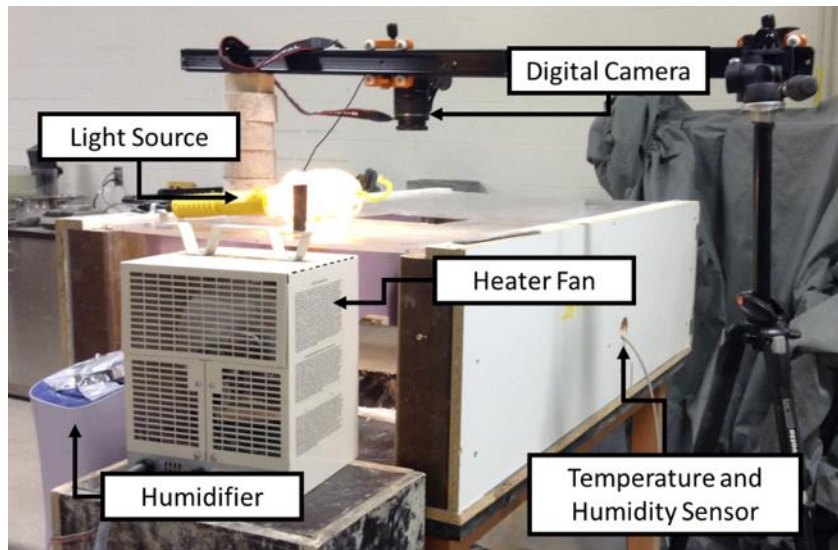


Figure 3.4. Setup of plastic shrinkage environmental test chamber

3.2.3.3. Absorption

Mortar specimens were tested for water absorption by total immersion, as per ASTM C642 [36]. Prior to immersion, two cylindrical specimens, with a diameter of 100 mm and thickness of 50 mm, were oven dried at 110°C ($\pm 2^\circ\text{C}$) for 24 hours. The mass of oven dried specimens and surface dried specimens after 24 hours of immersion was recorded. The total absorption after 48 hours of immersion is reported for each mixture at 28, 90, and 365 days after casting.

3.2.3.4. Rapid Chloride Permeability

Resistance to the penetration of chloride ions was assessed in accordance with ASTM C1202 [37]. Two 50 mm thick disks were cut from the center of cylindrical specimens with a diameter of 100 mm. The circumferential face of the mortar disks was coated with a rubber sealant and the disks were placed in a desiccator for 3 hours. The specimens were then mounted between plexiglass cells and sealed with a silicon rubber sealant. The reservoir of one cell was filled with 3% NaCl, while the other was filled with 0.3N NaOH. A potential difference of 60 ± 0.1 V DC was applied for 6 hours, and a computerized data acquisition system was used to record the charge passed at 30-minute intervals. Tests were conducted for each mixture at 28, 90, and 365 days after casting.

3.2.3.5. Thermal Conductivity

Thermal conductivity was measured in accordance with ASTM D5334 [38] using the TLS-100 Portable Thermal Conductivity/Thermal Resistivity Meter. Test specimens were prepared by casting 100 x 200 mm cement mortar cylinders. A hollow metal sleeve with a length of 100 mm and diameter of 2 mm was inserted at the center of the mortar

cylinder, approximately 30 minutes after placing the mortar mixture in the molds. Specimens were demolded after 3 days and stored in ambient temperature for the entire duration of the test. Prior to testing, thermal paste was applied to the sensor needle to provide better contact between the sensor and the metal sleeve. Figure 3.5 shows the method of testing. Measurements were taken 28, 90, and 365 days after casting. The average of 2 specimens is reported.



Figure 3.5. Testing procedure for thermal conductivity

3.3. Results and Discussion

3.3.1. Compressive Strength

The average 28, 90, and 365-day compressive strength of glass aggregate mortars under standard moist curing (20°C) are shown in Figure 3.6. The results indicate that an increase in glass content decreases compressive strength. At the age of 365 days, the decrease in strength is as much as 22% between the control specimen and the MG-100. Figure 3.6 also shows that strength increases with age. After 90 days, higher strength gain was observed for mortars containing glass aggregates, specifically MG-70 and MG-100. For specimen MG-100, the increase in compressive strength from 28 days to 365 days is

73%, whereas the increase is about 22% for the control specimen. A possible explanation for the greater strength development of glass aggregate mortars at later ages is the pozzolanic effect of the glass. According to Idir et al. [12], substantial pozzolanic activity occurs when glass particles are less than a transition fineness of 140 μm . The size of the glass beads used in the mixtures is within this range.

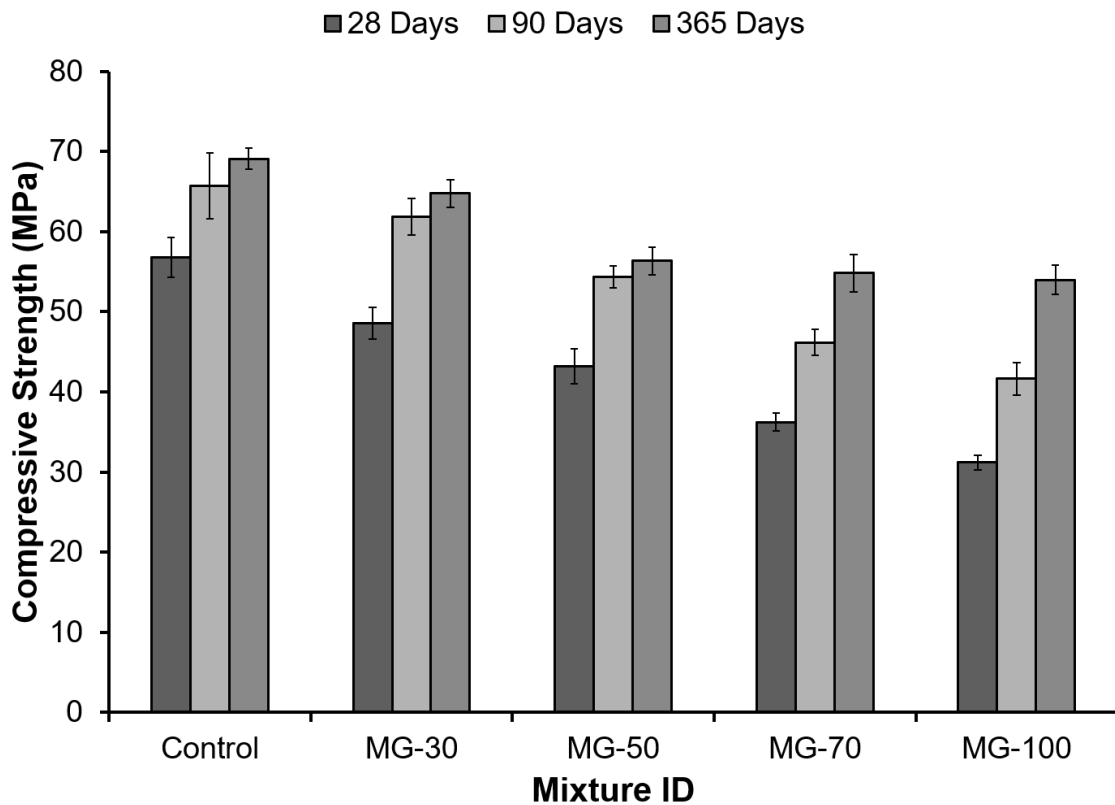


Figure 3.6. Compressive strength of glass aggregate mortar at 20°C curing condition

To further assess the strength of glass aggregate mortars, specimens were subjected to accelerated curing at 50°C (Figure 3.7). This method of curing is typically used to determine early age (28-day) strength as increased curing temperatures accelerate the process of hydration. In this study, accelerated curing was extended to evaluate compressive strength at later ages for comparison with results of standard 20°C curing.

Figure 3.7 shows that the high temperature curing of 50°C results in higher 28-day compressive strength for some glass aggregate mortars when compared with standard 20°C curing results. Specifically, MG-70 and MG-100 specimens experienced a 33% and 37% increase in 28-day compressive strength, respectively, when cured at 50°C compared to 20°C. However, the accelerated curing condition did not have a substantial effect on the control, MG-30, and MG-50 specimens. The difference in strength between glass aggregate specimens cured at 50°C and 20°C was also observed to decrease with age. For MG-70 and MG-100 specimens cured at 50°C, the strength at 365 days was less than the strength when cured at 20°C. Escalante-Garcia and Sharp [39] and Elkhadiri et al. [40] observed similar trends. According to these authors, although elevated curing temperatures significantly increases early age hydration rate, which causes higher early age strength, long term strength is decreased due to increased porosity and less uniform microstructures.

From Figure 3.7 it is also evident that all specimens containing glass aggregates exhibited insignificant strength development after 90 days, suggesting that the strength has almost stabilized after 90 days. On the other hand, there is still considerable strength development in the control specimen after 90 days. There is a 34% difference in strength between the control and MG-100 specimens after 365 days. This is 12% less than the difference found from standard 20°C curing. It is possible that the further reduction in strength is linked to the formation of delayed ettringite, which occurs because of the decomposition of primary ettringite at high temperatures, and/or high alkali silica reactivity of the glass aggregates [41]. Curing temperatures above 70°C have often been cited as the condition initiating delayed ettringite formation [42]. The extended curing condition of 50°C used in this study coupled with the low specific heat of glass could have caused the

water to absorb higher amounts of heat during hydration, thereby increasing the internal heat of hydration [43,44]. Figure 3.8 shows an SEM image of ettringite formation of an MG specimen after 365 days cured in accelerated conditions. It is important to note that it is unclear whether the ettringite observed is delayed ettringite; however, the image does indicate the maturity of the cement mortar.

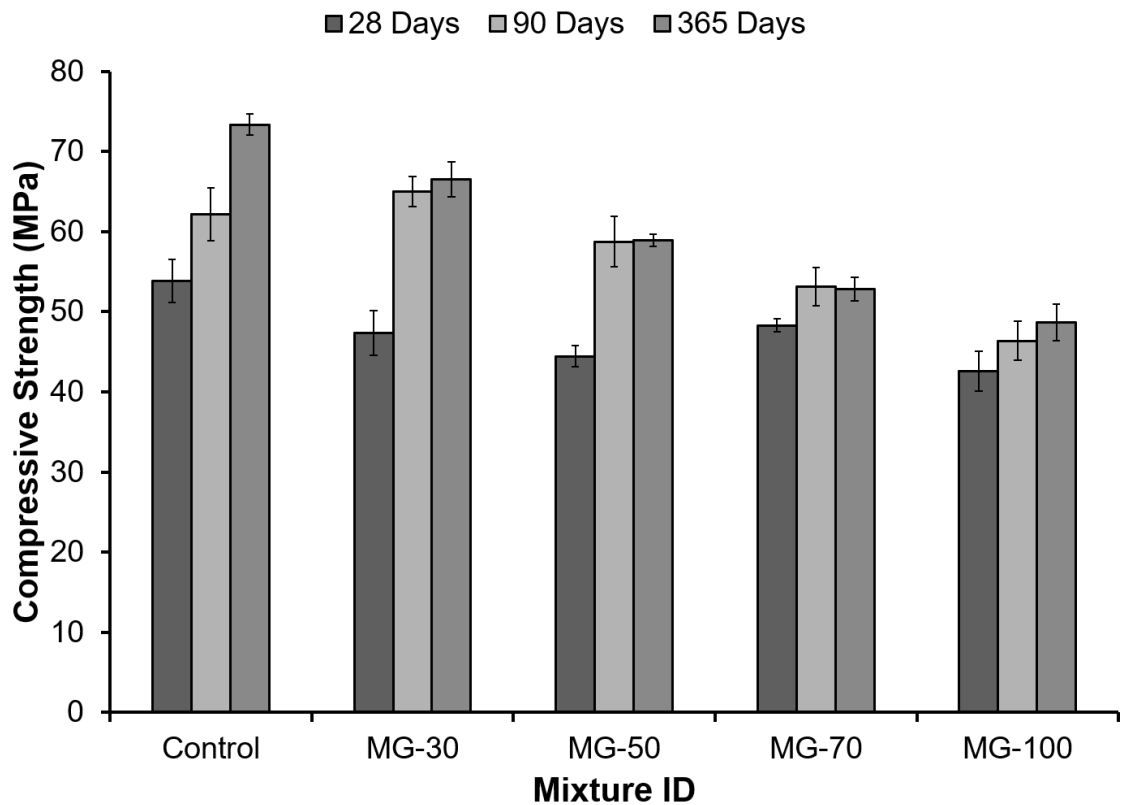


Figure 3.7. Compressive strength of glass aggregate mortar at 50°C curing condition

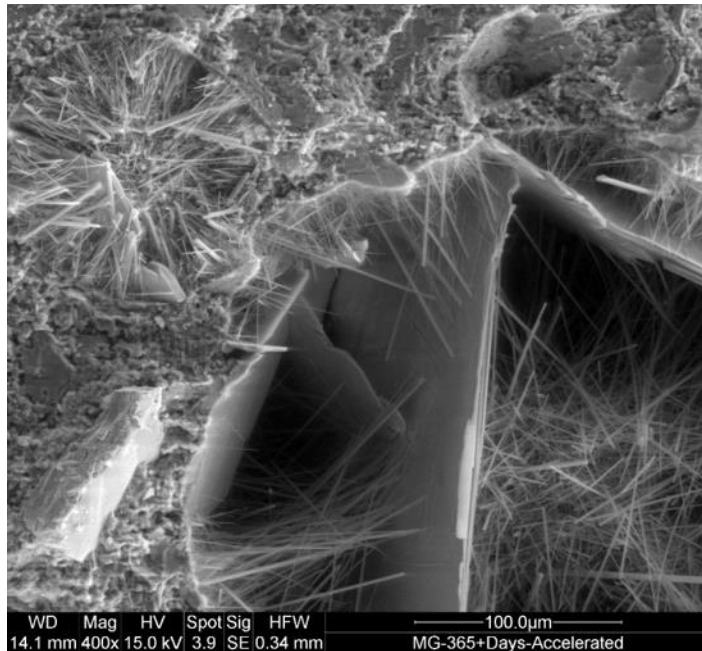


Figure 3.8. Ettringite formation in MG specimen after 365 days of 50°C curing

3.3.2. Plastic Shrinkage

Plastic shrinkage cracks mainly affect serviceability and durability of concrete and cement mortar; however, the growth of these cracks can affect strength over time. Rapid loss of moisture at the surface of freshly placed concrete or mortar induces shrinkage that often result in shallow cracks. The cracks form because of tensile stresses on plastic concrete or mortar. These stresses are developed due to restraints below the exposed surface. In this study, cracking due to plastic shrinkage was analysed using *ImageJ* software to provide better accuracy in the quantification of the surface crack properties. The captured images of the mortar surfaces were processed as an 8-bit image. Upon scaling the image, the black and white threshold was adjusted to attain the profile of the cracks. The total crack area and crack width were then determined by means of particle analysis. Figure 3.9 outlines the steps that were undertaken for the analysis.

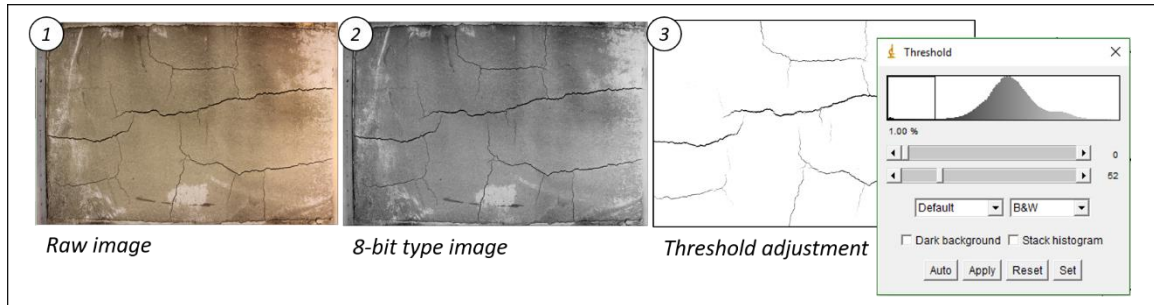


Figure 3.9. Crack area and crack width analysis using *ImageJ* software

The method of plastic shrinkage analysis allowed for the assessment of plastic shrinkage crack development. As shown in Figure 3.10, the first sign of cracking in the control mortar was observed after 60 minutes of placing. Sample images of how the cracks propagate are shown in Figure 3.11. Cracking of glass aggregate mortars ensued approximately 20 minutes later compared to the control mortar specimen. Additionally, comparison of the slope of the curves indicates that the cracks propagated faster in the control mortar compared to the glass aggregate mortars. The development of the cracks is slower for the glass aggregate mortars because of the lower absorption capacity of glass, which causes increased bleed rates. The availability of bleed water at the surface of the specimen delays drying of the surface [45]. In general, after approximately 2 hours of testing, the total crack area begins to stabilize, which indicates the setting of the mortar.

The addition of glass aggregates in mortar significantly decreases plastic shrinkage cracks. Specifically, Figure 3.12 shows that the total crack area was reduced by 81% for a glass replacement level of 30% (MG-30) when compared to the control mortar. Further, a full glass replacement (MG-100) experienced a 96% reduction in total crack area. As suggested by Tan and Du [9], dimensional stability of the mortar was likely improved by the glass aggregates. Nonetheless, the total crack area only amounted to 0.84%, 0.16%,

0.12%, 0.10%, and 0.03% of the total surface area of the control, MG-30, MG-50, MG-70, and MG-100 specimens, respectively. From the post-processed images of the cracking surface (Figure 3.13), it was also observed that there is no definite pattern in the cracks and that the width of the cracks become finer with the inclusion of glass aggregates. The maximum crack widths are quantified in Figure 3.12. These results confirm the assumption of Wright et al. [15], who stated that lower drying shrinkage, which can be achieved with glass aggregate mortars and concretes, may improve early-age cracking performance. Such reduction in total crack area and crack width indicates that glass aggregates can improve long-term durability by means of reducing passages for chlorides and other deleterious agents.

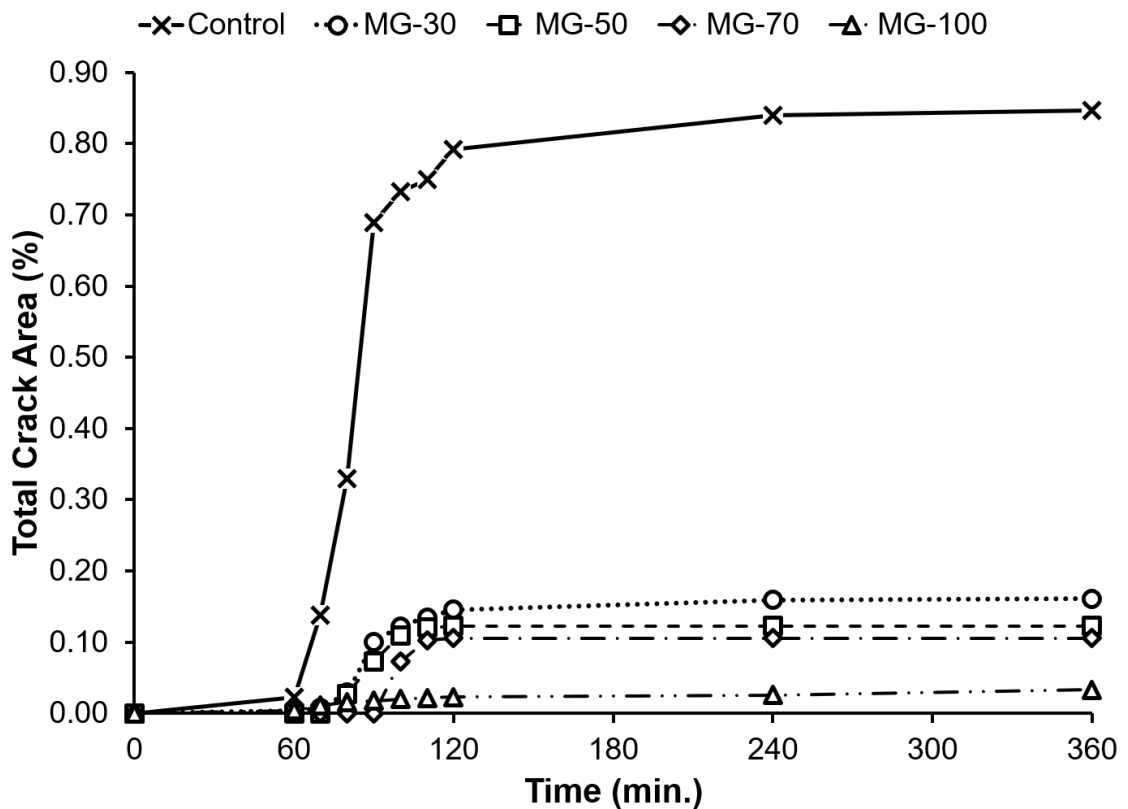


Figure 3.10. Development of plastic shrinkage cracks

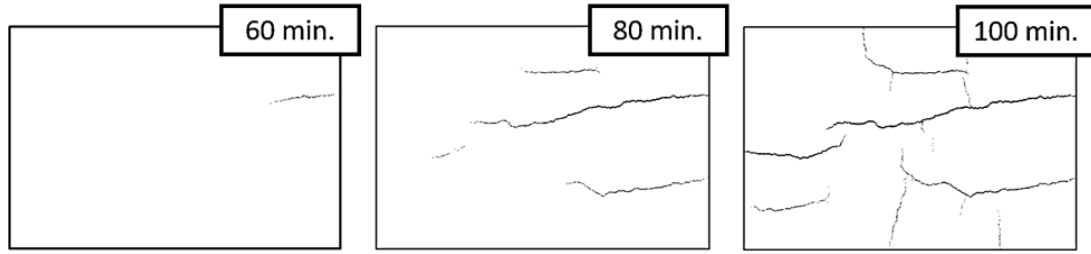


Figure 3.11. Propagation of cracks in control specimen

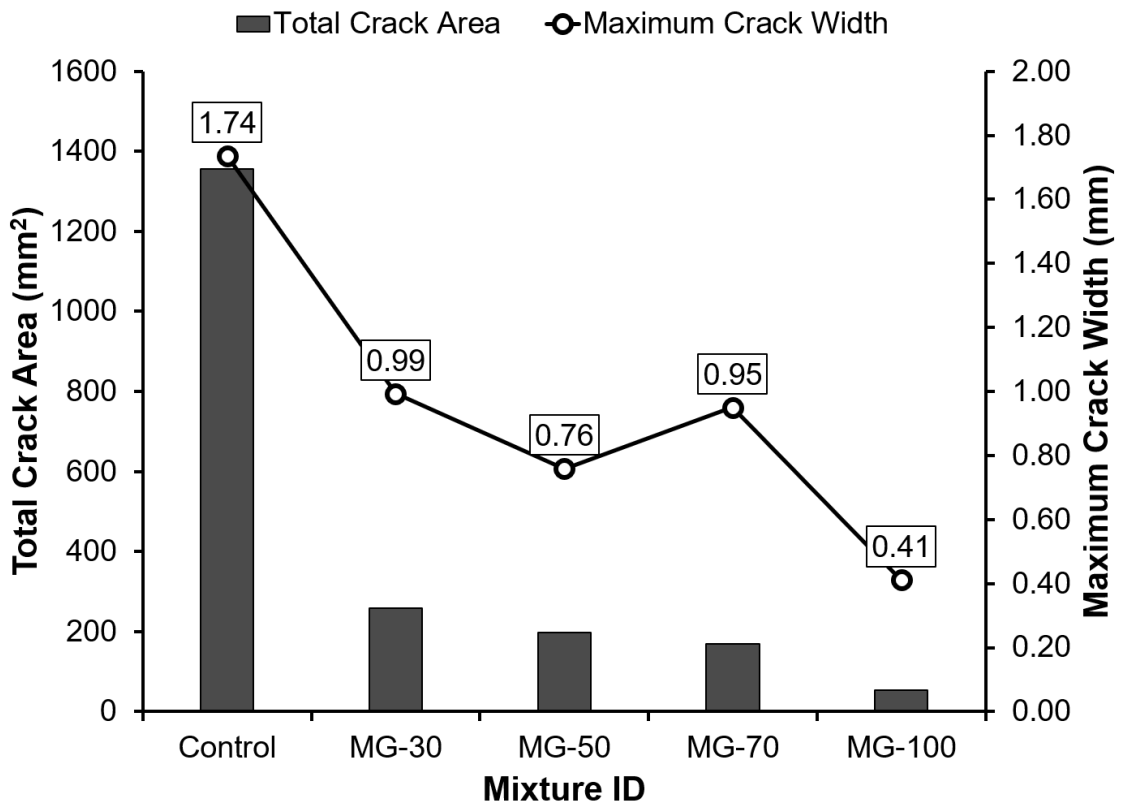


Figure 3.12. Total plastic shrinkage crack area and maximum crack width

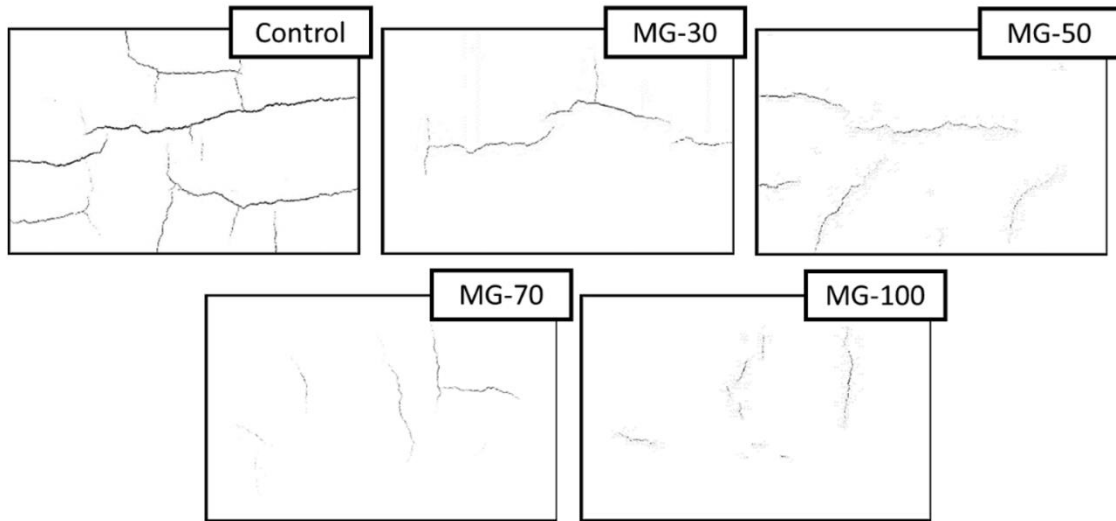


Figure 3.13. Plastic shrinkage crack patterns

3.3.3. Absorption

It was presumed that glass aggregates would reduce absorption because of their impermeable characteristic. Nonetheless, it is evident from Figure 3.14 that there is an insignificant difference between the absorption of the control mortar and the glass aggregate mortar, though the absorption of glass aggregate mortars is slightly lower. The difference in absorption after 24 hours of immersion is as much as 1.37%, 0.66%, and 0.28% at 28, 90, and 365 days, respectively. Similar results were observed by De Castro and De Brito [4] and Taha and Nounu [7]. It is possible that the shape of the crushed glass aggregates may have contributed to the minor influence of the glass on absorption as angular and irregular particles increase voids [46], and more voids increases absorption. The pre-conditioning of the specimens could have also affected the results as high temperature curing of the specimens may have caused shrinkage and microcracks in the microstructure of the mortar. Thus, regardless of glass impermeability, the improvement in immersion absorption was not realized. Furthermore, Figure 3.14 also indicates that the

amount of absorption significantly decreases with age. This is a reasonable result as the total porosity of cementitious materials generally decreases with the progress of the hydration process [47].

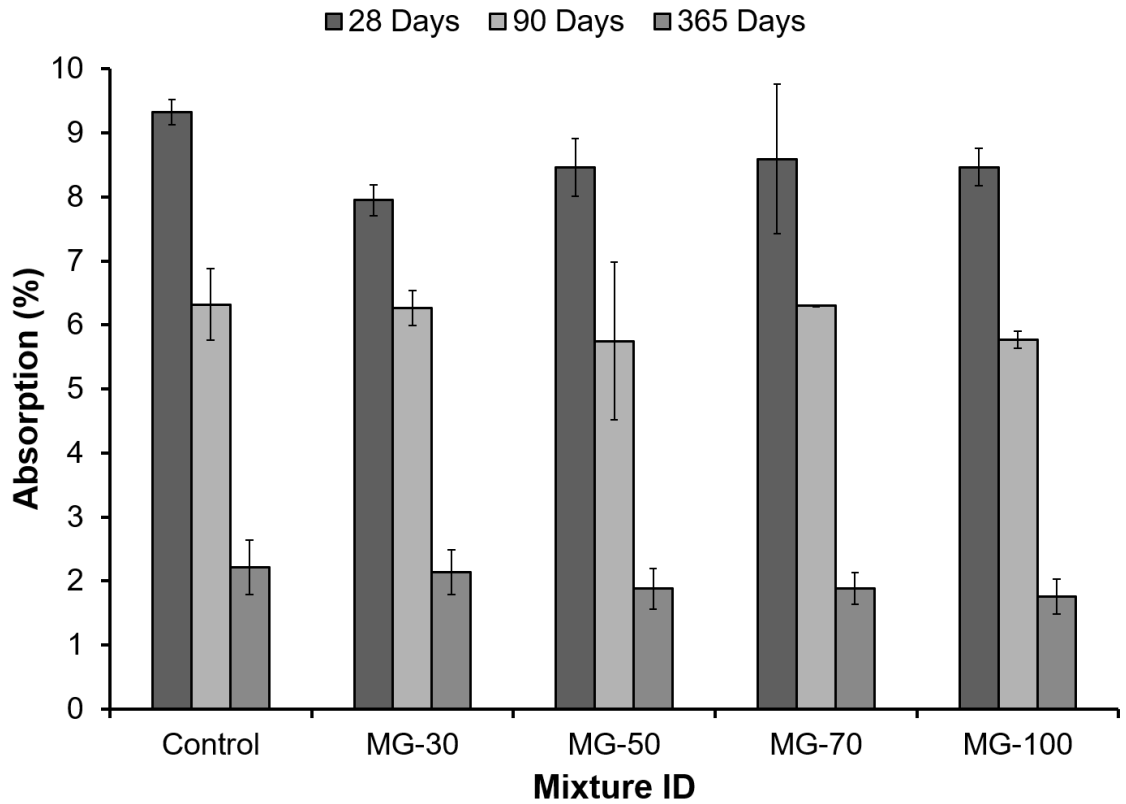


Figure 3.14. 24-hour immersion absorption of glass aggregate mortars

3.3.4. Rapid Chloride Permeability

Resistance of cementitious materials to chloride permeability is an indication of durability as permeation of chloride ions introduce problems in reinforcement corrosion and frost damage. Figure 3.15 shows the total charge passed for the glass aggregate specimens. As the amount of glass particles increases, the total charge passed is reduced. At the age of 28 days, the control mortar experienced the most chloride permeability with

a total charge passed of 9877 C, whereas MG-100 had the least charge passed of 5456 C. Thus, a reduction of about 45% was observed in MG-100. The difference after 90 days and 365 days were about 63% and 64%, respectively. These results are attributed to the lack of internal porosity of the glass particles compared to natural sand aggregates, as well as the low moisture absorption of the glass [48]. As per ASTM C1202 [37], better quality and durability is indicative of less charge passed. The results show that all cement mortar specimens in this study exhibited moderate (2000 – 4000 coulombs) to high (>4000 coulombs) values of total charge passed. Tan and Du [9] observed similar results and attributed these characteristics to the porous structure of the cement paste and the lack of coarse aggregates. In a similar manner as the absorption results, there is a substantial improvement in chloride permeability after 365 days due to the maturity of the hydration products in the pores, restricting the movement of the ions. Specifically, the 365-day permeability in all the mortar specimens was reduced to approximately half of the total charge passed at 28 days.

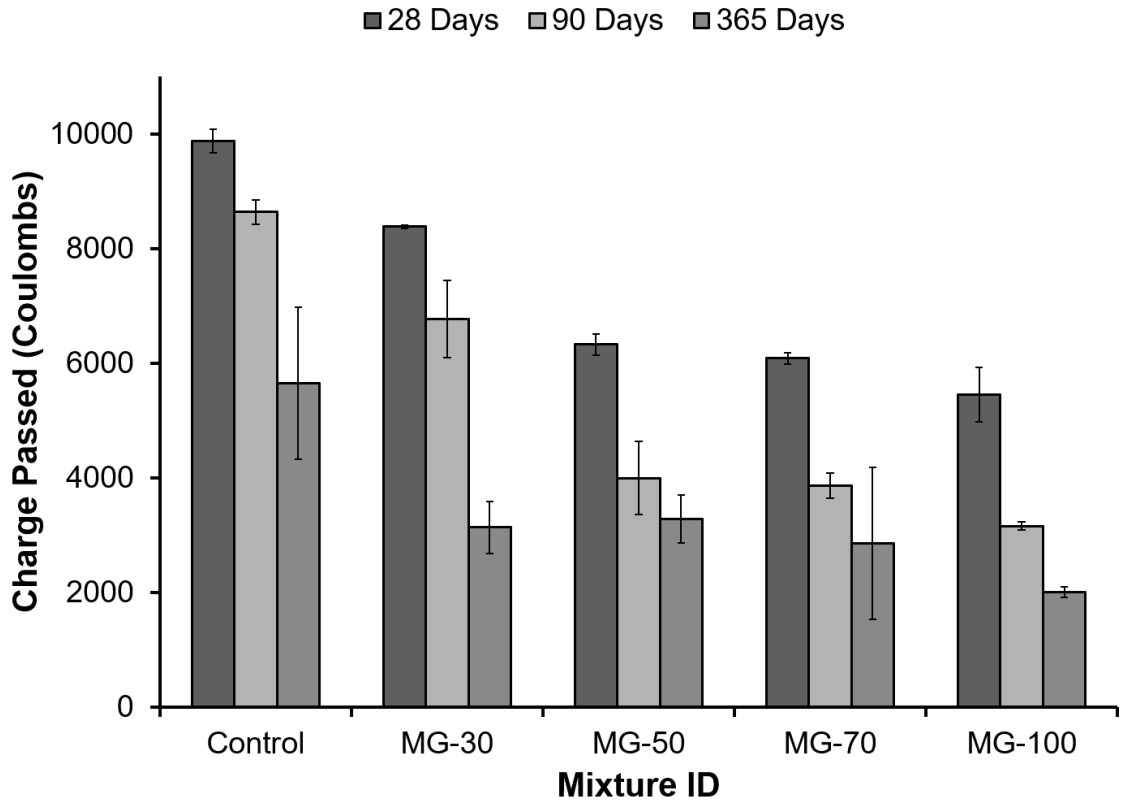


Figure 3.15. RCPT of glass aggregate mortars

3.3.5. Thermal Conductivity

In building applications, the thermal conductivity of building materials is better interpreted using the R-value. R-value is the measure of a material's ability to resist heat flow through a given thickness or, in other words, it indicates the effectiveness of insulation. Nonetheless, thermal conductivity, which is inversely related to the R-value, is commonly used in the assessment of thermal properties of materials as it is independent of thickness. Lower thermal conductivity or higher R-value means better thermal performance. Unfortunately, concrete and masonry do not contribute significantly to the R-value of typical wall assemblages [49]. Thus, typical concrete and masonry wall systems

generally consist of various insulating layers to meet standard thermal performance levels. Therefore, there is a need to improve the thermal performance of cementitious materials.

In general, glass materials have low thermal conductivity, thus it is intuitive that incorporating glass aggregates will improve the overall thermal conductivity of cementitious materials. As shown in Figure 3.16, thermal conductivity improvements of 13%, 26%, 40%, and 51% were obtained at glass replacement levels of 30%, 50%, 70%, and 100%, respectively, when compared to the control mortar at 28 days. After 365 days, there is a minor decrease in thermal conductivity, which is likely associated with the loss of water in the pores due to the hydration process. The placement of the test specimens in a controlled environment, free from excess moisture, could have also minimized the changes in thermal conductivity as moisture in the pores of the cement matrix can have a significant effect [26]. The difference between the three ages ranged from 0.010 W/(m·K) to 0.177 W/(m·K).

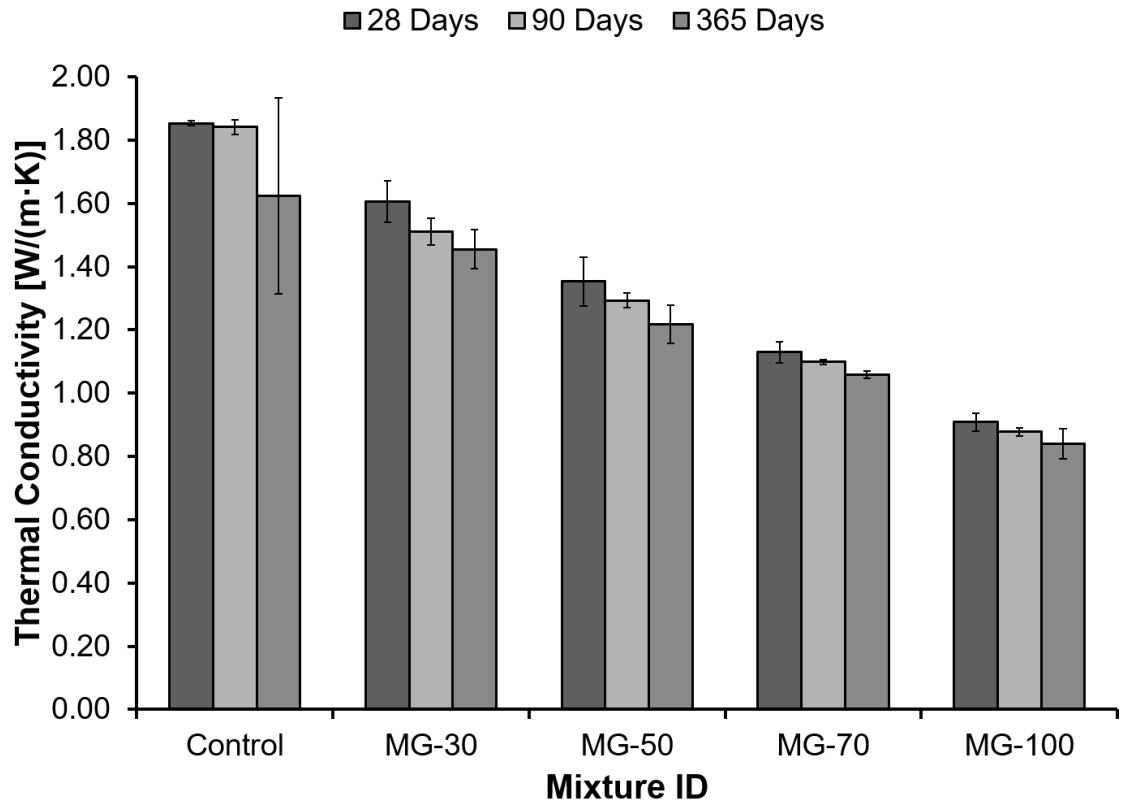


Figure 3.16. Thermal conductivity of glass aggregate mortars

3.4. Conclusions

This experimental work examined the performance of glass aggregate mortars in the areas of strength, durability, and thermal conductivity. Durability of glass aggregate mortar was qualitatively and quantitatively assessed through plastic shrinkage, immersion absorption, and rapid chloride permeability tests. The results of the study indicated that the addition of glass aggregates improves many of the properties tested in this experimental work, namely plastic shrinkage, chloride permeability, and thermal conductivity, which is beneficial in the building and construction industry. The major findings of this work are summarized as follows. It should be noted that the conclusions drawn herein may be limited to the scope of the work.

1. Glass aggregate mortars resulted in slightly lower strengths when compared to mortars containing natural sand aggregates. However, glass aggregate mortars experienced much greater strength development at later ages due to pozzolanic effect. In comparing the effects of standard (20°C) and accelerated (50°C) curing, higher 28-day strength was observed for glass aggregate specimens cured at 50°C due to the accelerated process of hydration. Nevertheless, higher temperature curing results in lower later age strength. In addition, the inherently low specific heat of glass likely increased internal heat of hydration and accelerated the hydration process. Nonetheless, delayed ettringite formation from increased curing temperatures likely caused the further reduction in strength of the glass aggregate mortars.
2. Cracking of the control mortar initiated after 60 minutes of placing under the set environmental conditions with an evaporation rate of 1kg/m²/h. Cracks in the control mortar developed earlier and propagated at faster rates compared to the glass aggregate mortar. This occurred because the availability of bleed water delayed the drying of the exposed surface. An 81% improvement in plastic shrinkage cracks was realized when 30% of glass aggregate was incorporated in mortar, whereas a 96% reduction was observed when full glass replacement was used. Glass aggregates also minimized the crack widths.
3. The various durability analyses performed indicated that glass aggregate mortars are effective in resisting penetration of aggressive agents not only through the minimization of plastic shrinkage cracks, but also through the minimization of transport of substances by absorption and permeation. Immersion absorption results of glass aggregate mortar were only slightly better than the control mortar as the angularity and

irregularity in the shape of the crushed glass may have introduced voids into the matrix. However, substantial improvements in chloride permeability was achieved with glass aggregates. The maturity of the specimens also contributed to the improvement in durability as the formation of hydration products in pores reduced the number of internal voids.

4. At 28 days, full replacement of sand with glass aggregates significantly decreased thermal conductivity by 51% when compared with the control mortar. The inherently low thermal conductivity of the glass aggregates is responsible for the reduction in the overall thermal conductivity of the mortar specimens. Minimal variation in thermal conductivity was observed over the ages of 28, 90, and 365 days. This result is likely due to the well controlled testing environment.

3.5. Acknowledgements

The authors acknowledge the Natural Sciences and Engineering Research Council of Canada for the financial support provided to Karla Gorospe in the form of the Canada Graduate Scholarship and the Discovery Grant to Dr. Sreekanta Das.

3.6. References

- [1] United States Environmental Protection Agency (USEPA), Facts and Figures about Materials, Waste and Recycling - Glass: Material-Specific Data. <https://www.epa.gov/facts-and-figures-about-materials-waste-and-recycling/glass-material-specific-data>, 2018 (accessed 3 July 2018).
- [2] C.W. Foster, Use of waste glass as asphaltic concrete aggregate, Masters Theses. 7187 (1970).
- [3] W.R. Malisch, D.E. Day, B.G. Wixson, Use of domestic waste glass as aggregate in bituminous concrete, Highway Research Board. (1970) 1–10.

- [4] S. De Castro, J. De Brito, Evaluation of the durability of concrete made with crushed glass aggregates, *Journal of Cleaner Production*. 41 (2013) 7–14.
- [5] İ.B. Topçu, M. Canbaz, Properties of concrete containing waste glass, *Cement and Concrete Research*. 34 (2004) 267–274.
- [6] H. Du, K.H. Tan, Use of waste glass as sand in mortar: Part II - Alkali-silica reaction and mitigation methods, *Cement and Concrete Composites*. 35 (2013) 109–117.
- [7] B. Taha, G. Nounu, Utilizing waste recycled glass as sand/cement replacement in concrete, *Journal of Materials in Civil Engineering*. 21 (2009) 709–721.
- [8] S.Y. Choi, Y.S. Choi, E.I. Yang, Effects of heavy weight waste glass recycled as fine aggregate on the mechanical properties of mortar specimens, *Annals of Nuclear Energy*. 99 (2017) 372–382.
- [9] K.H. Tan, H. Du, Use of waste glass as sand in mortar: Part I - Fresh, mechanical and durability properties, *Cement and Concrete Composites*. 35 (2013) 118–126.
- [10] A. Mardani-Aghabaglou, M. Tuyan, K. Ramyar, Mechanical and durability performance of concrete incorporating fine recycled concrete and glass aggregates, *Materials and Structures*. 48 (2015) 2629–2640.
- [11] Z.Z. Ismail, E.A. AL-Hashmi, Recycling of waste glass as a partial replacement for fine aggregate in concrete, *Waste Management*. 29 (2009) 655–659.
- [12] R. Idir, M. Cyr, A. Tagnit-Hamou, Use of fine glass as ASR inhibitor in glass aggregate mortars, *Construction and Building Materials*. 24 (2010) 1309–1312.
- [13] K. Afshinnia, P.R. Rangaraju, Impact of combined use of ground glass powder and crushed glass aggregate on selected properties of Portland cement concrete, *Construction and Building Materials*. 117 (2016) 263–272.
- [14] M. Kamali, A. Ghahremaninezhad, Effect of glass powders on the mechanical and durability properties of cementitious materials, *Construction and Building Materials*. 98 (2015) 407–416.
- [15] J.R. Wright, C. Cartwright, D. Fura, F. Rajabipour, Fresh and Hardened Properties of Concrete Incorporating Recycled Glass as 100% Sand Replacement, *Journal of Materials in Civil Engineering*. 26 (2014) 4014073.
- [16] T.C. Ling, C.S. Poon, A comparative study on the feasible use of recycled beverage and CRT funnel glass as fine aggregate in cement mortar, *Journal of Cleaner Production*. 29–30 (2012) 46–52.

- [17] N. Almesfer, J. Ingham, Effect of waste glass on the properties of concrete, *Journal of Materials in Civil Engineering* 26 (2014) 6014022.
- [18] S.B. Park, B.C. Lee, J.H. Kim, Studies on mechanical properties of concrete containing waste glass aggregate, *Cement and Concrete Research*. 34 (2004) 2181–2189.
- [19] National Ready Mixed Concrete Association (NRMCA), CIP 5 - Plastic Shrinkage Cracking. <https://www.nrmca.org/aboutconcrete/cips/05pr.pdf>, 2014.
- [20] J. Branston, S. Das, S.Y. Kenno, C. Taylor, Influence of basalt fibres on free and restrained plastic shrinkage, *Cement and Concrete Composites*. 74 (2016) 182–190.
- [21] A.E. Naaman, T. Wongtanakitcharoen, G. Hauser, Influence of different fibers on plastic shrinkage cracking of concrete, *ACI Materials Journal*. 102 (2005) 49–58.
- [22] M. Branch, J. and Rawling, A. and Hannant, D.J. and Mulheron, The effects of fibres on the plastic shrinkage cracking of high strength concrete, *Materials and Structures*. 35 (2002) 189–194.
- [23] J. Bisschop, J.G. van Mier, Effect of aggregates on drying shrinkage microcracking in cement-based composites, *Materials and Structures*. 35 (2002) 453–461.
- [24] E. Holt, M. Leivo, Cracking risks associated with early age shrinkage *Cement and Concrete Composites*. 26 (2004) 521–530.
- [25] L. Basheer, J. Kropp, D.J. Cleland, Assessment of the durability of concrete from its permeation properties: A review, *Construction and Building Materials*. 15 (2001) 93–103.
- [26] J.M.P.Q. Delgado, A.S. Guimarães, V.P. De Freitas, I. Antepará, V. Kočí, R. Černý, Salt Damage and Rising Damp Treatment in Building Structures, *Advances in Materials Science and Engineering*. 2016 (2016) 1–13.
- [27] ACI Committee 122, ACI 122R-02: Guide to Thermal Properties of Concrete and Masonry Systems, Technical Documents. (2002) 21.
- [28] T.S. Yun, Y.J. Jeong, K.S. Youm, Effect of surrogate aggregates on the thermal conductivity of concrete at ambient and elevated temperatures, *The Scientific World Journal*. 2014 (2014) 1–9.
- [29] A. Alani, J. MacMullen, O. Telik, Z.Y. Zhang, Investigation into the thermal performance of recycled glass screed for construction purposes, *Construction and Building Materials*. 29 (2012) 527–532.
- [30] CSA A3001, Cementitious materials used in concrete, Canadian Standards Association., Mississauga, Ontario, 2013.

- [31] ASTM C192, Standard Practice for making and curing concrete test specimens in the laboratory, ASTM International, West Conshohocken, PA, 2018.
- [32] ASTM C511, Standard specification for mixing rooms, moist cabinets, moist rooms, and water storage tanks used in the testing of hydraulic cements and concretes, ASTM International, West Conshohocken, PA, 2013.
- [33] ASTM C109, Standard test method for compressive strength of hydraulic cement mortars (using 2-in. or [50mm] cube specimens), ASTM International, West Conshohocken, PA, 2016.
- [34] ASTM C1579, Standard test method for evaluating plastic shrinkage cracking of restrained fiber reinforced concrete (using a steel form insert), ASTM International, West Conshohocken, PA, 2013.
- [35] N. Banthia, R. Gupta, Test method for evaluation of plastic shrinkage cracking in fiber-reinforced cementitious materials, *Experimental Techniques*. 31 (2007) 44–48.
- [36] ASTM C642, Standard test method for density, absorption, and voids in hardened concrete, ASTM International, West Conshohocken, PA, 2013.
- [37] ASTM C1202, Standard test method for electrical indication of concrete’s ability to resist chloride ion penetration, ASTM International, West Conshohocken, PA, 2012.
- [38] ASTM D5334, Standard test method for determination of thermal conductivity of soil and soft rock by thermal needle probe procedure, ASTM International, West Conshohocken, PA, 2014.
- [39] J.I. Escalante-García, J.H. Sharp, The microstructure and mechanical properties of blended cements hydrated at various temperatures, *Cement and Concrete Research*. 31 (2001) 695–702.
- [40] I. Elkhadiri, M. Elkhadiri, F. Puertas, Effect of curing temperature on cement hydration, *Journal Ceramics-Silikáty*. 53 (2009) 65–75.
- [41] Portland Cement Association (PCA), Ettringite Formation and the Performance of Concrete, PCA R&D, 2166 (2001) 1–16.
- [42] S. Diamond, Delayed ettringite formation - Processes and problems, *Cement and Concrete Composites*. 18 (1996) 205–215.
- [43] S. Poutos, K., and Nwaubani, Strength development of concrete made with recycled glass aggregates subjected to frost curing conditions, *International Journal of Application or Innovation in Engineering & Management*. 2 (2013) 19–28.

- [44] K.H. Poutos, A.M. Alani, P.J. Walden, C.M. Sangha, Relative temperature changes within concrete made with recycled glass aggregate, *Construction and Building Materials*. 22 (2008) 557–565.
- [45] G.M. Sadiqul Islam, S. Das Gupta, Evaluating plastic shrinkage and permeability of polypropylene fiber reinforced concrete, *International Journal of Sustainable Built Environment*. 5 (2016) 345–354.
- [46] D.D. Cortes, H.K. Kim, A.M. Palomino, J.C. Santamarina, Rheological and mechanical properties of mortars prepared with natural and manufactured sands, *Cement and Concrete Research*. 38 (2008) 1142–1147.
- [47] M.S. Meddah, A. Tagnit-Hamou, Pore structure of concrete with mineral admixtures and its effect on self-desiccation shrinkage, *ACI Materials Journal*. 106 (2009) 241–250.
- [48] S.C. Kou, C.S. Poon, Properties of self-compacting concrete prepared with recycled glass aggregate, *Cement and Concrete Composites*. 31 (2009) 107–113.
- [49] J. Straube, *Meeting and Exceeding Building Code Thermal Performance Requirements*, RDH Building Science, 2017.

CHAPTER 4

DURABILITY OF GLASS AGGREGATE MORTARS CONTAINING SUPPLEMENTARY CEMENTITIOUS MATERIALS

4.1. Introduction

Concrete is the world's leading building material. However, emissions from global cement production are staggeringly high and are of major concern. In 2016, it was estimated that 10.5 EJ of energy was consumed and 2.2 Gt of CO₂ was generated in the global production of cement [1]. In order to reduce the environmental impacts associated with concrete materials, the consumption of cement must be reduced. This can be achieved by using sustainable supplementary cementitious materials (SCMs). SCMs can be obtained naturally or from waste by-products of various processes. Natural SCMs include metakaolin, calcined shale or clay, and volcanic ash, to name a few. On the other hand, fly ash, slag, and silica fume are SCMs originating from waste by-products of coal, steel, and silicon metal and ferrosilicon alloy plants, respectively. Thus, partial replacement of cement with SCMs produces a sustainable and greener concrete material. Likewise, the quarrying of natural aggregates for concrete production also poses environmental impacts. Nonetheless, the use of recycled aggregates, such as glass, can further improve the sustainability of conventional concrete materials.

It has been well researched that the use of SCMs can enhance the fresh and hardened properties of concrete by improving its workability, strength, and durability. Specifically, the use of fly ash has been shown to reduce drying shrinkage and permeability through the enhancement of the concrete microstructure [2–5]. Fly ash has also been shown to reduce expansions due to alkali silica reaction (ASR); however, the reduction in expansion

depends on the class of the fly ash used. Studies in the literature have reported that class F fly ash performs better than class C fly ash because it contains less CaO [6]. It has also been reported that the use of fly ash as partial cement replacement reduces early-age compressive strength due to its slower reaction rate [7,8]. Unlike fly ash, slag exhibits high hydration activity, thereby resulting in improved early-age compressive strength [9]. In terms of durability, concrete containing slag blends exhibit similar benefits as concrete containing fly ash blends since slag is also effective in reducing permeability, chloride penetration, and ASR [10].

Silica fume is a very reactive SCM due to its chemical and physical properties. Hence, it is very effective even at lower replacement levels. Typical silica fume replacements range from 5% to 15% [11]. Silica fume in concrete can significantly improve strength and durability through pore-size refinement, matrix densification, and interfacial transition zone refinement between the cement paste and the aggregates [11]. At similar replacement levels, metakaolin has been found to be comparable to silica fume. Specifically, Poon et al. [12] reported that the chloride resistance of concrete containing SF and MK are similar at water-to-binder ratios of 0.3 and 0.5. However, there have been reports indicating that concrete with SF blends resists chloride ion penetration slightly better than concrete with MK blends [13]. Moreover, studies have shown that concrete containing SF exhibit marginally lower absorption characteristics compared to concrete containing MK [14]. Nonetheless, in terms of strength, MK outperforms SF [12].

Aside from binary blends, the effects of ternary and quaternary blends of SCMs in concrete materials have also been studied by several researchers [4,15–17]. In general, ternary and quaternary cementitious blends further improve the strength and durability

properties of cementitious materials. However, predicting the outcomes of varying combinations of SCMs is challenging as the interaction between multiple SCMs produces synergistic effects, which are often influenced by the chemical composition and physical properties of the SCMs used.

The combined use of glass aggregates and SCMs have been well documented in the literature. The primary reason for the use of SCMs in glass aggregate concrete and mortar is to mitigate and even eliminate deleterious expansions associated with alkali silica reaction [18–20]. The lower alkalinity of SCMs compared to ordinary cement is the foremost reason for its effectiveness in reducing ASR expansion. Nonetheless, the overall effectiveness of SCMs in glass aggregate concrete and mortar is still dependent on its chemical and physical characteristics. According to studies conducted by Du and Tan [21], the inclusion of SCMs in combination with glass aggregates further improves resistance to chloride ion penetration, drying shrinkage, compressive strength, split tensile strength, and flexural strength.

Although several studies have investigated the use of SCMs in glass aggregate concrete and mortar, many have only considered the effects of one, two, or even three types of SCM. There are also very few studies on glass aggregate concrete and mortar containing ternary cementitious blends. In addition, these studies have been limited to concrete and mortars containing one type of glass aggregates. Thus, this study was designed to provide a reasonable comparison between four different SCMs in binary and ternary combinations. The various SCM blends were used to produce mortars containing two types of glass aggregates. A comprehensive and extensive research was conducted on a total of 25 glass aggregate mortar mixtures. The binary and ternary blend mixtures were composed of

cement and either fly ash class F, slag, silica fume, or metakaolin. The effect of the SCM blends on compressive strength, alkali silica reaction, chloride permeability, and sorptivity was investigated and optimum SCM blends were determined.

4.2. Experimental Procedure

An experimental method was undertaken to determine the strength and durability properties of glass aggregate mortars containing supplementary cementitious materials (SCM). The influence of binary and ternary cementitious blends, consisting of fly ash, slag, silica fume, metakaolin, and a combination thereof, were investigated in this study. Tests on compressive strength, alkali silica reaction (ASR), chloride permeability, and sorptivity were conducted and the optimum combination and replacement level of SCM was determined.

4.2.1. Materials

All blended cement mortar specimens were prepared using fine aggregates composed of natural sand with a fineness modulus of 2.63 and commercially purchased glass particles made from 100% recycled glass. The glass aggregates used include crushed glass and glass beads. The crushed glass aggregates have particle sizes ranging from 600 to 850 μm and density of 2499 kg/m^3 , whereas the glass bead aggregates have particle sizes ranging from 40 to 125 μm and density of 1249 kg/m^3 . The cementitious materials used include general use Portland limestone cement (PC), conforming to CAN/CSA-A3001 [22], and fly ash class F (FA), slag (SG), silica fume (SF), and metakaolin (MK). The chemical composition of the cement and four SCMs are presented in Table 1. These properties were obtained through x-ray fluorescence analysis.

Table 4.1. Chemical composition of cementitious materials (%)

Analyte Symbol	PC	FA	SG	SF	MK
C ₃ O ₄	< 0.005	< 0.005	< 0.005	< 0.005	< 0.005
CuO	0.01	0.009	0.005	< 0.005	< 0.005
NiO	< 0.003	0.231	< 0.003	0.004	< 0.003
SiO ₂	19.78	61.3	36.9	85.39	63.49
Al ₂ O ₃	5.38	19.91	9.08	6.27	29.85
Fe ₂ O ₃ (T)	2.67	6.9	0.61	0.19	1.19
MnO	0.066	0.066	0.327	0.007	0.01
MgO	2.44	1.74	10.91	< 0.01	0.49
CaO	62.43	1.33	37.6	0.03	0.35
Na ₂ O	0.12	1.02	0.25	0.11	0.14
K ₂ O	0.49	2.26	0.26	0.04	1.81
TiO ₂	0.31	0.9	0.36	0.07	0.68
P ₂ O ₅	0.13	0.15	0.01	0.37	0.03
Cr ₂ O ₃	0.01	0.04	0.01	< 0.01	0.01
V ₂ O ₅	0.009	0.953	0.004	0.004	0.022
LOI	1.52	3.65	0.26	0.88	2.03
Total	95.38	100.5	96.58	93.38	100.1

4.2.2. Mixture Proportioning

For all blended cement mortar specimens, the binder to fine aggregate (sand and glass) ratio was maintained at 1:2 by mass. The water to binder ratio was also maintained at 1:2 by mass. Fine aggregates constituted 70% sand and 30% glass (20% crushed glass and 10% glass beads), which was kept unchanged for all mortar specimens. The control mortar was made with only standard Portland cement (PC), whereas binary blends consisted of PC and one type of supplementary cementitious material (SCM) – FA, SG, SF, or MK. The replacement levels of the SCMs were decided based on literature. FA and SG were used at replacement levels of 15% and 30% and were categorized as Group 1 SCMs, whereas SF and MK were used at replacement levels of 5% and 10% and were categorized as Group 2 SCMs. The mixture designation for binary blend mixtures is simply

the SCM abbreviation followed by the amount of replacement by mass. For example, mixture FA-15 indicates that 15% of the Portland cement was replaced with fly ash. Two sets of ternary blend mixtures were also investigated. The first set of ternary blend mixtures is FA-based, while the second set is SG-based. FA-based ternary blends consist of FA as the primary cement replacement and either SF or MK (Group 2 SCM) as the secondary cement replacement. Likewise, SG-based ternary blends consist of SG as the primary cement replacement and one Group 2 SCM as the secondary cement replacement. For the ternary blends, the mixture designation specifies the two levels of SCM replacement. For example, FA-15-SF-5 indicates that 15% of the cementitious material is fly ash, 5% is silica fume, and the remaining 80% is Portland cement. All 25 mixtures are summarized in Table 2. Superplasticizers were not required in any of the mixtures and ASTM C305 [23] was followed for the mixing procedure.

Table 4.2. Mass proportions of mortar mixtures

Mixture designation	Water	Sand	Glass	Cementitious Materials					
				PC	FA	SG	SF	MK	
Control	0.50	1.40	0.60	1.00	-	-	-	-	
Binary Blends	0.50	1.40	0.60	FA-15	0.85	0.15	-	-	-
				FA-30	0.70	0.30	-	-	-
				SG-15	0.85	-	0.15	-	-
				SG-30	0.70	-	0.30	-	-
				SF-5	0.95	-	-	0.05	-
				SF-10	0.90	-	-	0.10	-
				MK-5	0.95	-	-	-	0.05
				MK-10	0.90	-	-	-	0.10
Ternary Blends	0.50	1.40	0.60	FA-15-SF-5	0.80	0.15	-	0.05	-
				FA-30-SF-5	0.65	0.30	-	0.05	-
				FA-15-SF-10	0.75	0.15	-	0.10	-
				FA-30-SF-10	0.60	0.30	-	0.10	-
				FA-15-MK-5	0.80	0.15	-	-	0.05
				FA-30-MK-5	0.65	0.30	-	-	0.05
				FA-15-MK-10	0.75	0.15	-	-	0.10
				FA-30-MK-10	0.60	0.30	-	-	0.10
				SG-15-SF-5	0.80	-	0.15	0.05	-
				SG-30-SF-5	0.65	-	0.30	0.05	-
				SG-15-SF-10	0.75	-	0.15	0.10	-
				SG-30-SF-10	0.60	-	0.30	0.10	-
				SG-15-MK-5	0.80	-	0.15	-	0.05
				SG-30-MK-5	0.65	-	0.30	-	0.05
				SG-15-MK-10	0.75	-	0.15	-	0.10
				SG-30-MK-10	0.60	-	0.30	-	0.10

4.2.3. Test Methodology

4.2.3.1. Compressive Strength

A compressive strength test of 50 mm mortar cube specimens was performed using a universal testing machine, as per ASTM C109 [24]. Specimens were cured in lime-water at 20°C and were surface dried prior to testing. For each mixture, a total of five specimens were casted and tested at the ages of 28 and 90 days.

4.2.3.2. Alkali Silica Reaction

Expansion due to ASR was determined in accordance to ASTM C1567 [25]. Four standard mortar bar specimens (25 mm x 25 mm x 250 mm) were cast for each mixture. The specimens were demolded after 24 hours of casting and were placed in a water bath at 80°C. The specimens were removed from the water bath after 24 hours and a length reading was taken prior to placing the specimens in NaOH solution at 80°C. The change in length of the specimens was periodically measured using a length comparator and the average expansion after 14 days of exposure to the NaOH solution was reported. It is important to note that the testing procedure followed provides a very aggressive alkaline environment, resulting in very conservative values of expansion.

4.2.3.3. Chloride Permeability

ASTM C1202 [26] was followed to determine the resistance of the mortar specimens to the penetration of chloride ions. For each mixture, cylindrical specimens (100 mm diameter x 200 mm height) were cast and cured in lime-water. Two 50 mm thick disks, cut from the mid-length of the cylindrical specimens, were placed in a desiccator for 3

hours prior to testing. The specimens were then mounted between two plexiglass cells. One cell was filled with 0.3 mol NaOH solution, while the opposite cell was filled with 3% NaCl solution. A potential difference of 60 V DC was applied for 6 hours, and a data acquisition system was used to record the charge passed in coulombs (C) at 30-minute intervals. Tests were conducted at the ages of 28 days and 90 days.

4.2.3.4. Sorptivity

The sorptivity of glass aggregate mortar specimens was determined as per ASTM C1585 [27]. Two cylindrical specimens with a diameter of 100 mm and thickness of 50 mm were oven dried at 110°C ($\pm 2^\circ\text{C}$) for 24 hours. A silicon coating was applied along the periphery of the mortar specimens to prevent the evaporation of moisture. The initial mass of the specimens was recorded prior to its placement on top of supports in a pan filled with water. The water level in the pan was maintained at 1 mm to 3 mm above the supports. The mass of the specimens was measured after 1, 4, 9, 16, 25, 49, and 64 minutes of contact with water and the absorption was calculated by dividing the change in mass by the product of the nominal surface area exposed to water and the density of water. In plotting the absorption against the square root of time, initial sorptivity was determined from the slope of the line of best fit. The test was performed after 28 days and 90 days of casting.

4.3. Results and Discussion

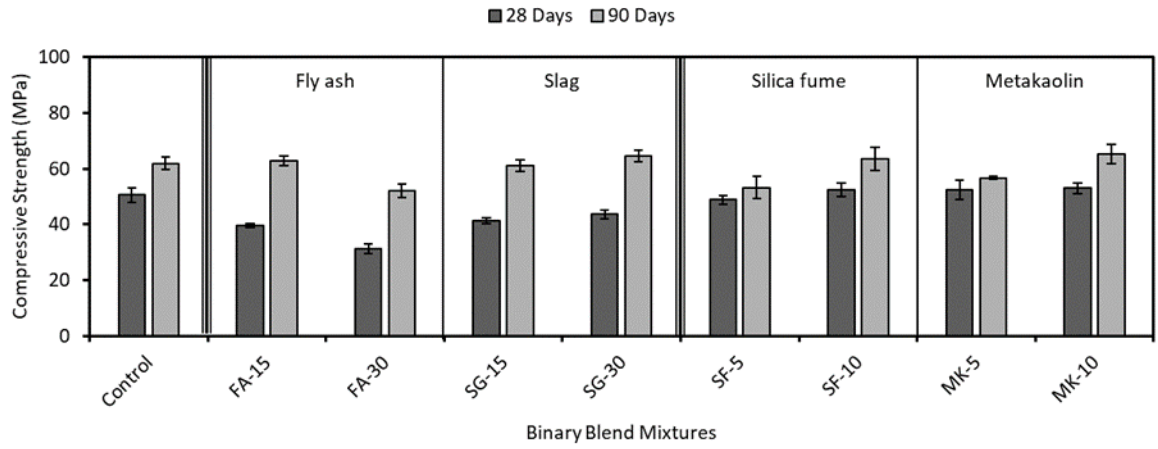
4.3.1 Compressive Strength

The average compressive strength of glass aggregate mortars containing SCM binary blends is presented in Figure 1(a). At 28 days, an insignificant increase in strength was observed when SG, SF, and MK content was increased. However, an apparent decrease in strength of 21% was found when FA content was increased. The difference in strength with increasing amount of SCM was more evident at 90 days for mixtures containing Group 2 SCM binary blends (SF and MK). Between SF-5 and SF-10, the increase was 19%, whereas the increase between MK-5 and MK-10 was 15%. For SG binary blend mixtures, the increase in strength between SG-15 and SG-30 was 5.9% at 90 days, which is comparable with the 5.7% increase observed at 28 days. Again, at 90 days, a decrease in strength (17%) was observed when FA content was increased. In general, the inclusion of FA decreases the strength of cementitious materials at early ages due to its slower process of pozzolanic reaction [28–30]. Hence, among all binary blend mixtures, FA-30 exhibited the lowest strength of 31.3 MPa and 52.2 MPa at 28 and 90 days, respectively. Between the SCMs in each group, it was found that SG was more effective in improving strength compared to FA, while MK marginally outperformed SF. The compressive strength of all Group 1 SCM binary blend mixtures, at 28 days, was significantly lower than the control, which contains no SCM. On the other hand, binary blend mixtures containing Group 2 SCMs were within 3% lower (SF-5) or higher (SF-10, MK-5, and MK-10) than the control. Nonetheless, SG-30, SF-10, and MK-10 all exhibited higher strength compared to the control at 90 days.

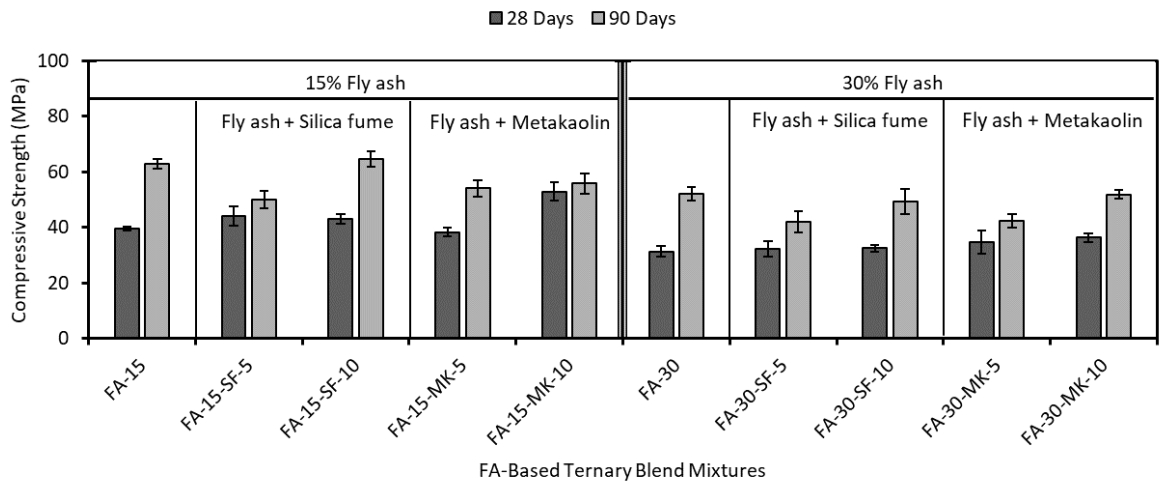
The compressive strength of FA-based ternary blend mixtures is shown in Figure 1(b). At 28 and 90 days, it is evident that increasing the FA content decreases the strength, regardless of the Group 2 SCM added. This trend is similar to the results obtained for FA binary blend mixtures. Furthermore, when FA content is kept unchanged, increasing the replacement level of the Group 2 SCM caused a general increase in strength. At 28 days, all ternary blend mixtures were comparable to or higher than their corresponding base binary blend mixtures (FA-15 and FA-30), and mixture FA-15-MK-10 even exhibited a compressive strength (52.9 MPa) higher than the control (50.6 MPa). Thus, the addition of Group 2 SCMs as secondary cement replacement was effective in improving compressive strength. Conversely, it was found that the strength at 90 days is generally lower than the strength of the base binary blend mixtures. This contradicts several studies that have observed improvements in compressive strength with ternary blends compared to a relative binary blend [30,31]. However, a possible reason for the lower 90-day strength of the FA-based ternary blend mixtures containing SF is the formation of a layer of reaction product in the matrix that inhibits further reaction of SF with calcium hydroxide [16,32]. Similarly, for ternary blend mixtures containing MK, Wild et. al [33] reported that a critical change in the reaction between MK and calcium hydroxide can inhibit further reaction of MK, even with ample supply of MK present. Further, Gesoğlu et al. [15] reported similar findings in compressive strength and suggested that among the other SCMs used, FA governed the reduction in strength of the ternary blends.

SG-based ternary blend mixtures exhibited similar trends as the FA-based ternary blend mixtures; however, the strength of SG-based ternary blend mixtures was relatively higher, as shown in Figure 1(c). This was expected since the pozzolanic reaction of SG is

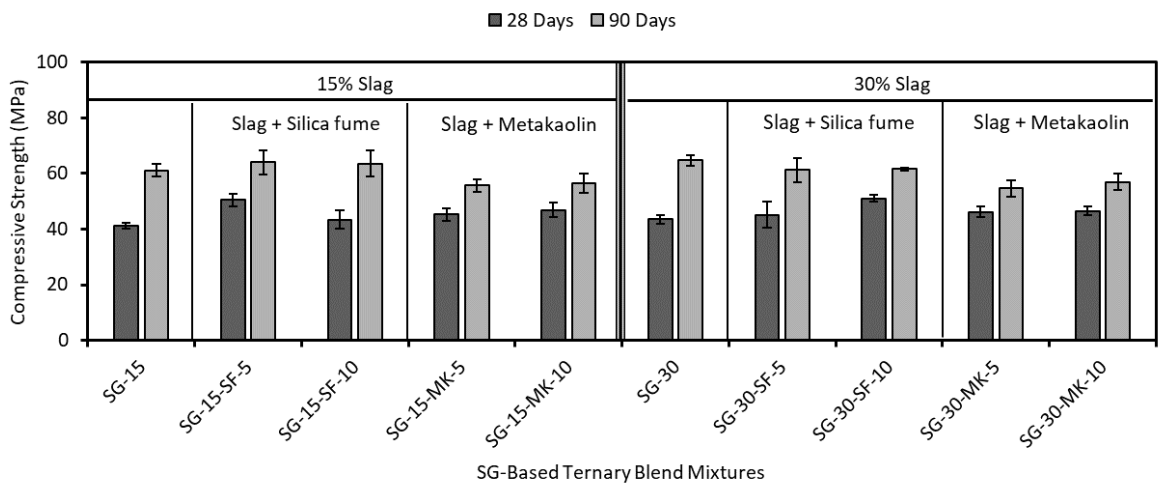
faster than FA [28]. At 28 days, all SG-based ternary blend mixtures were comparable to or higher than the corresponding base binary mixtures (SG-15 and SG-30) and mixture SG-30-SF-10 exhibited compressive strength (51.0 MPa) comparable to the control (50.6 MPa). Again, for the same reasons discussed earlier, the strength of SG-based ternary blend mixtures at 90 days was generally lower than the base binary blend mixtures.



(a)



(b)



(c)

Figure 4.1. Compressive strength of (a) binary, (b) FA-based ternary, and (c) SG-based ternary blend mixtures

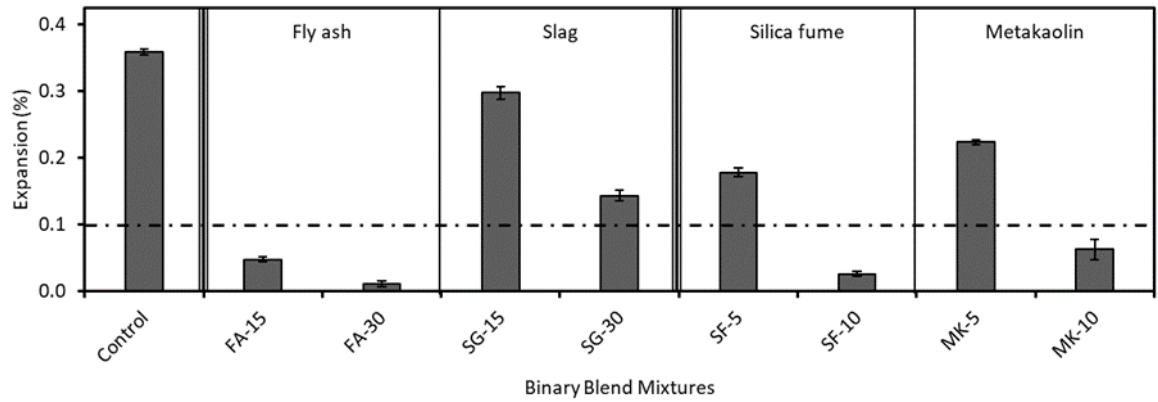
4.3.2. Alkali Silica Reaction

Incorporating glass aggregates in cementitious materials generally induces deleterious internal expansion due to alkali silica reaction (ASR). However, as reported in many studies, ASR expansion can be controlled through the addition of SCMs [8,34,35]. From Figure 2(a), it is evident that the glass aggregate mortar consisting of only ordinary cement (control) exhibited excessive ASR expansion. However, the inclusion of SCM binary blends significantly reduced the expansion. It was found that increasing the replacement level of SCM further reduced ASR expansion, regardless of the SCM type. This reduction in expansion is attributed to the SCMs reacting with and consuming alkalis in the pore solution of the cementitious material, thereby minimizing the concentration of free alkalis [35]. The most effective SCM from Group 1 was FA. All binary blend mixtures containing FA exhibited expansions that were less than the specified ASTM threshold of 0.1% [25]. On the other hand, for Group 2, SF was more effective in reducing ASR expansion compared to MK. Nonetheless, the expansion of mixtures SF-10 and MK-10 were less than 0.1%. Although the results of the two groups of SCMs cannot be directly compared due to their differing replacement levels, studies have found that the order of SCMs, in terms of effectiveness in controlling ASR, is SF, MK, FA class F, and SG [34,36–38]. The results obtained in this study agrees with such findings.

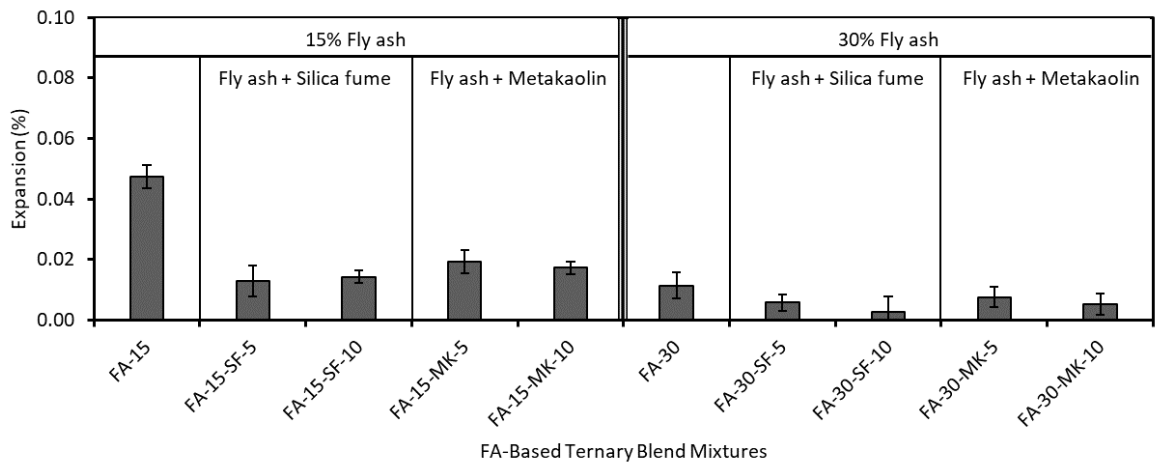
In analyzing the effects of FA-based ternary blend mixtures (Figure 2(b)), it is apparent that the trends in the results correspond to the findings for the binary blend mixtures. Specifically, the increase in FA content from 15% to 30% decreased ASR expansion, regardless of the Group 2 SCM added. Likewise, at fixed FA replacement levels, increasing the content of the Group 2 SCM generally reduced expansion. As

expected, all FA-based ternary blend mixtures exhibited expansions less than the ASTM threshold (0.1%) and all the FA-based ternary blend mixtures had expansions lower than its corresponding base binary blend mixture (FA-15 and FA-30). The combination of FA and SF provided the optimum performance with mixture FA-30-SF-10 exhibiting the lowest expansion of 0.003%.

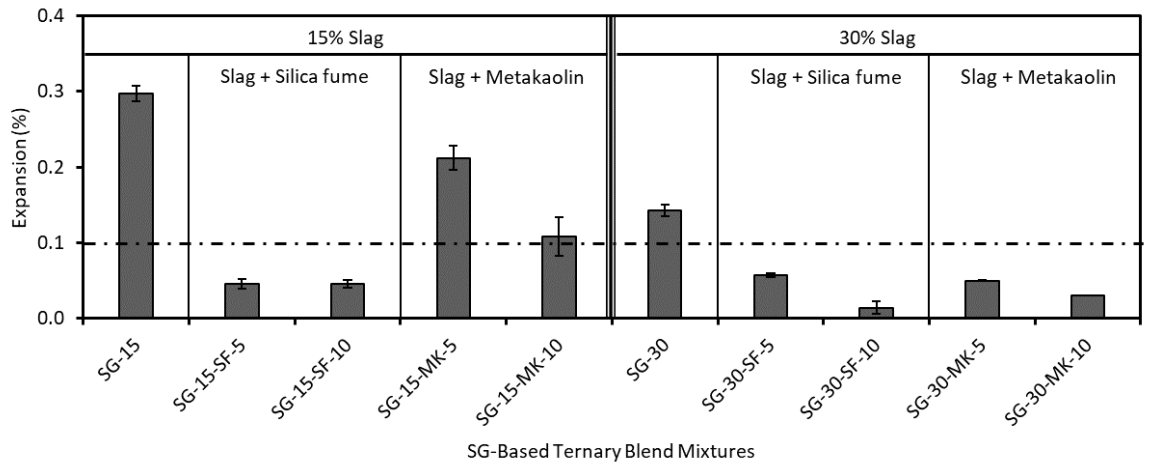
The behaviour of SG-based ternary blend mixtures was very similar to the FA-based ternary blend mixtures. As shown in Figure 2(c), the main difference between the two sets of data was the level of expansion. Unlike the FA-based ternary blend mixtures, not all SG-based ternary blend mixtures were found to have expansions below 0.1%. However, all SG-based ternary blend mixtures containing SF expanded less than 0.1%. Thus, as previously reported, SF is more effective than MK in controlling ASR expansion. This result can be further validated by examining the silica (SiO_2) content of the SF and MK used. As shown in Table 1, the SF used is composed of 85.4% silica, whereas the MK used is composed of 63.5% silica. Therefore, based on chemical compositions alone, SF is expected to outperform MK in terms of expansion reduction as greater levels of silica content in SCMs increases the consumption of available alkalis [35]. Moreover, the higher expansion observed for SG-based ternary blend mixtures compared to FA-based ternary blend mixtures is acceptable since the silica content of SG (36.9%) is much less than the FA (61.3%).



(a)



(b)



(c)

Figure 4.2. 14-day ASR expansion of (a) binary, (b) FA-based ternary, and (c) SG-based ternary blend mixtures

4.3.3. Chloride Permeability

Chloride ingress into cementitious materials can adversely affect durability. Nonetheless, the inclusion of glass aggregates, which have inherently low absorption capacity, can improve chloride permeability. From previous studies completed, the chloride permeability of ordinary cement mortars, with the same mixture proportions as the one used in this study (water to binder ratio and binder to fine aggregate ratio of 1:2 by mass), is 9.88×10^3 C (see Chapter 3.3.4.). Replacing 30% of the fine aggregates with glass reduced chloride permeability to 8.38×10^3 C. However, according to ASTM C1202 [26], the total charge passed for cement mortars containing 30% glass aggregates is still considered as “high”. The current study demonstrates that the chloride permeability of glass aggregate mortars can be further reduced by incorporating SCM blends.

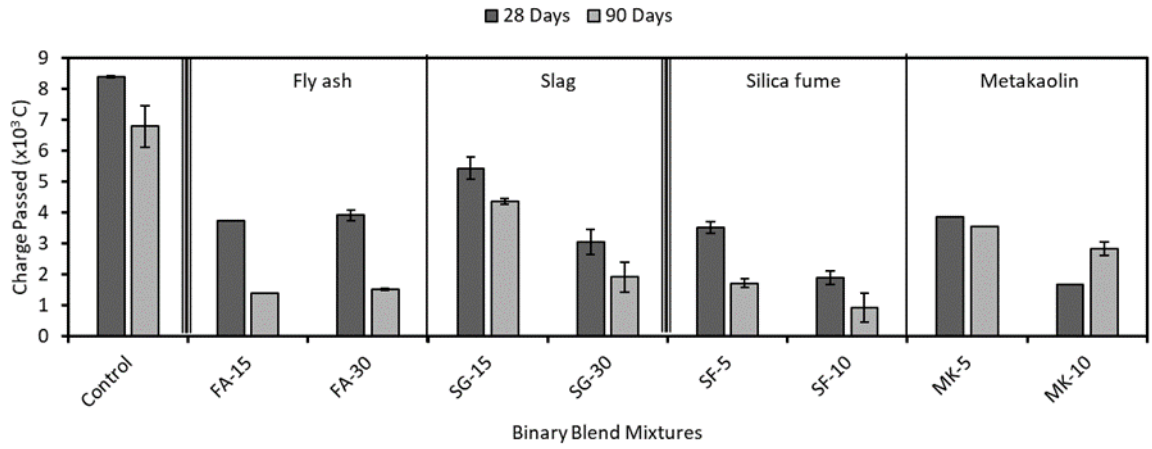
Figure 3(a) shows the improvement in chloride permeability for binary blend mixtures. From this figure, it was found that increasing SG, SF, and MK content results in a significant decrease in chloride permeability, regardless of the test age; however, changes in permeability was not realized when FA content was increased from 15% to 30%. Nevertheless, all binary blend mixtures exhibited chloride permeations less than the control. This is attributed to the ability of SCMs to enhance the microstructure of the cement matrix by reducing interconnecting voids [3,31,39]. At the test age of 90 days, it was observed that SG-15 is still characterized as having “high” chloride permeability (above 4×10^3 C), whereas FA-15, FA-30, and SG-15 exhibited “low” permeability (between 1×10^3 and 2×10^3 C). Many studies have reported that SG is more effective in reducing chloride permeability compared to FA [15,28,40]. However, a possible reason for the lower chloride permeability of the FA binary blend mixtures compared to the SG binary blend mixtures

in this study is the higher alumina (Al_2O_3) content of FA (19.9%) compared to SG (9.1%). Higher alumina content leads to the formation of calcium aluminum silicate hydrates (C-A-S-H) and other aluminate hydrates, which increases chloride binding, thereby minimizing free chlorides [41,42]. Thus, it is evident that for Group 1, FA is more effective in reducing chloride permeability compared to SG. For Group 2 binary blend mixtures, SF-5 and MK-5 exhibited “moderate” chloride permeability (between 2×10^3 and 4×10^3 C), while SF-10 and MK-10 exhibited “low” chloride permeability (between 1×10^3 and 2×10^3 C) at 28 days. All Group 2 binary blend mixtures exhibited either “low” or “very low” chloride permeability at 90 days. SF was more effective than MK in reducing chloride permeability and mixture SF-10 exhibited the lowest total charge passed of 0.92×10^3 C. This agrees with the findings of Jian Tong & Zongjin [13].

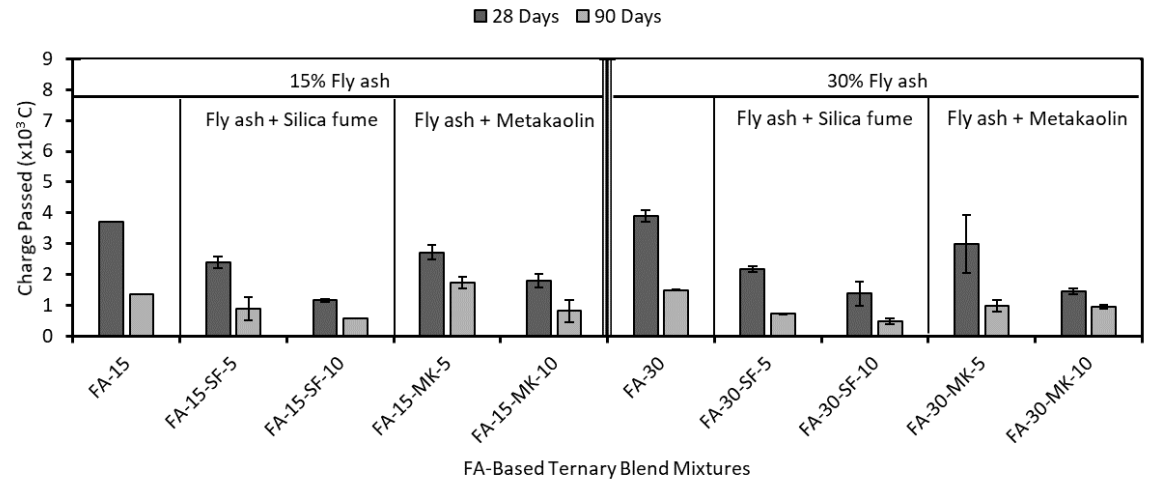
The chloride permeability of FA-based ternary blend mixtures is presented in Figure 3(b). At both test ages of 28 and 90 days, it was found that increasing the FA content to 30% resulted in chloride permeability that was comparable to or lower than ternary blend mixtures containing 15% FA. Similarly, at fixed FA levels, increasing the Group 2 SCM content significantly decreased chloride permeability. These findings correspond with the results obtained for the Group 2 binary blend mixtures. Compared to the respective base binary blend mixtures (FA-15 and FA-30), the ternary blend mixtures are generally lower in permeability. At 90 days, it was found that mixture FA-30-SF-10 exhibited the lowest total charge passed of 0.50×10^3 C.

The trends observed in chloride permeability for SG-based ternary blend mixtures is similar to the FA-based ternary blend mixtures as increasing the SG content generally decreased chloride permeability. At fixed SG levels, a general decrease in permeability

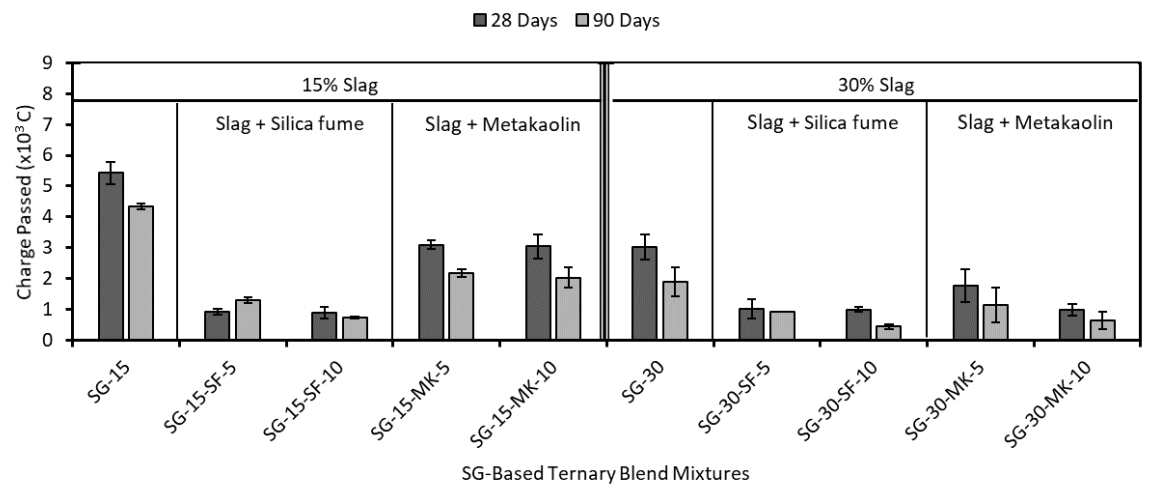
was observed when the amount of the Group 2 SCM was increased. Compared to the base binary blend mixtures (SG-15 and SG-30), all ternary blend mixtures exhibited lower permeability, regardless of the test age. Specifically, the combination of SG and SF was the most effective in reducing chloride permeability. In fact, among all ternary blend mixtures, it was determined that the optimum combination at 28 and 90 days was SG-15-SF-10 (0.90×10^3 C) and SG-30-SF-10 (0.45×10^3 C), respectively. This contradicts the results obtained for the binary blend mixtures in which FA was found to be more effective than SG; however, the results obtained agrees with the conclusions of Gesoğlu et al. [15] since this study reported that the ternary use of SG and SF provides better performance in chloride permeability compared to FA and SF combinations.



(a)



(b)



(c)

Figure 4.3. Chloride permeability of (a) binary, (b) FA-based ternary, and (c) SG-based ternary blend mixtures

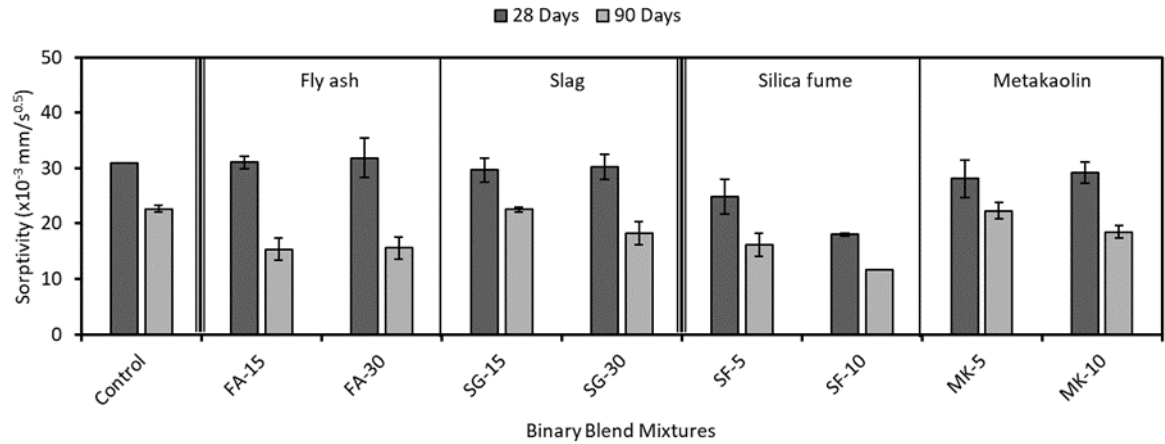
4.3.4. Sorptivity

The sorptivity indices of SCM binary blend mixtures are presented in Figure 4(a). At 28 days, a marginal difference in the sorptivity index was observed when FA, SG, and MK content was increased; however, a significant decrease (28%) was observed when SF content was increased. At 90 days, a considerable reduction in the sorptivity index was observed when SG, SF, and MK content was increased. The reduction in the sorptivity index was 19%, 28%, and 17% respectively. Nonetheless, there was still an insignificant change in the sorptivity index when FA content was increased at 90 days. The sorptivity index of all Group 1 binary blend mixtures was comparable at 28 days; however, at 90 days, FA binary blend mixtures clearly performed better than SG binary blend mixtures with sorptivity indices of $15.3 \times 10^{-3} \text{ mm/s}^{0.5}$ and $15.6 \times 10^{-3} \text{ mm/s}^{0.5}$ for FA-15 and FA-30, respectively. For Group 2 binary blend mixtures, it was found that SF-10 exhibited the lowest sorptivity index of $18.0 \times 10^{-3} \text{ mm/s}^{0.5}$ and $11.7 \times 10^{-3} \text{ mm/s}^{0.5}$ at 28 and 90 days, respectively. Compared to the control mixture, all binary blend mixtures exhibited lower sorptivity indices by the age of 90 days. This can be attributed to progress of hydration, which enhanced the microstructure of the mortars. Furthermore, the combined pozzolanic and filler effect of SCMs refined internal pores and densified the cementitious paste [12,29,43,44].

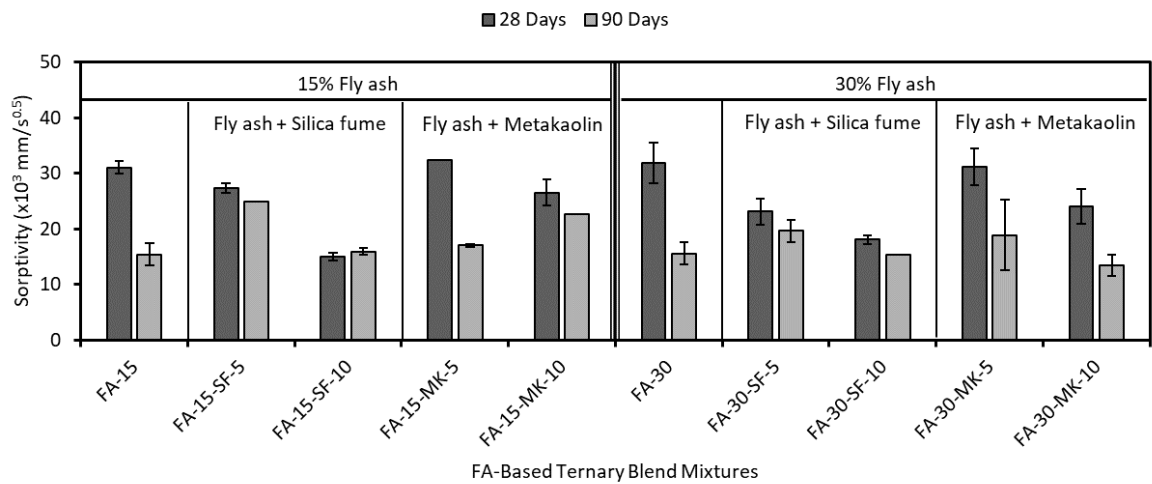
For FA-based ternary blend mixtures, it was found that increasing the FA content generally decreased the sorptivity index at both 28 and 90 days (Figure 4(b)). This trend in sorptivity also occurred when the FA content was fixed and the Group 2 SCM content was increased. At 28 days, all FA-based ternary blend mixtures were either comparable to or lower than their relative base binary blend mixtures (FA-15 and FA-30). Nonetheless,

similar to the behaviour observed for compressive strength, a comparison between the relative base binary blend mixtures and the ternary blend mixtures at 90 days contrasts the 28-day trends. The obtained 90-day sorptivity indices are opposite of the expected result as the sorptivity indices of the ternary blend mixtures are either comparable to or higher than the base binary blend mixtures. The reasons provided in the compressive strength discussion can be applied to explain the behaviour of the 90-day sorptivity data. Nevertheless, it is just right that the 28 and 90-day results of compressive strength and sorptivity concur since it has generally been found that these two properties are correlated [45]. Despite the differing trends, it is evident that SF is more effective in reducing sorptivity compared to MK, which agrees with reports found in the literature [14,46].

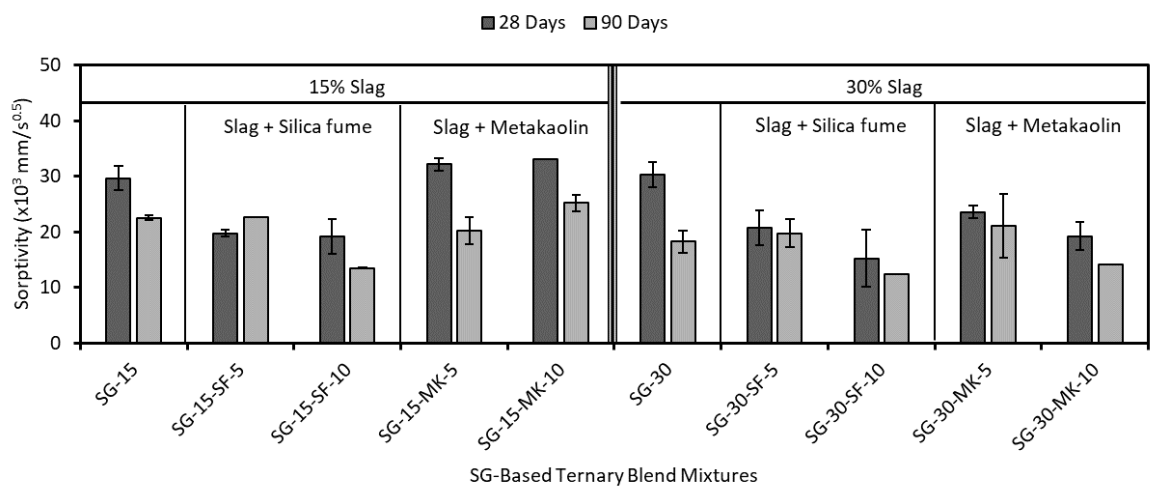
The sorptivity results for SG-based ternary blend mixtures is presented in Figure 4(c). Similar to the FA-based ternary blend mixtures, increasing the SG and Group 2 SCM content generally decreases the sorptivity index at both 28 and 90 days. Compared to its relative base binary blend mixtures, the sorptivity index of the ternary blend mixtures are either comparable to or much lower at 28 days. Surprisingly, at 90 days, the ternary blend mixtures were also comparable to or lower than the base binary blend mixtures, which is in contrast with the trends observed for the FA-based ternary blend mixtures. Again, it was evident that SF is more effective in reducing the sorptivity index compared to MK with SG-30-SF-10 exhibiting the lowest sorptivity index of $12.4 \times 10^{-3} \text{ mm/s}^{0.5}$ at 90 days.



(a)



(b)



(c)

Figure 4.4. Sorptivity of (a) binary, (b) FA-based ternary, and (c) SG-based ternary blend mixtures

4.3.5. Optimization

Design Expert software was used to determine the optimum combinations of the SCMs. Predictive models were developed for each property (response) investigated, as shown in Table 4.3. The developed models were based on quadratic models, which produced the best fit for the data. It is important to note that variables *FA*, *SG*, *SF*, and *MK* indicate the linear effect of the SCMs, while FA^2 , SG^2 , SF^2 , and MK^2 indicate the quadratic effect and $FA \cdot SF$, $FA \cdot MK$, $SG \cdot SF$, and $SG \cdot MK$ indicate the interaction effect of the SCMs [17]. The equations presented in Table 3 includes only the statistically significant coefficients ($p < 0.05$). As such, it is evident that not all SCMs have a significant effect on the responses.

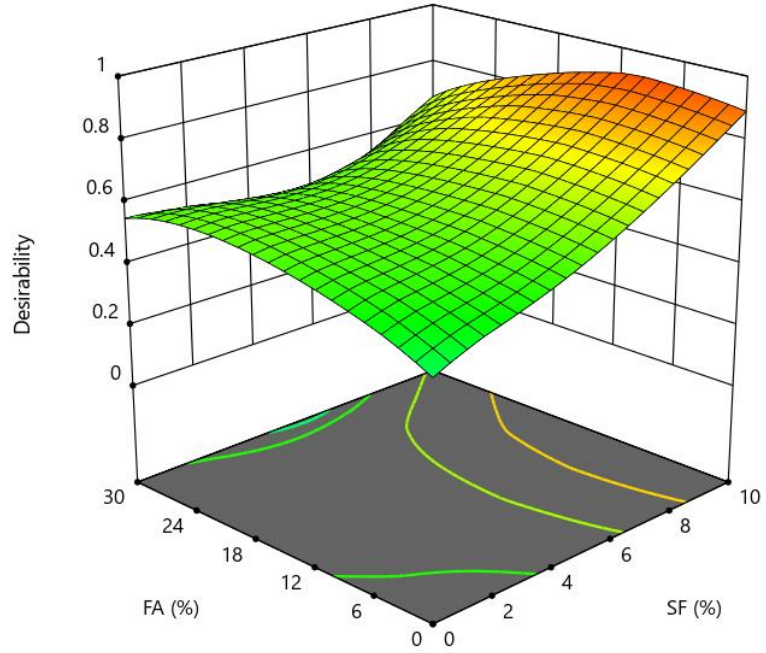
Goals were assigned to each factor (*FA*, *SG*, *SF*, and *MK*) and response as specified in the optimization criteria outlined in Table 4.4. These goals were transformed by the software into a scale ranging from zero to one – zero being the least desirable and one being the most desirable – to produce desirability functions. The geometric mean of the transformed responses (individual desirability functions) results in the overall desirability index. The highest desirability that was obtained for the set of data in this study was 0.92. From the desirability curves presented in Figure 4.5, this level of desirability (0.92) can be achieved with the combinations of 9% *FA* + 10% *SF* or 9% *FA* + 10% *MK*. Likewise, from Figure 4.6, the highest desirability of 0.92 can be obtained with the combinations of 0% *SG* + 10% *SF* or 0% *SG* + 10% *MK*. Hence, maximizing the Group 2 SCMs results in the optimal performance, which coincides with the experimental results.

Table 4.3. Statistical models of glass aggregate mortar properties

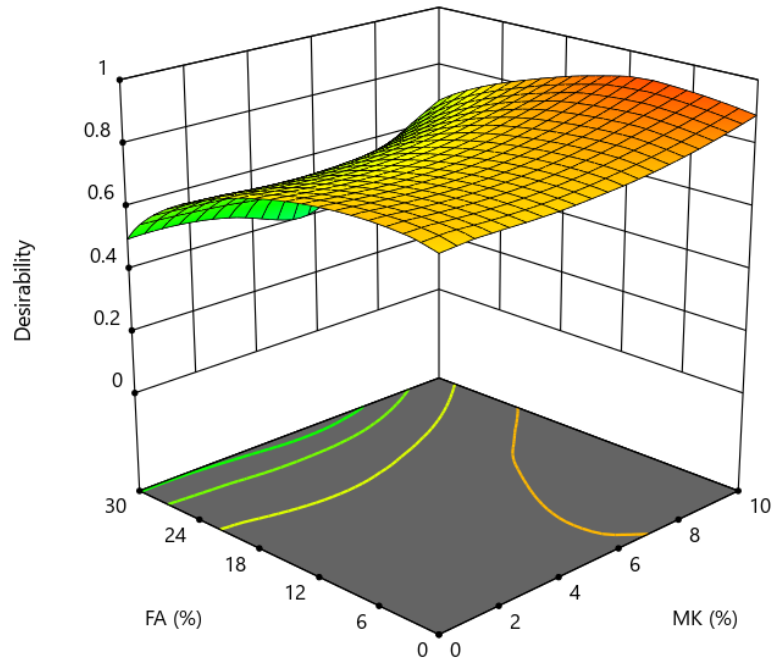
Derived models	R ²	p-value
Alkali Silica Reaction (%) = exp [− 4.68449 − 1.3055·FA − 0.45012·SG − 0.81265·SF − 0.5124·MK]	0.95	< 0.0001
Compressive Strength - 28d (MPa) = 39.7998 − 8.78849·FA	0.89	0.0005
Compressive Strength - 90d (MPa) = 45.7691 − 6.97022·FA + 6.40824·SF ² + 6.1992·MK ²	0.85	0.0028
Chloride Permeability - 28d (C) = − 671.897 − 1081.3·SF − 863.824·MK + 940.545·FA·SF + 884.966·SG·SF + 953.448·SG·MK	0.87	0.0012
Chloride Permeability - 90d (C) = [− 0.0416346 − 0.00664831·FA + 0.00799441·SG + 0.0103648·SF + 0.00568142·MK + 0.00268592·SG·MK − 0.00443272·FA ²] ⁻²	0.96	< 0.0001
Sorptivity - 28d (x10 ⁻³ mm/s ^{0.5}) = 22.5227 − 3.08592·SG − 7.34567·SF − 3.81183·MK	0.87	0.0012
Sorptivity - 90d (x10 ⁻³ mm/s ^{0.5}) = [0.034872 − 0.00873273·FA·SF + 0.0145626·SF ²] ⁻¹	0.78	0.0190

Table 4.4. Optimization Criteria

Factors/Responses	Goal	Lower Limit	Upper Limit
FA (%)	In Range	0	30
SG (%)	In Range	0	30
SF (%)	In Range	0	10
MK (%)	In Range	0	10
Alkali Silica Reaction (%)	Minimize	0.0026	0.3582
Compressive Strength - 28d (MPa)	Maximize	31.3	53.0
Compressive Strength - 90d (MPa)	Maximize	42.1	65.3
Chloride Permeability - 28d (C)	Minimize	900	8383
Chloride Permeability - 90d (C)	Minimize	447	6771
Sorptivity - 28d ($\times 10^{-3}$ mm/s ^{0.5})	Minimize	15.0	33.0
Sorptivity - 90d ($\times 10^{-3}$ mm/s ^{0.5})	Minimize	11.7	25.2

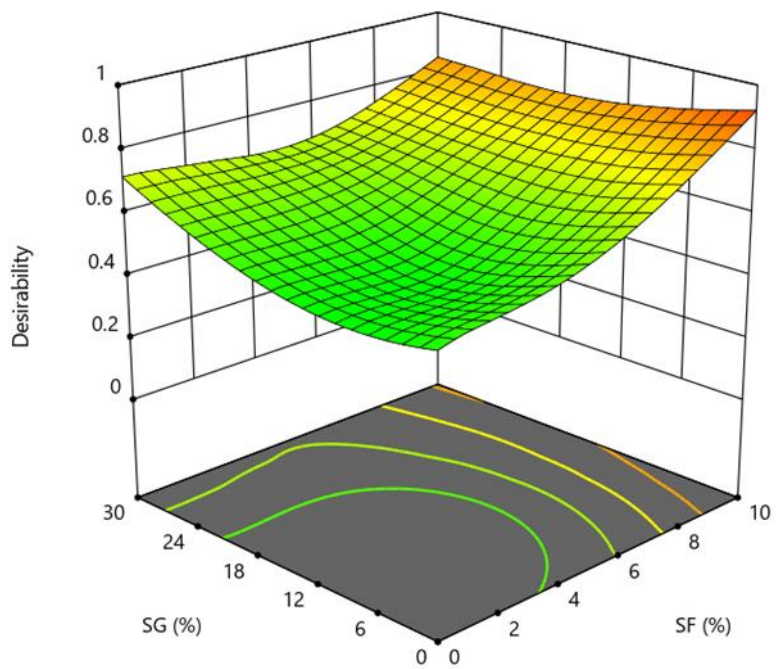


(a)

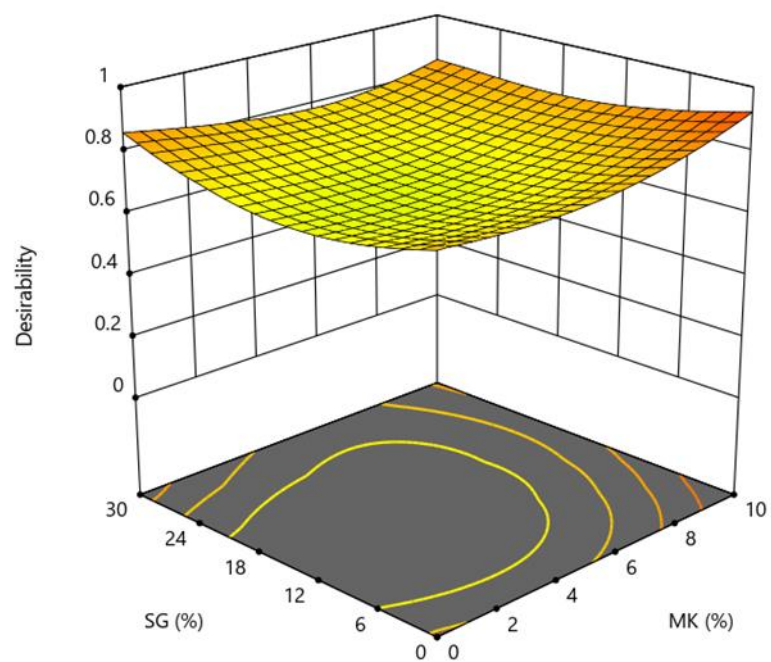


(b)

Figure 4.5. Desirability of mixtures containing FA and (a) SF (b) MK



(a)



(b)

Figure 4.6. Desirability of mixtures containing SG and (a) SF (b) MK

4.4. Conclusions

The experimental work undertaken in this study examined the effects of various SCM blends in glass aggregate mortars. Strength and durability in terms of ASR expansion, chloride permeability, and sorptivity were investigated and the optimal SCM combinations were determined. The significant findings of this study are summarized as follows. It should be noted that the conclusions drawn here may be limited to the scope of the work.

1. FA reduces compressive strength, whereas all other SCMs (SG, SF, and MK) improve strength. Between the Group 1 SCMs, binary blend mixtures containing SG exhibited higher compressive strengths compared to binary blend mixtures containing FA. Consequently, SG-based ternary blend mixtures exhibited greater strength compared to FA-based ternary blend mixtures. For Group 2 SCMs, SF and MK were found to be comparable in strength.
2. SCMs are very effective in mitigating the expansions of glass aggregate mortars. Among the Group 1 SCMs, FA was the most effective in reducing ASR expansion. All binary and ternary blend mixtures containing FA exhibited expansions well below the ASTM threshold of 0.1%. For Group 2 SCMs, SF was found to be more effective than MK. The underlying explanation for the effectiveness of FA and SF compared to SG and MK, respectively, is the higher SiO₂ content of FA and SF.
3. Chloride permeability and sorptivity are significantly reduced when SCMs are used as partial cement replacement. SCMs enhance the microstructure of the cement paste through pozzolanic and filler effect. The ternary combination of SG and SF resulted in the lowest chloride permeability and sorptivity index.

4. The optimal glass aggregate mortar performance can be obtained by maximizing Group 2 SCMs. Mixtures containing 9% FA + 10% SF, 9% FA + 10% MK, 0% SG + 10% SF, and 0% SG + 10% MK provide the highest desirability of 0.92.

4.5. Acknowledgements

The authors acknowledge the Natural Sciences and Engineering Research Council of Canada and the University of Windsor for the financial support provided to Karla Gorospe in the form of the Canada Graduate Scholarship, and the Queen Elizabeth II Graduate Scholarship in Science and Technology, respectively.

4.6. References

- [1] International Energy Agency (IEA), Cement: Tracking Clean Energy Progress. <https://www.iea.org/tcep/industry/cement/>, 2019 (accessed 3 March 2019).
- [2] P. Dinakar, K.G. Babu, M. Santhanam, Durability properties of high volume fly ash self compacting concretes, *Cement and Concrete Composites*. 30 (2008) 880–886.
- [3] A.K. Saha, Effect of class F fly ash on the durability properties of concrete, *Sustainable Environment Research*. 28 (2018) 25–31.
- [4] M. Sharfuddin Ahmed, O. Kayali, W. Anderson, Chloride penetration in binary and ternary blended cement concretes as measured by two different rapid methods, *Cement and Concrete Composites*. 30 (2008) 576–582.
- [5] W. Wongkeo, P. Thongsanitgarn, A. Chaipanich, Compressive strength and drying shrinkage of fly ash-bottom ash-silica fume multi-blended cement mortars, *Materials & Design*. 36 (2012) 655–662.
- [6] C.S. Shon, S.L. Sarkar, D.G. Zollinger, Testing the effectiveness of class C and class F fly ash in controlling expansion due to alkali-silica reaction using modified ASTM C 1260 test method, *Journal of Materials in Civil Engineering*. 16 (2004) 20–27.
- [7] R.O. Lane, J.F. Best, Properties and use of fly ash in portland cement concrete, *Concrete International*. 4 (1982) 81–92.
- [8] D.S. Lane, C. Ozyildirim, Preventive measures for alkali-silica reactions (binary and

- ternary systems), *Cement and Concrete Research*. 29 (1999) 1281–1288.
- [9] M.F. Bazhuni, M. Kamali, A. Ghahremaninezhad, An investigation into the properties of ternary and binary cement pastes containing glass powder, *Frontiers of Structural and Civil Engineering*. (2018) 1–10.
- [10] G.J. Osborne, Durability of Portland blast-furnace, *Cement and Concrete Composites*. 21 (1999) 11–21.
- [11] R. Siddique, Utilization of silica fume in concrete: Review of hardened properties, *Resources, Conservation and Recycling*. 55 (2011) 923–932.
- [12] C.S. Poon, S.C. Kou, L. Lam, Compressive strength, chloride diffusivity and pore structure of high performance metakaolin and silica fume concrete, *Construction and Building Materials*. 20 (2006) 858–865.
- [13] D. Jian Tong, L. Zongjin, Effects of metakaolin and silica fume on properties of concrete, *ACI Materials Journal*. 99 (2002) 393–398.
- [14] H.A. Razak, H.K. Chai, H.S. Wong, Near surface characteristics of concrete containing supplementary cementing materials, *Cement and Concrete Composites*. 26 (2004) 883–889.
- [15] M. Gesoğlu, E. Güneyisi, E. Özbay, Properties of self-compacting concretes made with binary, ternary, and quaternary cementitious blends of fly ash, blast furnace slag, and silica fume, *Construction and Building Materials*. 23 (2009) 1847–1854.
- [16] E. Güneyisi, M. Gesoğlu, S. Karaoğlu, K. Mermerdaş, Strength, permeability and shrinkage cracking of silica fume and metakaolin concretes, *Construction and Building Materials*. 34 (2012) 120–130.
- [17] S. Aydın, A ternary optimisation of mineral additives of alkali activated cement mortars, *Construction and Building Materials*. 43 (2013) 131–138.
- [18] H. Du, K.H. Tan, Use of waste glass as sand in mortar: Part II - Alkali-silica reaction and mitigation methods, *Cement and Concrete Composites*. 35 (2013) 109–117.
- [19] S. Guo, Q. Dai, X. Sun, X. Xiao, R. Si, J. Wang, Reduced alkali-silica reaction damage in recycled glass mortar samples with supplementary cementitious materials, *Journal of Cleaner Production*. (2017).
- [20] D. Serpa, A. Santos Silva, J. De Brito, J. Pontes, D. Soares, ASR of mortars containing glass *Construction and Building Materials*. 47 (2013) 489–495.
- [21] H. Du, K.H. Tan, Concrete with recycled glass as fine aggregates, *ACI Materials Journal*. 111 (2014) 47–57.

- [22] CSA A3001, Cementitious materials used in concrete, Canadian Standards Association., Mississauga, Ontario, 2013.
- [23] ASTM C305, Standard practice for mechanical mixing of hydraulic cement pastes and mortars, ASTM International, West Conshohocken, PA, 2015.
- [24] ASTM C109, Standard test method for compressive strength of hydraulic cement mortars (using 2-in. or [50mm] cube specimens), ASTM International, West Conshohocken, PA, 2016.
- [25] ASTM C1567, Standard test method for determining the potential alkali-silica reactivity of combinations of cementitious materials and aggregate (accelerated mortar - bar method), ASTM International, West Conshohocken, PA, 2013.
- [26] ASTM C1202, Standard test method for electrical indication of concrete's ability to resist chloride ion penetration, ASTM International, West Conshohocken, PA, 2016.
- [27] ASTM 1585, Standard test method for measurement of rate of absorption of water by hydraulic-cement concretes, ASTM International, West Conshohocken, PA, 2013.
- [28] O. Sengul, M.A. Tasdemir, Compressive Strength and Rapid Chloride Permeability of Concretes with Ground Fly Ash and Slag, *Journal of Materials in Civil Engineering*. 21 (2009) 494–501.
- [29] T.K. Erdem, Ö. Kirca, Use of binary and ternary blends in high strength concrete, *Construction and Building Materials*. 22 (2008) 1477–1483.
- [30] T. Nochaiya, W. Wongkeo, A. Chaipanich, Utilization of fly ash with silica fume and properties of Portland cement-fly ash-silica fume concrete, *Fuel*. 89 (2010) 768–774.
- [31] M.F. Bazhuni, M. Kamali, A. Ghahremaninezhad, An investigation into the properties of ternary and binary cement pastes containing glass powder, *Frontiers of Structural and Civil Engineering*. (2018) 1–10.
- [32] M. Mazloom, A.A. Ramezani pour, J.J. Brooks, Effect of silica fume on mechanical properties of high-strength concrete, *Cement and Concrete Composites*. 26 (2004) 347–357.
- [33] S. Wild, J.M. Khatib, A. Jones, Relative strength, pozzolanic activity and cement hydration in superplasticised metakaolin concrete, *Cement and Concrete Research*. 26 (1996) 1537–1544.
- [34] M.H. Shehata, M.D.A. Thomas, Use of ternary blends containing silica fume and fly ash to suppress expansion due to alkali-silica reaction in concrete, *Cement and*

Concrete Research. 32 (2002) 341–349.

- [35] M. Thomas, The effect of supplementary cementing materials on alkali-silica reaction: A review, *Cement and Concrete Research*. 41 (2011) 1224–1231.
- [36] M.H. Shehata, M.D.A. Thomas, R.F. Bleszynski, The effects of fly ash composition on the chemistry of pore solution in hydrated cement pastes, *Cement and Concrete Research*. 29 (1999) 1915–1920.
- [37] T. Ramlochan, M. Thomas, K.A. Gruber, Effect of metakaolin on alkali-silica reaction in concrete, *Cement and Concrete Research*. 30 (2000) 339–344.
- [38] R. Bleszynski, R.D. Hooton, M.D.A. Thomas, C.A. Rogers, Durability of ternary blend concrete with silica fume and blast-furnace slag: Laboratory and outdoor exposure site studies, *ACI Materials Journal*. 99 (2002) 499–508.
- [39] J. Bijen, Benefits of slag and fly ash, *Construction and Building Materials*. 10 (1996) 309–314.
- [40] A.A. Ramezani-pour, V.M. Malhotra, Effect of curing on the compressive strength, resistance to chloride-ion penetration and porosity of concretes incorporating slag, fly ash or silica fume, *Cement and Concrete Composites*. 17 (1995) 125–133.
- [41] H. Justnes, A review of chloride binding in cementitious systems, *Nordic Concrete Research Publications*. 21 (1998) 48–63.
- [42] Q. Yuan, C. Shi, G. De Schutter, K. Audenaert, D. Deng, Chloride binding of cement-based materials subjected to external chloride environment - A review, *Construction and Building Materials*. 23 (2009) 1–13.
- [43] B. Sabir, S. Wild, J. Bai, Metakaolin and calcined clays as pozzolans for concrete: A review, *Cement and Concrete Composites*. 23 (2001) 441–454.
- [44] P. Duan, Z. Shui, W. Chen, C. Shen, Effects of metakaolin, silica fume and slag on pore structure, interfacial transition zone and compressive strength of concrete, *Construction and Building Materials*. 44 (2013) 1–6.
- [45] C. Tasdemir, Combined effects of mineral admixtures and curing conditions on the sorptivity coefficient of concrete, *Cement and Concrete Research*. 33 (2003) 1637–1642.
- [46] R. Saleh Ahari, T.K. Erdem, K. Ramyar, Permeability properties of self-consolidating concrete containing various supplementary cementitious materials, *Construction and Building Materials*. 79 (2015) 326–336.

CHAPTER 5

CONCLUSIONS AND RECOMMENDATIONS

The mechanical, durability, and thermal properties of glass aggregate mortars containing various types of glass and supplementary cementitious materials (SCM) were examined in this thesis. This chapter summarizes the main findings of the experimental work undertaken and presents recommendations for future work.

5.1. Mechanical Properties

Incorporating glass aggregates in cement mortar generally reduced compressive strength. The temperature of curing also affected the strength as elevated temperatures led to the formation of delayed ettringite. Nonetheless, glass aggregates of finer particle size possess inherent pozzolanic properties, which was shown to improve strength. Binary blends of slag, silica fume, and metakaolin are also effective in improving mortar strength, thereby offsetting the loss of strength associated with the addition of glass aggregates. However, the use of fly ash resulted in a further reduction in strength due to its slow reaction rate. Extending the tests to later ages should be considered in future works to better perceive the effects of the SCMs, specifically fly ash. Furthermore, the mixture design should be modified to exhibit more realistic mortar strength, and other mechanical properties, such as flexural and split-tensile strength, should be studied.

5.2. Durability Properties

Durability was assessed quantitatively and qualitatively by means of alkali silica reaction (ASR), chloride ion permeability, immersion absorption, sorptivity, and plastic

and drying shrinkage tests. As expected, glass aggregate mortars are susceptible to deleterious ASR expansions; however, the level of expansion is dependent on the size of the glass aggregates. The use of SCMs, specifically fly ash and silica fume, significantly reduced mortar bar expansions to acceptable levels (below 0.1%). Glass aggregate mortars also exhibited improved immersion absorption, sorptivity, and chloride ion permeability. Furthermore, it was found that glass aggregates are effective in reducing plastic and drying shrinkage of mortar.

For future works, it is recommended that long-term ASR tests be considered to validate the results obtained using the accelerated mortar bar method. More SEM and EDS analyses should also be conducted to further evaluate the microstructure and interfacial transition zones in the cement mortars. In addition, the capillary pressure and the rate of bleeding of the mortar overlay specimens should be measured to better understand the underlying mechanisms that cause plastic shrinkage.

5.3. Thermal Properties

Glass aggregate mortars were found to be very effective in reducing thermal conductivity. Therefore, it has great potential in improving thermal insulation properties if used as a building material. This advantageous property of glass aggregate mortars is a result of the inherently low thermal conductivity of glass. Further testing on glass aggregate mortars, specifically at a larger scale, should be done.

VITA AUCTORIS

NAME: Kayle Karla Mei Mamitag Gorospe

PLACE OF BIRTH: Dagupan City, Pangasinan, Philippines

YEAR OF BIRTH: 1995

EDUCATION: University of Windsor, Windsor, ON, Canada

- B.A.Sc. (Honours Civil Engineering Co-op) With Great Distinction, 2013-2017
- M.A.Sc. (Civil Engineering), 2017-2019